DISSERTATION

submitted to the

Combined Faculties for the Natural Sciences and for Mathematics

of the Ruperto-Carola University of Heidelberg, Germany

for the degree of

Doctor of Natural Sciences

presented by

Ionut Gabriel Dumitru, M. Sc.

born in Bucharest, Romania

SGZ adult neurogenesis is regulated by Diazepam Binding Inhibitor

Referees: Prof. Dr. Hannah Monyer

Dr. Julieta Alfonso

Oral examination:……

Declaration according to § 8 (3) b) and c) of the doctoral degree regulation: I hereby declare that the submitted dissertation, entitled: ‘SGZ adult neurogenesis is regulated by Diazepam Binding Inhibitor’ was written by myself and in this process I used no other sources or materials than those indicated. Where the work of others has been quoted or reproduced, the source is always given. I hereby declare that I did not already present this thesis or parts of it to a university or any other institution as part of an examination or degree.

Date Signature

Table of Contents

Summary

Adult neurogenesis adds an entirely new level of plasticity to the brain and raises hope to use stem cell therapy to repair damaged nervous tissue. To understand the role of neurogenesis in the adult brain and to harness its potential it is of utmost importance to understand the regulation of the stem cell niches. Our group previously showed that the endozepine DBI is expressed in neuronal progenitors in the SVZ and that it reduces GABA signalling in these cells. Via this mechanism, DBI promotes the proliferation of fast dividing progenitors which leads to a strong increase in neurogenesis. Here I investigated the presence of DBI in other neurogenic niches and its role in regulating postnatal and adult neurogenesis. I found that DBI is strongly expressed in the SGZ and in the walls of the 3rd ventricle both postnatally and in adult mice. Furthermore, I showed that DBI is present in RG cells during embryonic development. I found that DBI is expressed not only in all mouse postnatal and adult neurogenic niches but also across species in the SGZ of the Rhesus monkey and in humans. High expression levels of DBI were detected in all stem cells and in the early population of amplifying progenitors, suggesting that this protein could be considered as an indicator for stemness in the nervous tissue. Focusing on the SGZ, I showed that DBI negatively modulates the activity of the $GABA_A$ receptor in stem cells, thereby increasing their proliferation, self-renewal and astrocyte production. In summary, DBI together with GABA regulate the balance between preserving the stem cell pool and neuronal production.

External factors such as environmental enrichment and physical exercise strongly enhance neurogenesis. I found in this study that DBI is essential for the pro-proliferative and pro-neurogenic effects of enriched environment and exercise. Therefore, DBI and GABA regulate SGZ neurogenesis in a close partnership enabling multiple levels of control which makes the niche dynamic and capable of reacting promptly to changes in the environment.

Zusammenfassung

Adulte Neurogenese trägt zu einem völlig neuen Niveau an Plastizität des Gehirns bei und weckt die Hoffnung, Stammzelltherapie zur Reparatur von beschädigtem Nervengewebe zu verwenden. Um die Rolle von Neurogenese im adulten Gehirn zu verstehen und sich ihr Potenzial zunutze zu machen, ist es von höchster Wichtigkeit, die Regulierung der Stammzellnischen zu verstehen. Unsere Forschungsgruppe hat zuvor gezeigt, dass das endozepine DBI in neuronalen Progenitoren in der Subventrikulären Zone exprimiert wird und dass es die GABA-Signalisierung in diesen Zellen reduziert. Durch diesen Mechanismus fördert DBI die Vermehrung von sich schnell teilenden Progenitoren, was zu einem starken Anstieg von Neurogenese führt. Hier habe ich die Anwesenheit von DBI in anderen neurogenen Nischen und seine Rolle bei der Regulierung der postnatalen und adulten Neurogenese erforscht. Ich habe herausgefunden, dass DBI sowohl in neugeborenen als auch in adulten Mäusen in der Subgranulare Zone und in den Wänden des dritten Ventrikels stark exprimiert wird. Außerdem habe ich aufgezeigt, dass DBI in RG-Zellen während der Embryo-Entwicklung vorhanden ist. Ich habe herausgefunden, dass DBI bei Mäusen nicht nur in allen postnatalen und adulten neurogenen Nischen exprimiert wird, sondern auch artübergreifend in der SGZ der Rhesusaffen und in Menschen. Große Mengen an DBI wurden in allen Stammzellen und in der frühen Population von wechselnden Progenitoren gefunden, was andeutet, dass dieses Protein als Indikator für Stammzellpotenzial im Gehirn angesehen werden könnte. Bei genauerer Betrachtung der SGZ konnte ich aufzeigen, dass DBI die Aktivität des $GABA_A$-Rezeptors in Stammzellen negativ beeinflusst und dabei deren Ausbreitung, Selbsterneuerung und Astrozyten-Produktion anhebt. Zusammenfassend bedeutet dies, dass DBI zusammen mit GABA das Gleichgewicht zwischen der Erhaltung des Stammzellpools und der neuronalen Produktion reguliert.

Externe Faktoren wie eine angereicherte Umgebung und körperliche Aktivität fördern die Neurogenese stark. Ich habe durch diese Studie herausgefunden, dass DBI essenziell ist für die Förderung von Neurogenese in angereicherter Umgebung. Somit

regulieren DBI und GABA die SGZ Neurogenese in enger Zusammenarbeit durch die Aktivierung mehrerer Kontrollebenen, was die Nische dynamisch macht und befähigt, schnell auf Änderungen in der Umgebung zu reagieren.

1. Introduction

At the beginning of the 20th century when the base of neuroscience were laid, researchers believed that after birth the number of neurons in the human brain would not change, or if so, only slightly. The complex structure of the brain, the large number of neurons, the intricate connections between them and the lack of improvement after neurodegeneration or injury supported this hypothesis. Using ^{3}H-thymidine experiments, Altman and Das provided the first proofs that new neurons are produced postnatally in the rat brain, opening a new research field (Altman and Das, 1965). Altman also showed the presence of labeled cells in the subventricular zone (SVZ) of the lateral ventricles and the migration of these cells towards the olfactory bulbs (OB) via a structure he termed the rostral migratory stream (RMS) (Altman, 1969). These findings raised the hope to harness neurogenesis in the adult for repair following damage of nervous tissue. Furthermore, neurogenesis in the adult represents yet another mode of plasticity in the mammalian brain, which was thought to subside during/after development. In the course of the next fifty years, great advances were made regarding molecular and cellular characteristics of neural stem cells, composition of the neurogenic niches, regulation and functions of adult neurogenesis (Bond et al., 2015). *In vitro* experiments showed the presence of putative stem cells with self-renewal and multipotency capacities in the adult rodent brain (Reynolds and Weiss, 1992). Using the synthetic thymidine analogue bromodeoxiuridine (BrdU) in vivo, the group of Fred Gage showed that neurons are born in the adult rat dentate gyrus (DG) (Kuhn et al., 1996). Final proofs that the new-born neurons integrate in mature circuits of the brain were brought by Dayer and colleagues With the help of label retention studies they showed that some of the new-born neurons remain in the brain throughout the life of the animal (Dayer et al., 2003). Furthermore, Carlen and colleagues, showed that newborn neurons integrate functionally in brain circuits and contribute to their function (Carlen et al., 2002). These early papers were followed by a vast literature investigating the behavior of neural progenitors and the factors regulating them (Bond et al., 2015). The first indication of adult neurogenesis in the human brain was brought by Eriksson

and colleagues, who showed the presence of BrdU positive neurons in the hippocampus of cancer patients that received the thymidine analogue for diagnostic purposes (Eriksson et al., 1998). The group of Arturo Alvarez-Buylla also found the presence of neurogenic activity in the SVZ of human infants. However, this activity seems to decrease steeply during childhood and has virtually subsided in adults (Sanai et al., 2011). Furthermore, the authors showed the presence of postnatally generated neurons in the RMS and in a migratory pathway towards the prefrontal cortex and the frontal latter migratory route was described for the first time in humans and may correspond to the pathway identified by Inta and colleagues in the mouse (Inta et al., 2008; Paredes et al., 2016). Based on C^{14} dating, the lab of Jonas Frisén demonstrated that adult neurogenesis takes place in the human SVZ, hippocampus and striatum. However, in contrast to what had been reported in studies with rodents, the authors found almost no new neurons that integrated in the olfactory bulb in humans, pointing towards species differences (Bergmann et al., 2015; Ernst et al., 2014; Ernst and Frisen, 2015; Spalding et al., 2013).

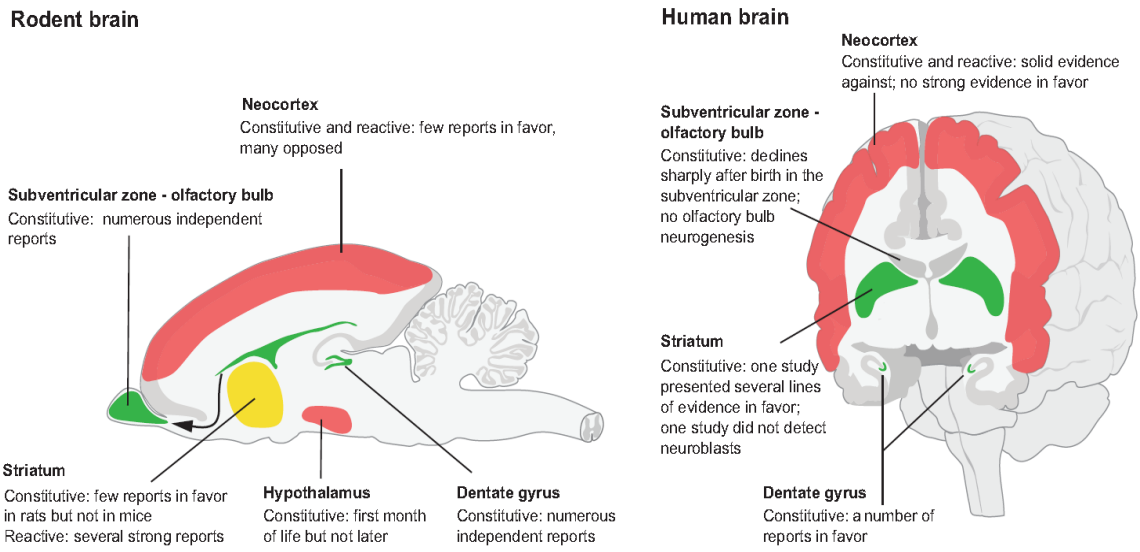

Figure 1.1. The main postnatal and adult neurogenic niches present in the mouse and human brain. Adapted after Magnsson and Frisén (Magnusson and Frisen, 2016).

1.1 Adult neurogenesis

Many reports described the two most important adult neurogenic niches in the rodent brain: the SVZ and the subgranular zone (SGZ) of DG (Bond et al., 2015). Recent studies also indicate neurogenic activity at the walls of the 3rd ventricle (Dietrich and Horvath, 2012; Lee et al., 2012). Furthermore, there are studies indicating the potential of other brain regions, non-neurogenic in normal conditions, which get activated and produce glial cells and neurons in certain circumstances. For example the striatal astrocytes were shown to have a latent stem cell potential and get activated after stroke leading to production of both glial cells and neurons (Magnusson et al., 2014).

1.1.1 Adult neurogenesis in the SVZ

The walls of the lateral ventricles in rodents are populated with several thousands of neural stem cells (NSC), also known as B1 cells (Fuentealba et al., 2015; Furutachi et al., 2015; Lim and Alvarez-Buylla, 2016). SVZ NSCs share many properties with astrocytes, for instance expression of the markers glial-fibrillary acidic protein (GFAP), glutamate aspartate transporter (GLAST), brain lipid-binding protein (BLBP) and sex determining region Y-box 2 protein (SOX2), but not of the astrocytic marker S100β (Doetsch et al., 1997; Lim and Alvarez-Buylla, 2016). However, they also express Nestin, a marker associated with neural stem cells (Doetsch et al., 1997). SVZ NSCs come in direct contact with the ventricle and are surrounded by ependymal cells forming a so-called ‘pinwheel structure’. NSCs extend an apical process that contacts the ventricle and a long basal process, which, similar to gray matter astrocytes, wraps around blood vessels (Lim and Alvarez-Buylla, 2016; Mirzadeh et al., 2008). SVZ NSCs are mostly quiescent, but can be activated by several factors, upon which they divide asymmetrically to self-renew and produce transit amplifying cells (TAC), also termed type C cells, which express mammalian achaete scute homolog-1 (Mash1) (Lim and Alvarez-Buylla, 2016). After about three symmetric divisions, TACs develop into neuroblasts (type A cells), which in turn divide one or two times in the RMS on

their migratory route towards the OB (Ponti et al., 2013a; Ponti et al., 2013b). Neuroblasts express doublecortin (DCX) and polysialylated neural-cell-adhesion molecule (PSA-NCAM) (Lim and Alvarez-Buylla, 2016). Ensheathed by astrocytes forming a network of interconnected paths in the RMS, they migrate in chains towards the OB (Doetsch et al., 1997; Lois et al., 1996). After reaching the OB, neuroblasts migrate radially to their final position where they differentiate into interneurons (Lim and Alvarez-Buylla, 2016).

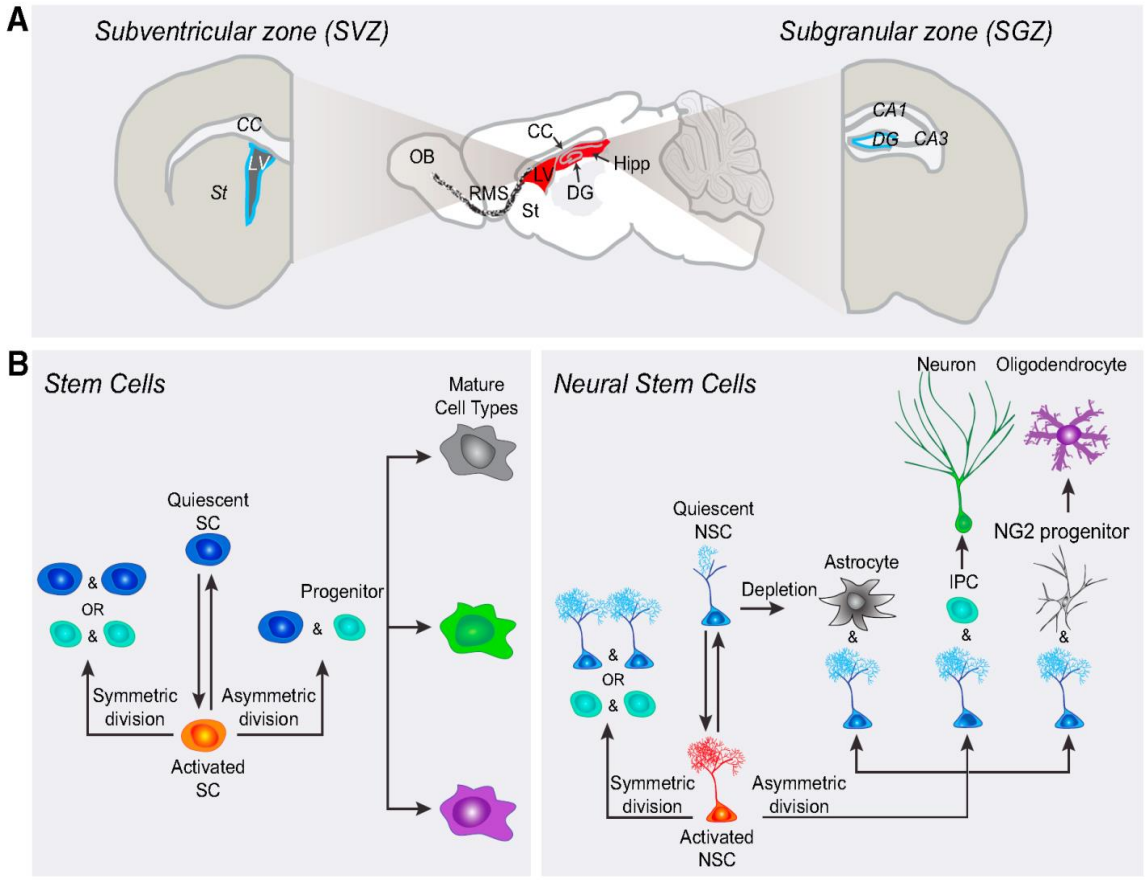

Figure 1.2. Main adult neurogenic regions in the mouse brain, i.e. the SVZ and the SGZ. (A) The SVZ and SGZ in coronal and sagittal sections in the mouse brain. (B) Neural progenitors and balance between the indicated cell types in the SVZ and SGZ. Adapted after Bond, Ming and Song (Bond et al., 2015).

SVZ NSCs were shown *in vitro* to produce cells belonging to both the neuronal and glial lineage thereby generating neurons, oligodendrocytes and astrocytes.

Furthermore, when co-cultured on support astrocyte monolayer, single stem cells formed colonies that comprised both neurons and glia, indicating that SVZ NSCs are multipotent (Menn et al., 2006). However, *in vitro* time-lapse experiments showed that acutely isolated SVZ progenitors produce either neurons or oligodendrocytes, but not both, and no astrocyte production was found (Ortega et al., 2013). *In vivo* clonal analysis from individual stem cells in SVZ showed only the generation of cells belonging to neuronal lineages. Furthermore, SVZ NSCs were shown to be short-lived and to get exhausted after several asymmetric divisions, indicating that the life-long generation of OB neurons is achieved at a population level, while individual SVZ NSCs have limited self-renewal capacity (Calzolari et al., 2015). Thus, single cell data both *in vivo* and *in vitro* indicate that the SVZ has a mosaic organization comprising a heterogeneous pool of stem cells that exhibit certain stem cell properties such as self-renewal and multipotency only at the population level (Chaker et al., 2016).

1.1.2 Adult neurogenesis in the SGZ

The SGZ is a thin layer of cells located between the granule cell layer of the DG and the hilus, and harbors a special and complex microenvironment that supports neurogenesis in the adult mammalian brain. NSCs populating this niche were thought to originate from the dentate neuroepithelium. According to this hypothesis, descendants of these progenitors, which produce granule cells during development, relocate to the SGZ and continue to produce granule cells also postnatally and in the adult (Goncalves et al., 2016b). However, a recent study showed that SGZ NSCs originate from a population of progenitors in the ventral hippocampus, and relocate to the dorsal hippocampus during late gestation (Li et al., 2013). SGZ NSCs (Type 1 progenitors) have a radial glia-like (RG-like) morphology, with the cell body residing in the SGZ and a long radial process extending through the granular cell layer into the molecular layer of the DG where it branches out extensively and forms a bushy tuft-like termination (Bond et al., 2015). Similarly to SVZ NSCs, SGZ NSCs express the glial markers GFAP, GLAST, BLBP, SOX2 and the stem cell marker Nestin, but do

not the astrocytic marker S100β (Kempermann et al., 2015). Furthermore, they extend end-feet processes to the elaborate vasculature in the niche and are strongly regulated by factors in the blood (Filippov et al., 2003; Kempermann et al., 2015). SGZ stem cells are mostly quiescent accounting for less than 5% of all proliferation in the SGZ, but can get activated and proliferate asymmetrically to self-renew and produce TACs (Type 2 progenitors) (Kempermann et al., 2004). Whether SGZ NSCs are capable of symmetric division, thereby expanding the stem cell pool, still is a matter of debate in the field.

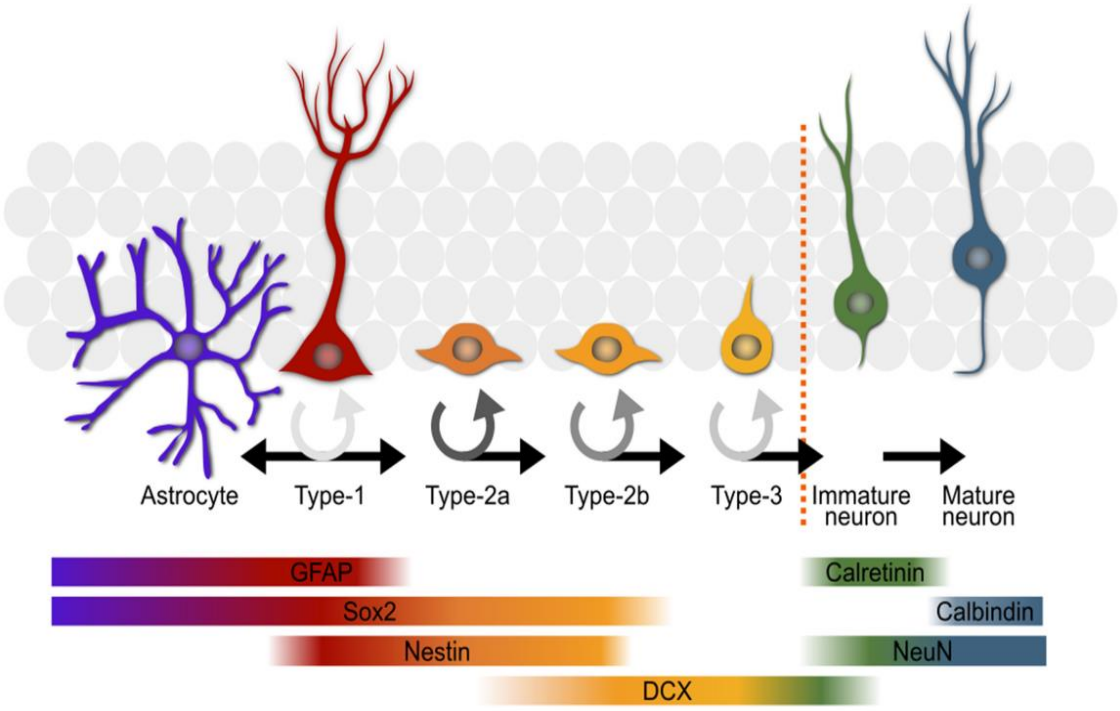

Figure 1.3. SGZ adult neurogenesis. The scheme presents SGZ neural progenitors and the most important markers used to identify them. Figure adapted after Overall and colleagues. (Overall et al., 2016).

According to Encinas and colleagues, upon activation stem cells rapidly undergo asymmetric division (on average three divisions) leading to self-renewal and TAC production. Apparently, a proportion of the activated, stem cells transform into astrocytes after several rounds of asymmetric division, and would thus account for the ensuing depletion of stem cells. The data of Encinas and colleagues indicate that SGZ

NSCs cannot undergo symmetric division, which would explain the decrease in the stem cell pool and in neurogenesis with age (Encinas et al., 2011). However, Dranovsky and colleagues used *in vivo* lineage tracing in the SGZ starting from the GFAP positive stem cells and found that certain cell lineages persist for long time in the DG and at the same time found an expansion of the stem cell pool, which would contradict the previous proposed model. Most interestingly these authors found that the ratio between stem cells and neurons is experience-dependent and the change is more pronounced in the dorsal versus the ventral blade of the DG (Dranovsky et al., 2011). Bonaguidi and colleagues used long term *in vivo* lineage tracing that allowed them to follow the progeny derived from single Nestin-positive RG-like NSCs. The authors found that SGZ NSCs undergo both asymmetric and symmetric self-renewal and are able to expand the stem cell pool. Furthermore, they found multiple clones comprising both neurons and astrocytes, but no oligodendrocytes (Bonaguidi et al., 2011). In the same study, the authors provide evidence that SGZ NSCs exhibit the two fundamental properties of stem cells, namely self-renewal and multipotency. Different experimental approaches and genetically modified mouse lines might account for the divergent conclusions and the derived models. Alternatively, in the studies mentioned above, different stem cell populations might have been targeted/studied (Bonaguidi et al., 2012). Indeed, similarly to the SVZ, different populations of NSCs co-exist in the SGZ. They might exhibit different regulatory mechanisms and functions (Gebara et al., 2016; Lugert et al., 2010).

A common characteristic of the presented models is that upon activation SGZ NSCs most often divide asymmetrically to produce a new stem cell and a TAC. TACs express SOX2, Mash1, T-box transcription factor Eomes (Tbr2) and are highly proliferative, leading to an expansion of the progenitor pool. They present different levels of specification and have been accordingly classified into Type 2a-1, Type 2a-2 (or Type 2ab) and Type 2b (or Type 3). Type 2a-1 cells are the most undifferentiated type, and like stem cells they express Nestin, SOX2, BLBP and GFAP (at early stages). They lack a radial process and present plump short process which are oriented horizontally (Kempermann et al., 2004). Type 2a-2 progenitors are BLBP- and GFAP-negative and continue to express SOX2 and low levels of Nestin. In addition, Type 2a-

2 progenitors express cell markers for immature cells such as Mash1 and Tbr2, which, by decreasing SOX2 expression, are essential for the transition from the stem cell towards the TAC stage. Furthermore, Type 2a-2 progenitors start to express NeuroD and Prox1, i.e. factors that are important in delineating the neuronal lineage and that are essential for the subsequent maturation of the cell. Type 2b cells are the most differentiated TACs. They begin to express DCX and PSA-NCAM, which are markers for young neurons, and exhibit noticeable processes (Kempermann et al., 2015). The transition between stem cells and TACS as well as between the different stages of TAC development, is not well-defined, as the down-regulation of some markers and the increasing expression of others overlap. Thus, there is a gradual transition from one stage to the other, and marker expression does not allow a clear-cut delineation of the different stages.

Early TACs are highly proliferative and are positive for the proliferation markers Ki67 and minichromosome maintenance complex component 2 (MCM2). They divide symmetrically to produce two other TACs, thus expanding the progenitor pool, or neuroblasts (Kempermann et al., 2015; Ming and Song, 2011). Three to four days after stem cell division, late Type b progenitors begin to differentiate into DCX-expressing neuroblasts. Neuroblasts express also calretinin, PSA-NCAM, NeuroD, Prox1, and at a later stage they begin to express the mature neuron marker NeuN. Neuroblasts can still divide but to a lesser extent than TACs. They have reached the last stage in the development of a progenitor on the way to a granule cell, bearing dendrites and an axon projecting to the CA3 region (Kempermann et al., 2015; Song et al., 2016).

1.1.2.1 Survival

Similarly to neurogenesis during development, many cells generated in the adult SGZ do not survive. Depending on the context, 30% to 70% progenitors survive two weeks after their generation (Ryu et al., 2016). Most SVZ-derived, postnatally-generated neurons die by apoptosis and are removed via phagocytosis by resident microglia (Sierra et al., 2010). This process is strongly regulated and has most likely

the role to assure that the right number of cells is integrated in the network. There are two important selection steps. Most cells die one to four days after birth, at the TAC stage or the transition stage between TAC and neuroblast (Ryu et al., 2016; Sierra et al., 2010). A second selection step takes place between two and four weeks after birth when the cells compete for synaptic input. The cells that manage to get integrated in the network survive while the ones that do not make enough connections die via apoptosis. However, the number of cells that perish during this second selection step is much lower than the large number of cells selected out at the stage of TAC (Kempermann et al., 2015; Sierra et al., 2010). Programmed cell death is a fundamental mechanism regulating the number of adult-born neurons, and thereby assuring that the 'right' cells that can contribute to the activity of the network survive and get integrated (Kempermann et al., 2015; Ryu et al., 2016).

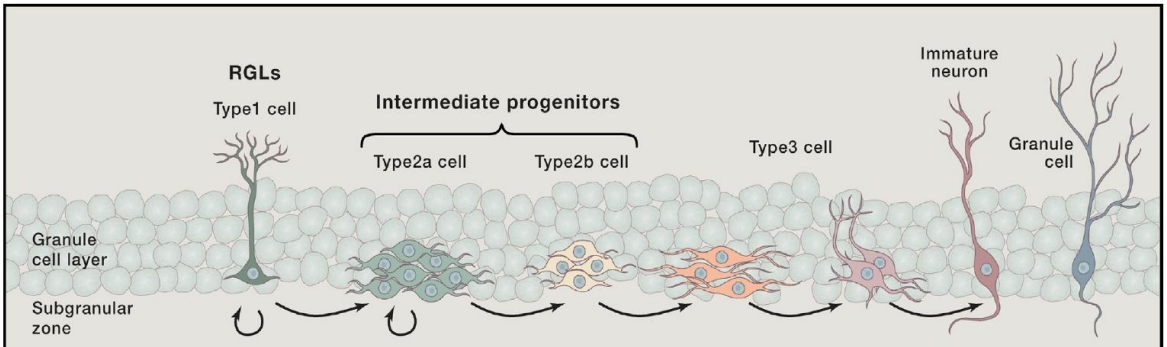

	Quiescence	Proliferation/ Activation	Fate specification	Morphogenesis and differentiation	Maturation
Signals	BMP, Notch, GABA	Canonical Wnt, IGF, Shh, FGF-2, EGF, Dopamine	Canonical Wnt, NT-3	Wnt/PCP, Notch, BDNF, Reelin, GABA	Glutamate, NRG2, Neuronal activity
Transcription factors	Hes5, FoxO, REST	Sox2, Tlx	Tbr2, Ascl1/Mash1, NeuroD1, Prox1	NeuroD1,Prox1, CREB, AP-1?	CREB
Epigenetic regulation		Gadd45b, LSD1	Fmrp, Mbd1	Gadd45b, MeCP2	MeCP2, HDAC2

Figure 1.4. Regulation of SGZ adult neurogenesis. The scheme presents SGZ neural progenitors and the most important factors regulating their activity. Figure adapted after Gonçalves and colleagues. (Goncalves et al., 2016b).

1.1.2.2 Differentiation

The first signs of neuronal fate become apparent already at three/four days after cell birth, i.e. the time point of transition from Type 2b progenitor to neuroblast. One week after birth, cells begin to express DCX and the calcium binding protein calretinin, and exhibit non-oriented dendritic processes (Goncalves et al., 2016b; Kempermann et al., 2015). Furthermore, at this stage, before full development of neurites, neuroblasts receive onto their soma the first input, which is GABAergic, and at this point in development excitatory in nature (Aguilar-Arredondo et al., 2015; Esposito et al., 2005; Zhao et al., 2006). As soon as four to ten days after cell birth, the axon extends through the hilus towards the CA3, and most fibers reach the CA3 region ten to eleven days after birth (Aguilar-Arredondo et al., 2015; Hastings and Gould, 1999; Zhao et al., 2006). After one and a half weeks, young neurons present prominent apical dendrites which extend in the molecular layer of the DG, and at two weeks they already show developed, however, still aspiny dendritic arborization and extensive GABAergic input (Esposito et al., 2005; Zhao et al., 2006). At this time, the chloride gradient is about to change. Thus, the decrease in expression of the Na^+-K^+-$2Cl^-$ transporter NKCC1 and the concomitant increase in expression of the K^+-coupled Cl^- transporter KCC2 determine that GABA receptor-mediated currents become hyperpolarizing and therefore inhibitory (Ge et al., 2006). At about two and a half weeks after birth, the first dendritic spines appear at a time when first glutamatergic/excitatory input from the medial entorhinal cortex (MEC) becomes evident. This step is also associated with the switch in the expression of calretinin to calbindin, a calcium binding protein specific for mature granule cells (Aguilar-Arredondo et al., 2015; Esposito et al., 2005; Kempermann et al., 2015).

Physiologically, one to seven days old cells are still silent and do not present postsynaptic responses even after stimulation. Starting with day eight after cell birth, the young developing neurons commence to have immature electrophysiological properties, generating only few action potentials upon current injection (Aguilar-Arredondo et al., 2015; Esposito et al., 2005). One month after birth the cells exhibit

both GABA receptor- and glutamatergic receptor-mediated responses and receive abundant glutamatergic afferents. Furthermore, they acquire an action potential threshold of -43mV and present spontaneous spiking activity with increasing frequency after stimulation of the local network or the perforant path (Aguilar-Arredondo et al., 2015; Esposito et al., 2005; Mongiat et al., 2009; van Praag et al., 2002). Between two and six weeks after birth, adult born neurons have distinct electrophysiological properties with a more depolarized resting membrane potential than mature granule cells and low input resistance. Furthermore, they have a lower LTP threshold indicating a high degree of plasticity. The enhanced plasticity of newborn neurons has been at least partially attributed to their transiently increased expression of the NR2B containing N-methyl-D-aspartate (NMDA) receptors. NR2B subunits are expressed more than NR2A subunits in the early postnatal brain. However, later in development, NR2A expression increases causing a switch in the NR2B-NR2A ratio in many brain regions, including the hippocampus (Ge et al., 2007; Monyer et al., 1994). NR2B subunits were shown to determine a longer opening of the NMDA channel. which plays an important role in controlling plasticity-associated changes (Fox et al., 2006; Matta et al., 2011; Zhuo, 2009).

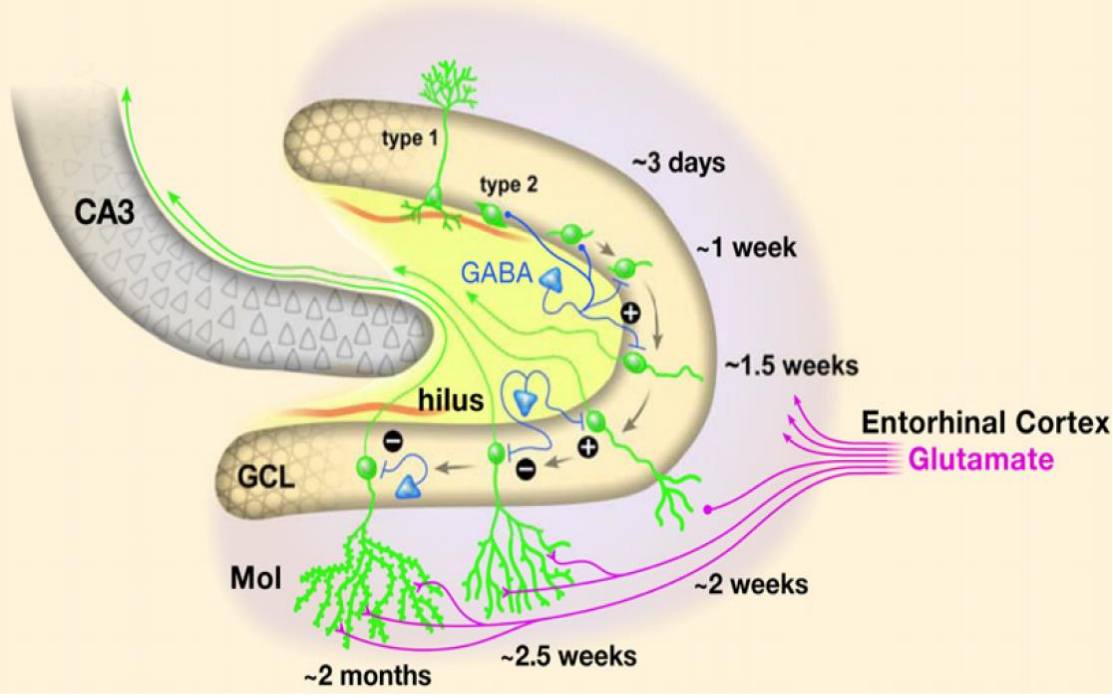

Figure 1.5. Morphological and physiological developmental stages in postnatal SGZ neurogenesis. The scheme presents the morphological and physiological changes undertaken by SGZ progenitors on their way to DG granule neurons. The progenitors first receive GABAergic input (blue) followed by the glutamatergic input (pink). Figure adapted after Gonçalves et al. (Goncalves et al., 2016b).

By eight weeks after birth, new-born neurons are completely integrated in the network and have reached a maturation level at which the morphological and electrophysiological properties are indistinguishable from the ones of granule cells generated during development (Aguilar-Arredondo et al., 2015; Esposito et al., 2005; van Praag et al., 2002). The developmental stages of adult-born neurons appear to be akin to those of granule cells that are generated perinatally, indicating that they follow a cell-autonomous program rather than being influenced by local or external cues (Esposito et al., 2005). However, the speed of differentiation is slower in adult neurogenesis, and it seems to further decrease with age, indicating that the differentiation of adult born neurons is influenced by the environment and not the activity of the local network (Rao et al., 2005; Riddle and Lichtenwalner, 2007).

1.1.3 Adult neurogenesis in the 3rd ventricle

While neurogenesis in the adult SVZ and SGZ has been well characterized, adult neurogenesis in other brain regions has remained controversial. Several recent studies reported the presence of adult neurogenesis in the walls of the 3rd ventricle (Lee et al., 2012; Xu et al., 2005). Lining the walls of the 3rd ventricle there is a population of cells called tanycytes (‘cells with drawn out process’) that have a similar morphology to radial glia (Goodman and Hajihosseini, 2015). They are present in the ventral hypothalamic ventricular region and have long radial processes, some of which extend to the hypothalamic nuclei regulating appetite and energy metabolism. Like SVZ NSCs, tanycytes have contact with the cerebrospinal fluid in the ventricle and have access to the factors in the blood through fenestrated local capillaries. Furthermore,

they express stem cell markers like Nestin and SOX2 (Goodman and Hajihosseini, 2015; Lee et al., 2012). Based on of BrdU incorporation and viral infection studies, tanycytes were shown to proliferate and produce progenitors that migrate in the median eminence and generate local neurons, which in turn integrate in the local network and become functional (Lee et al., 2012; Xu et al., 2005). The data obtained by Lee and colleagues (2012), indicates that overfeeding in adult mice induces an increase in neurogenesis in the median eminence. Furthermore, the authors showed that following a high fat diet, new-born neurons contribute to a reduction in baseline energy consumption and in energy storage in form of fatty acids and glycerides (Kokoeva et al., 2005; Lee et al., 2012). The discovery of adult neurogenesis in the hypothalamus revealed not only a new neurogenic niche, but also a new function for adult neurogenesis, raising the question as to the presence of yet other neurogenic areas in the adult brain which have been overlooked because of the low number of newly generated neurons (Magnusson and Frisen, 2016; Magnusson et al., 2014).

1.2 External factors influencing adult neurogenesis

Among the most important functions of the mammalian brain is its ability to adapt quickly to external circumstances to assure survival and reproduction of the organism. Indeed, the mammalian brain is extremely plastic and supports adaption (Lledo et al., 2006). A most remarkable feature of the mammalian brain is its plasticity, i.e. the ability to adapt quickly to changes in the environment. As a result of a previous experience, new synapses are formed and existing ones are modified, which will affect the way new information is processed (Green and Bavelier, 2008). Adult neurogenesis represents a whole new level of plasticity in the adult brain offering the possibility to change the pre-established neuronal networks by the addition of new cells that are more plastic, at least initially, compared to neurons generated during embryogenesis (Goncalves et al., 2016b; Lledo et al., 2006). The increased plasticity of adult-born neurons and the ease with which they can be recruited makes them highly suitable to change preexisting DG neuronal networks.

1.2.1 Adult hippocampal neurogenesis after enriched environment and voluntary physical exercise

Adult neurogenesis is not only a source of plasticity but is itself modulated by external factors. The dynamics of neurogenesis in both SVZ and SGZ are under the influence of the environment and were proposed to adapt the number of neurons to the necessities of the local network (Lledo et al., 2006). Adult SVZ neurogenesis plays an important role in olfactory discrimination and in olfactory memory formation. Olfactory enrichment was shown to increase the number of adult-born neurons in the OB by increasing cell survival (Lledo et al., 2006). Adult hippocampal neurogenesis supports several hippocampus-dependent functions such as the balance between pattern separation and pattern integration to avoid memory interference, temporal encoding of memories, cognitive flexibility for learning new tasks and context-dependent memory formation (Goncalves et al., 2016b). In adult DG, the dynamics of neurogenesis and the fate specification of progenitor cells were shown to be regulated by the environment (Dranovsky et al., 2011). The best described external factors found to regulate adult neurogenesis are environmental enrichment (EE) and physical exercise (Vivar et al., 2013). Both voluntary as well as forced running were shown to improve spatial memory in tasks like the Morris water maze, the T-maze, the Y-maze and the radial arm maze. Furthermore, running was also shown to improve the performance in tasks that do not require spatial navigation like novel object recognition, passive avoidance, and contextual fear conditioning (Vivar et al., 2013). First evidence that EE and physical activity influence adult neurogenesis was brought by Kempermann and colleagues (1997). They found that housing mice in an EE with free access to running wheels had a pro-proliferative effect, leading to an increase in the number of adult-born neurons in the SGZ, which subsequently enhanced the performance of the mice in the Morris water maze (Kempermann et al., 1997). Later studies separated EE from running and found that both have a pro-neurogenic effect but influence neurogenesis at different levels. Most of the increase in neuron production was found to be induced by physical exercise. Housing mice or rats with free access to running wheels leads to a

two to threefold increase in SGZ cell proliferation, which is the strongest pro-proliferative effect at the level of TACs (Kronenberg et al., 2003; van Praag et al., 1999). Furthermore, physical exercise also enhances the activation and proliferation of SGZ NSCs (Dranovsky et al., 2011; Gebara et al., 2016). The higher number of adult-born neurons produced following physical exercise is associated with an increase in synaptic plasticity in DG and a better performance in spatial memory tasks such as the Morris water maze. Experiments testing the effect of EE devoid of running wheels showed that environmental enrichment also has a pro-neurogenic effect. However, this setting does not influence the proliferation of progenitors (Olson et al., 2006; van Praag et al., 2000), but enhances the survival and the development of TACs and neuroblasts. Furthermore, DG adult-born neurons in mice housed in EE showed increased dendritic complexity and higher synaptic plasticity. Therefore, adult DG neurogenesis is responsive to both physical exercise and to EE (Goncalves et al., 2016b; van Praag et al., 2000). Furthermore, enriched odor exposure resulted in an increase in adult SVZ neurogenesis and ultimately in more neurons that integrated in the OB (Rochefort et al., 2002; Vivar et al., 2013). Together, these changes in the environment lead to a strong increase in neuron production both neurogenic niches and to an increase in the complexity and connectivity of the new neurons adapting local neuronal networks to new challenges of the environment (Goncalves et al., 2016a; Lledo et al., 2006). An enriched environment would mean more space to be explored but also to be remembered. As indicated above, increased neurogenesis would support better pattern integration in the hippocampus or smell discrimination and memory in the OB. enabling mice to remember more details of their environment and differentiate better similar situations, rendering them maybe more successful in the search of food or in the avoidance of predators.

1.2.2 Factors proposed to support stimulus-induced adult neurogenesis

One of the most important questions in the field of adult neurogenesis concerns the mechanisms that regulate the stem cell niches. In spite of the vast literature regarding the effect of EE and physical exercise on adult neurogenesis, very little is known about the mechanisms mediating these effects. A first possible mechanisms pertains to factors provided by the vasculature in the niche (Vivar et al., 2013). It has been shown that running caused an increase in the DG microvasculature. Furthermore, both SGZ and SVZ stem cells are strongly associated with blood vessels and are regulated by circulating factors (Fabel et al., 2003; Palmer et al., 2000). However, in old mice voluntary exercise still led to an increase in adult SGZ neurogenesis which was not mirrored by an increase in the DG vasculature indicating that this mechanism alone cannot account for the pro-neurogenic effect of physical exercise (van Praag et al., 2007; Vivar et al., 2013). It was also observed that running was associated with an increase in circulating neurotrophic factors, which were produced most likely by the musculature (Overall et al., 2016; Vivar et al., 2013). Furthermore, for many neurotrophic factors increased expression was observed also in the adult neurogenic niches. Among the best documented and most important are brain derived neurotrophic factor (BDNF), fibroblast growth factor 2 (FGF-2), nerve growth factor (NGF), vascular endothelial growth factor (VEGF) and insulin growth factor (IGF) (Vivar et al., 2013). Running increased the expression of these factors in the hippocampus, the most pronounced being BDNF, which was expressed specifically in the DG, but not in the CA1 region (Berchtold et al., 2005; Berchtold et al., 2002; Farmer et al., 2004). Infusion of these factors augmented SGZ neurogenesis by increasing proliferation, survival and maturation of adult-born neurons (Vivar et al., 2013). This effect is especially prominent for BDNF. Its overexpression (OE) in the DG mimicked the effect of running, leading to an increase in neurogenesis, synaptic plasticity and an improvement in the Morris water maze (Scharfman et al., 2005). Knocking down (KD) or blocking neurotrophic factors had the opposite effect (Taliaz et al., 2010).

Furthermore, blocking BDNF and VEGF signaling prevented the increase in proliferation induced by running, indicating that these factors mediated this effect at least in part (Clark et al., 2009; Li et al., 2008). However, these factors have a multitude of cellular functions and so far there is no causal effect linking them to neurogenesis (Vivar et al., 2013).

There is good evidence that GABA signaling is an important determinant supporting stimulus-induced neurogenesis in the niche is. GABA is present in both neurogenic niches and plays important roles in regulating neurogenesis at multiple levels. Both in the SVZ and SGZ, GABA regulates the activation and proliferation of stem cells (Liu et al., 2005; Song et al., 2014; Song et al., 2016). At the level of the SGZ, GABA regulates also the survival and development of TACs and neuroblasts (Song et al., 2013). The source of GABA are local PV-positive interneurons. These cells are connected to DG granule cells and are modulated by the physical activity of the animal (Hu et al., 2014). GABA released from PV-positive interneurons could provide information to the stem cell niche regarding the degree of local network activity, that in turn reflects the animal's activity (Song et al., 2014; Song et al., 2016). Notably, optogenetic inhibition of PV-positive interneurons canceled the EE-mediated survival effect (Song et al., 2013). Thus, GABA signaling is a strong candidate for mediating external changes to the neurogenic niches. However, a large body of literature shows that the regulation of the neurogenic niches is complex. There are most likely several mechanisms and many players, some of which may be redundant, that regulate neurogenesis in defined situations.

1.3 GABA and adult neurogenesis

1.3.1 GABA and GABAergic receptors

Gamma-aminobutyric acid (GABA) is the main inhibitory neurotransmitter in the mammalian brain. GABA is present in a large and heterogeneous population of

neurons, many of which project locally (interneurons). GABAergic neurotransmission is essential in modulating and synchronizing neuronal networks (Mann and Paulsen, 2007). GABA is produced by glutamic-acid decarboxylase mediated decarboxylation of glutamate (Awapara et al., 1950; DeFelipe et al., 2013; Feldblum et al., 1993). GABA is generated in the cytoplasm of GABAergic neurons and is taken up into vesicles at the axon terminals (Farrukh et al., 1998; McIntire et al., 1997; Roth and Draguhn, 2012). Action potentials reaching the axon terminals induce Ca^{2+} influx which triggers the release of GABA into the synaptic cleft (Levy et al., 1973; Suudhof, 2008). GABA can bind to synaptic receptors thus exerting a phasic action, but it can also diffuse rapidly from the synaptic cleft and activate extrasynaptic receptors thereby exerting a tonic action. Excess GABA is taken up by surrounding astrocytes (Minelli et al., 1995; Minelli et al., 1996; Stell and Mody, 2002). The effect of GABA depends on the type of receptor it binds to and on the intracellular Cl^- concentration. There are two classes of GABA receptors, namely ionotropic $GABA_A$ receptors, which are ligand-gated ion channels, and metabotropic $GABA_B$ receptors, which are G protein-coupled receptors (Nicoll and Alger, 1979). $GABA_A$ receptors are heteropentameric proteins that can have in their composition 19 potential subunits: α1-6, β1-3, γ1-3, δ, ε, θ, π and ρ1-3 (Cutting et al., 1991; Davies et al., 1997; Hadingham et al., 1993; Hedblom and Kirkness, 1997; Jin et al., 2004; Moragues et al., 2000; Olsen and Sieghart, 2009; Schofield et al., 1987; Schofield et al., 1989; Sibbe and Kulik, 2016; Whiting et al., 1997; Yang et al., 1995; Ymer et al., 1989a; Ymer et al., 1989b; Ymer et al., 1989c). The subunit composition of the receptor determines the subcellular localization, conductance, kinetics and pharmacology (Sibbe and Kulik, 2016). $GABA_A$ receptors are ion channels permeable both for Cl^- and $HCO3^-$ (bicarbonate) ions. GABA has an equilibrium potential of approximately -70mV, close to the membrane resting potential in neurons (Olsen and Sieghart, 2009). Mature neurons express the K^+-coupled Cl^- transporter KCC2, which exports Cl^- ions from the cell, leading to a lower intracellular Cl^- concentration. Binding of GABA to the receptor determines an influx of Cl^- into the cell, which leads to a hyperpolarization of the cell membrane. Thus, in mature neurons GABA acts as an inhibitory neurotransmitter. Neural progenitors and young neurons express the Na^+-K^+-$2Cl^-$ transporter NKCC1, and have a higher Cl^- intracellular

concentration compared to the extracellular space (Ge et al., 2006). Hence GABA is depolarizing when binding to the $GABA_A$ receptor in immature neurons. During neuronal maturation the expression of NKCC1 decreases while KCC2 starts being expressed, leading to a reversion of the chloride gradient and as a consequence to a switch from a depolarizing, activatory GABA action to a hyperpolarizing, inhibitory action (Ge et al., 2006; Kaila et al., 2014). $GABA_A$ receptors are localized both synaptically and extrasynaptically. The former are activated by high GABA concentrations released into the synaptic cleft and generate fast inhibitory postsynaptic currents (IPSCs), thus governing phasic GABA inhibition (Brickley et al., 1999; Kullmann et al., 2005). Extrasynaptic $GABA_A$ receptors are present peri- and extrasynaptically. These receptors are activated by GABA spilled over from nearby synapses and they mediate tonic inhibition. Phasic and tonic GABAergic inhibition support different functions in the course of neurogenesis. For example, tonic inhibition in stem cells has an anti-proliferative effect, while phasic inhibition in TACs promotes survival (Song et al., 2002; Song et al., 2013). GABA receptors containing α1, α2 and γ2 subunits are often present at the synapse and mediate phasic inhibition, while receptors containing α5 and δ are often extrasynaptically localized and mediate tonic inhibition (Charara et al., 2005; Farrant and Nusser, 2005; Passlick et al., 2013).

Metabotropic $GABA_B$ receptors are coupled to guanosin triphosphate (GTP)-binding proteins (G proteins) and are responsible for mediating slow effects. GABA binding leads to a conformational change of the receptor, which is transmitted to the G_α subunit of the G protein, leading to the exchange of GDP for GTP (Bettler et al., 2004; Ulrich and Bettler, 2007). The GTP bound G_α subunit then dissociates from the other two subunits of the G protein, the β and γ subunit. G_α subunit can activate phospholipase C or inhibit the enzyme adenylyl cyclase, which reduces the levels of secondary messenger cyclic adenosine monophosphate (cAMP), this in turn leads to the inactivation of the cAMP dependent protein kinase A (PKA). The two pathways activated by G_α are some of the most important cellular signalling hubs and can regulate different processes like protein expression vesicle priming, modulation of the activity of different ion channels, etc. (Franek et al., 1999; Rosenbaum et al., 2009). Furthermore, the $G_{\beta\gamma}$ subunit can itself regulate ion channel gating and several other

cellular processes. $GABA_B$ receptors are heteromultimeric receptors associated with auxiliary proteins that regulate the subcellular localization, the kinetics and pharmacology of $GABA_B$ receptors. They can be present both pre- and the postsynaptically. Presynaptic $GABA_B$ receptors inhibit neurotransmitter release by negatively modulating voltage-activated Ca^{2+} channels, while postsynaptic receptors lead to formation of slow IPSPs. $GABA_B$ receptors are essential for many important brain processes such as learning, cognition, anxiety and have been shown to modulate adult neurogenesis (Fritschy et al., 1999; Jones et al., 1998; Rosenbaum et al., 2009).

1.3.2 $GABA_A$ receptors and benzodiazepines

GABA binds to the $GABA_A$ receptor at the GABA binding site situated extracellularly at the interface between the α and the β subunit. Most $GABA_A$ receptors comprise two α and two β subunits and have two GABA binding sites (Krall et al., 2015; Sieghart, 2015). Biding of GABA to one site can open the channel, however, occupation of both binding sites enhances greatly the opening probability (Baumann et al., 2003). Furthermore, the effect of GABA after binding to the site has been shown to be influenced by the flanking subunits present in the composition of the channel. Besides the well characterized binding site of the GABA between the α and the β subunits there are data indicating the presence of another GABA binding site at the interface of the δ subunit in the receptors containing it (Sieghart, 2015).

$GABA_A$ receptors present several other binding sites and can be modulated by numerous ligands which leads to a very complex pharmacology (Sieghart, 2015). Many binding sites are present at the interface between two subunits of the pentameric receptor, and the subunit composition determines whether a ligand can bind and exert its action or not (Krall et al., 2015; Sieghart, 2015). Among the best characterized molecules that modulate the activity of $GABA_A$ receptors are barbiturates, benzodiazepines, steroids, anaesthetics, alcohol, cannabinoids and picrotoxin, which all act as allosteric modulators of the channel (Sieghart, 2015). Benzodiazepines, among the best known is diazepam, were first introduced in clinics in the 1960s and are used

mostly for their sedative, anxiolytic and anticonvulsant effects (Farzampour et al., 2015; Sieghart, 2015). Based on the crystal structure of the $GABA_A$ receptor with bound diazepam, the benzodiazepine binding site has been mapped to the extracellular part of the receptor at the interface between the α and the γ subunit (Buhr and Sigel, 1997). Binding of benzodiazepines modulates the receptor allosterically and causes an increase in GABA binding affinity and in channel opening frequency, which leads to a change in $GABA_A$ receptor mediated currents (Baur and Sigel, 2005; Bianchi, 2010; Bianchi et al., 2009; Buhr et al., 1997; Macdonald and Barker, 1978). $GABA_A$ receptors comprising the subunits α1, α2, α3 and α5 are sensitive to benzodiazepines, while the receptors containing the subunits α4 and α6 are insensitive (Rudolph and Mohler, 1999). Subunits α1, α2, α3 and α5 contain a conserved histidine residue at position 101, 101, 126, and 105, respectively, which are essential for benzodiazepine binding. In contrast, receptors containing the α4 and α6 subunits that are insensitive to benzodiazepines as they have an arginine residue at the corresponding position (Rudolph and Mohler, 1999). Furthermore, mutations of histidine 101 in α1, renders the respective $GABA_A$ receptors insensitive to benzodiazepines (Rudolph et al., 1999; Wieland et al., 1992). Using chimeric α_1 and γ_2 subunits, two domains of the γ_2 subunit were identified which are necessary and sufficient for the high affinity binding at the benzodiazepine binding site, namely Lys 41 - Trp 82 and Arg 114 – Asp161 (Kucken et al., 2000; Sieghart, 2015). An aminoacid residue which was shown to be important for binding at the benzodiazepine binding site is phenylalanine 77 on the γ_2 subunit (γ_2 F77). Mutations at this site (F77I γ_2) leads to a drastic decrease or even abolishment in binding of most benzodiazepines (Buhr et al., 1997; Buhr and Sigel, 1997).

The before mentioned site is the most important for high affinity benzodiazepine binding at the $GABA_A$ receptor. However, other binding sites were also described. Diazepam was shown to bind also to a lower affinity site, which is responsible for its anaesthetic properties (Krall et al., 2015; Sieghart, 2015). Diazepam and some benzodiazepines bind furthermore to a third site located extracellularly at the interface between the α and the β subunit in the position homologous to the classical high affinity benzodiazepine binding site (Sieghart, 2015). Furthermore, crystal structures of the $GABA_A$ receptor with bound benzodiazepines indicated the presence

of yet other binding sites. Binding to these sites has, in most cases, similar effects as binding to the classical site, namely allosteric modulation of the $GABA_A$ receptor (Baur et al., 2008; Ramerstorfer et al., 2010; Sieghart, 2015; Spurny et al., 2012; Walters et al., 2000). Crystallographic studies using $GABA_A$ receptors and various benzodiazepines showed that the binding sites of benzodiazepines and their action on these sites depends strongly on the structural characteristics of the individual subunits and therefore on the subunit composition of the channel (Sieghart, 2015).

1.3.3 The regulatory role of GABA in adult neurogenesis

Adult neurogenesis is regulated by multiple factors, of which GABA plays a major role. In both the SVZ and SGZ neural stem cells express $GABA_A$ receptors (Liu et al., 2005; Song et al., 2012). In the SVZ, GABA produced by neuroblasts and released by terminals of striatal neurons bind to $GABA_A$ receptors on the surface of stem cells and reduce their proliferation (Liu et al., 2005; Young et al., 2014). Also in the SGZ, stem cells bearing $GABA_A$ receptors are responsive to GABA (Song et al., 2012). $GABA_A$ receptors in SGZ stem cells were shown to express predominantly the subunits α_5, β_3 and γ_2. SGZ NSCs show no spontaneous or evoked synaptic currents in response to field stimulation of the DG (Song et al., 2012). However, Song and colleagues showed the presence of GABA responses in SGZ NSCs and the currents were enhanced by inactivating the GABA reuptake transporter GAT1, indicating GABA spill-over from nearby synapses. The GABA currents recorded from SGZ NSCs are potentiated by diazepam indicating the presence of γ_2 subunits in the $GABA_A$ receptors (Song et al., 2012). Diazepam administration reduced significantly the proliferation of SGZ NSCs promoting their quiescence. Conditional knockout of the γ_2 subunit in stem cells reduced their responsiveness to activation and increased the production of stem cells and glial cells. This phenotype was not rescued by diazepam administration, indicating a direct involvement of the γ_2 subunit in $GABA_A$ receptor regulating quiescence and fate choice of SGZ NSCs (Song et al., 2012). The authors identified parvalbumin-positive local interneurons as the source of GABA. They found

close associations between SGZ NSCs and PV-positive neurons. Optogenetic activation of PV-positive interneurons led to GABA receptor-mediated responses in stem cells and to a decrease in stem cell proliferation, similar to the effects found subsequent to diazepam treatment (Crowther and Song, 2014; Song et al., 2012).

Four days after SGZ retroviral injection, the labelled progenitors include TACs and DCX-positive neuroblasts. Whole cell recording in acute slice showed that 95% of the four days old SGZ progenitors are responsive to GABA. At this age SGZ progenitors have postsynaptic currents after 5 Hertz but not after 0.1 Hertz field stimulation, suggesting the presence of immature synapses (Song et al., 2013). Immuno-electron microscopy revealed symmetric synaptic contacts between PV-positive axon terminals and new-born progeny, suggesting the PV-positive neurons as a possible source of GABA for SGZ progenitors. Optogenetic activation of DG PV-positive neurons led to the appearance of GABAergic postsynaptic currents in the new-born cells and to an increase in their survival and development (Song et al., 2013). Four days old SGZ progenitors, namely TACs and neuroblasts, express at high levels the Cl^- transporter NKCC1 (in contrast to mature cells which express at high levels the Cl^- transporter KCC2). High NKCC1 expression levels determine a high intracellular Cl^- concentration in the young progenitors compared to mature granule cells. Thus, GABA has a depolarizing effect in the four days old progenitors and enhances their survival. At approximately two weeks after birth the progenitors decrease NKCC1 expression and start to express KCC2, which leads to a reversal in the Cl^- gradient. Thereafter, GABA has a hyperpolarizing effect and is inhibitory (Ge et al., 2006).

Thus, GABA provides at the level of the SGZ a ‘diametric regulation’ of stem cell proliferation and of TAC and neuroblast survival which could serve several roles (Song et al., 2016). One can envisage a situation when the activity of the DG is high. Consequently the activity of PV-positive interneurons will also be high leading to an increased survival of TACS and neuroblasts, and eventually and enhanced number of neurons in the network. At the same time, the increase in PV-positive interneuron activity would keep stem cells quiescent and preserve them for later usage. In contrast, when DG activity is low, GABA release from PV-positive interneurons would also be low and the short-term effect would be decreased cell survival. At the same time,

reduced GABA release would lead to an increase in the activation of stem cells and hence future activity in the DG would occur in a network with an increased stem cell pool (Song et al., 2014; Song et al., 2016).

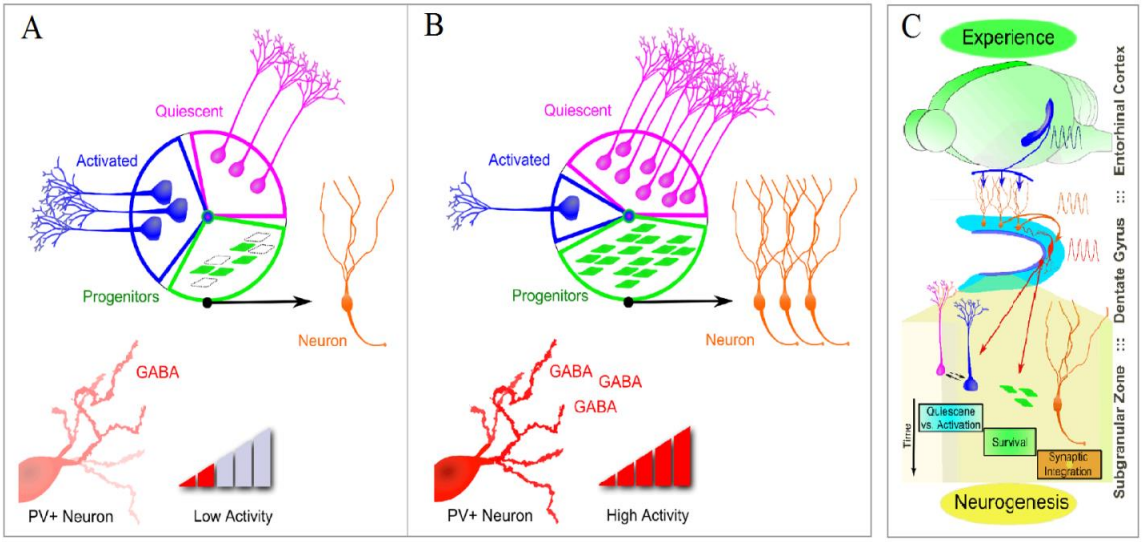

Figure 1.6. Diametric regulation of stem cell proliferation and of TAC and neuroblast survival. (A) Decreased network activity leads to reduced GABA release from the PV-positive neurons which determines an increase in stem cell activation and proliferation but a decrease in the survival of Type 2b TACs and neuroblasts. (B) Increased network activity leads to enhanced GABA release from the PV-positive neurons which determines a decrease in stem cell activation and proliferation but an increase in the survival of the Type 2b TACs and neuroblasts. (C) Experience leads to modifications in the activity of the DG network which are translated in differences in GABA release. GABA regulates SGZ neurogenesis at multiple levels and has been proposed to mediate the effects of external experience on the dynamics of the stem cell niche. Figure adapted after Song et al., 2014 (Song et al., 2013; Song et al., 2012).

The regulation provided by GABA in the SGZ might be well suited to 'time-stamp' adult-born neurons. DG postnatal neurons were proposed to play a role in temporally linking events that take place in close time proximity. As young neurons go through a window of enhanced plasticity, they will very likely respond even to low DG stimulation. However, as they become less plastic, and responsive with time, they

would exhibit sparse coding akin to adult granule cells. Hence adult-born neurons might serve to link events that take place close in time by participating in the memory engrams of these events. The regulation of the niche by GABA could determine an increase in the number of neurons produced at a given time point, and at the same time would inhibit or decrease the production of adult-born neurons immediately after that event, which would lead to a better temporal coding of the event (Song et al., 2014; Song et al., 2016). DG PV-positive interneurons receive direct excitatory input from granule cells and their activity is thus an indicator of the activity in the local DG network. Moreover, GABA regulates neurogenesis at multiple levels. Thus, GABA was proposed to couple the activity of the local network to the dynamics of the stem cells niche thereby affecting SGZ neurogenesis in response to changes in the environment (Song et al., 2014; Song et al., 2016). EE has a strong impact on SGZ neurogenesis leading to an increase in survival and in the development of TACs and neuroblasts. Silencing the activity of PV-positive interneurons while the animals are subjected to EE practically abolishes the increase in survival normally found after environmental enrichment (Song et al., 2013). This indicates that GABA released from PV-positive interneurons are likely to link environmental enrichment, local activity of the DG network and survival of adult-born neurons (Song et al., 2014).

1.4 Diazepam binding inhibitor (DBI)

1.4.1 DBI and its cleavage products

After the discovery of the benzodiazepine binding site on the $GABA_A$ receptor, an intensive search started for the presence of endogenous benzodiezepines, i.e. endozepines. The best known example so far is diazepam binding inhibitor (DBI). DBI is a 87 aminoacid, 10 kDa protein discovered in the rat brain which was found to displace radioactive diazepam from whole brain membrane preparates (Costa and Guidotti, 1991; Farzampour et al., 2015; Guidotti et al., 1983). In humans 10 low-

abundance DBI isoforms were identified and were shown to have a tissue-specific distribution (Ludewig et al., 2011a; Ludewig et al., 2011b; Nitz et al., 2011). In mammals, DBI is expressed at low levels in most cell types in the body (Sandberg et al., 2005). Higher expression was found in the brain and in tissues with intense metabolic activity such as kidney, heart, skeletal muscle, and liver (Bovolin et al., 1990). High DBI expression was also found in tissues important for the production of steroid compounds, such as testes and ovaries (Bovolin et al., 1990). In the nervous system, DBI is expressed at intermediate levels in astrocytes, in Bergmann glia, in ependymal cells and also in a restricted population of neurons in the thalamus (Christian et al., 2013). The highest expression level of DBI is in the DG, RMS, SVZ, in the ependymal layer lining the walls of the third ventricle, in area postrema, in the cerebellar cortex, in hypothalamus, in amygdala and in certain regions of the thalamus and of the cerebral cortex. Intermediate DBI levels were found in OB, in pontine nuclei, in inferior colliculi, in the arcuate nucleus and in the pineal gland (Alfonso et al., 2012; Alho et al., 1989; Alho et al., 1985; Alho et al., 1991; Alho et al., 1995). DBI expression is regulated by multiple factors. The DBI promoter presents binding sites for several transcription factors with different functions: Activator protein-1 and 2 (AP-1/2), specificity protein 1 (SP1), EGFR-specific transcription factor (ETF), Y-box binding protein; nuclear factor 1 (NF1), CCAAT/enhancer binding protein (C/EBP), hepatocyte nuclear factor 3 (HNF3), peroxisome proliferator response element (PPREs), and others (Elholm et al., 1996; Farzampour et al., 2015). The DBI promoter also comprises the glucocorticoid response element GRE and the steroid response element SRE (Sandberg et al., 2005; Swinnen et al., 1998). A survey of these factors and their functions prompts a putative function for DBI in cell proliferation and cell metabolism (Farzampour et al., 2015).

DBI was found not only in mammals, but in all eukaryotes tested from yeast to mammals and it is highly conserved across species (Gray et al., 1986; Lihrmann et al., 1994; Mocchetti et al., 1986; Owens et al., 1985, 1986). Using yeast genetics, the DBI orthologue Acb1 was found to be secreted via an unconventional mechanism mediated by autophagosomes, namely exophagy (Duran et al., 2010). Further studies showed that rat brain astrocytes secrete DBI through a non-conventional secretory pathway, an

autophagy activated mechanism similar to the one described in yeast (Loomis et al, 2010). DBI secretion from cultured astrocytes is controlled by various factors, indicating multiple regulatory mechanisms. Steroid hormones, elevated K^+ concentrations, PAC1-R ligands, urotensin-II and β-amyloid increase DBI secretion while activation of $GABA_B$ receptors and somatostatin (SOM) have an opposite effect (Ferrarese et al., 1987; Jarry et al., 2010; Loomis et al., 2010; Masmoudi et al., 2003; Masmoudi et al., 2005; Qian et al., 2008; Tokay et al., 2008).

Together with DBI several cleavage products were isolated and characterized: triakontatetraneuropeptide (TTN, DBI 17-50), octadecaneuropeptide (ODN, DBI 33-50) and octapeptide (OP, DBI 43-50). TTN is 34 aminoacids long, ODN 18 and OP 8 (Ferrero et al., 1986). There are no in depth studies addressing the question whether DBI is cleaved intra- or extracellularly. Also the identity of the enzymes responsible for DBI cleavage has remained elusive. DBI itself comprises several putative endoprotease sites and might be capable of self-cleavage and self-activation (Farzampour et al., 2015). Both DBI and all its cleavage fragments have the ability to displace benzodiazepines from the benzodiazepine binding site and are therefore considered endozepines. However, only DBI and ODN bind with high affinity to the $GABA_A$ receptor (Ki=4µM measured via displacement of $_3H$-diazepam) (Bormann, 1991; Costa and Guidotti, 1991; Mohler, 2014). DBI was found to displace radioactivily marked benzodiazepines and it was therefore inferred that it occupies the same site on the $GABA_A$ receptor. Experiments in mouse embryonic spinal cord neurons showed that DBI alone does not induce GABA receptor-mediated currents or any other type of currents. However, micromolar concentrations of the protein reduced GABA receptor-mediated Cl^- currents measured by whole cell path clamp recordings. This effect was dose dependent at concentrations between 1 and 10 µM DBI and was inhibited by Flumazenil, a synthetic benzodiazepine (Bormann, 1991). Further studies clearly showed that DBI and its cleavage products ODN bind to the benzodiazepine binding site of the $GABA_A$ channel. Their binding not only displaces other benzodiazepines, but also induces allosteric modifications of the receptor that leads to a reduction in GABA-receptor induced currents (Costa and Guidotti, 1991; Farzampour et al., 2015). Thus, DBI and ODN have an opposite effect compared to benzodiazepines.

Furthermore, administration of DBI or ODN in rodents showed a pro-conflict action, which antagonized the well characterized anti-conflict effect of the synthetic bendoziazepines (Corda et al., 1984; De Mateos-Verchere et al., 1998). ODN administration also has an anxiogenic effect, which is antagonized by co-administration of benzodiazepines (Ferrero et al., 1986). Notably, although a large body of literature showed that DBI and ODN act as negative allosteric modulators of the $GABA_A$ receptor, it was recently found that DBI can also enhance GABA currents. Christian and colleagues demonstrated a potentiation of GABAergic synaptic transmission in the reticular thalamic nucleus. The potentiation was absent in mice DBI knockout mice and in mice with a mutation that abolishes the binding of benzodiazepines at the benzodiazepine binding site in the α_3 subunit (Christian et al., 2013). Based on these data it can be inferred that in the nRT DBI acts as a positive modulator of $GABA_A$ receptors by binding to the benzodiazepine binding site, in contrast to its previous well described role as negative modulator of the GABA receptor-induced currents. Furthermore, the authors found that DBI reduces thalamo-cortical oscillations, which might be an endogenous mechanism to prevent seizures (Christian et al., 2013). Low doses of DBI efficaciously suppressed seizures, while high concentrations had a seizure-promoting effect. Therefore, the authors proposed low DBI concentrations enhance GABA induced currents, while high DBI concentrations would negatively modulate the activity of the receptor (Christian et al., 2013; Farzampour et al., 2015).

In addition to modulating the activity of the $GABA_A$ receptor, the DBI cleavage product TTN was shown to have yet other functions. Thus, TTN that binds only with low affinity to the $GABA_A$ receptor, binds with high affinity to a receptor on the outer mitochondrial membrane called the peripheral benzodiazepine receptor (PBR) (Mohler, 2014; Mukhin et al., 1989; Selvaraj et al., 2015). PBR interacts with the steroidogenic acute regulatory protein (StAR) thereby promoting the transport of cholesterol into mitochondria, facilitating the production of steroid compounds (Bovolin et al., 1990). PBR is present in all cells and is especially enriched in the kidney (Braestrup and Squires, 1977).

DBI also binds with high affinity to C(14)-C(22) acyl-CoA esters and acts as an intracellular acyl-CoA transporter and pool former (Frolov and Schroeder, 1998;

Rosendal et al., 1993). Thus, DBI also termed acyl-CoA binding protein (ACBP). The protein is able to desorb acyl-CoA esters from membranes, to transport and deliver them for the mitochondrial β-oxidation and stimulate the production of acyl-CoA esters by removing them from the acyl-CoA synthetase. Furthermore, by binding the acyl-CoA esters and transporting them to other subcellular compartments, DBI was also shown to protect the acetyl-CoA carboxylase and the mitochondrial ADP/ATP translocase from acyl-CoA inhibition (Knudsen et al., 1993; Neess et al., 2015; Rosendal et al., 1993). Hence DBI plays an important role in lipid metabolism regulating cell growth and proliferation. Mice that lack DBI are viable, fertile and develop normally till weaning. However, at weaning they show a state of weakness and delayed growth. This state is caused by an impaired start in the liver lipogenic program, the lack of DBI interfering with the normal metabolic adaptation program to weaning (Bloksgaard et al., 2012; Knudsen et al., 1993).

1.4.2 DBI and adult neurogenesis

GABA was shown to regulate postnatal and adult SVZ neurogenesis. GABA spilled-over from synapses of local medium spiny neurons or produced by the neuroblasts reduced the proliferation of stem cells and of TACs and keeps stem cells quiescent (Alfonso et al., 2012; Liu et al., 2005; Young et al., 2014). DBI is enriched in cells lining the walls of the lateral ventricle. Careful immunohistological analysis performed in our lab showed that DBI is strongly expressed in the SVZ and the RMS indicating a possible role in regulating neurogenesis. In the postnatal SVZ DBI is present in NSCs and in 67% of TACs, while in adult mice the percentage of TACs expressing DBI drops to 32% (Alfonso et al., 2012). No DBI signal is detected in neuroblasts nor in mature neurons. With the help of *in vivo* viral gain and loss of function studies, our group found that DBI plays an important role in regulating postnatal and adult SVZ neurogenesis. Retroviral DBI KD led to a reduction in the proliferation of SVZ progenitors while DBI OE had the opposite effect. Manipulating DBI expression affected not only the pool of progenitors but also the number of adult

neurons produced (Alfonso et al., 2012). By enhancing the proliferation of TACs, DBI OE increased the number of neurons in the OB, while DBI KD had the opposite effect and reduced neurogenesis. *In vivo* cell cycle analysis showed that, in TACs, DBI does not influence the length of the cell cycle, but promotes re-entry into the cell cycle and thus increases the number of cell division (Alfonso et al., 2012). The pro-proliferative effect of DBI was blocked by flumazenil, a benzodiazepine binding to the $GABA_A$ receptor, but not by PK-11195, an inhibitor of the peripheral benzodiazepine receptor, indicating that DBI regulates adult neurogenesis via the $GABA_A$ receptor. The DBI cleavage product ODN, when overexpressed, reproduced the phenotype of DBI overexpression (OE). ODN is known to bind with high affinity to the central benzodiazepine receptor, but not to the peripheral one (Alfonso et al., 2012). Furthermore, electrophysiological recordings showed that ODN inhibits GABA receptor-mediated currents in TACs. Thus, DBI and ODN enhance postnatal and adult SVZ neurogenesis by negatively modulating the GABA induced currents (Alfonso et al., 2012). Unpublished data from our lab show that olfactory enrichment increases the percentage of TACs expressing DBI in the SVZ, suggesting that DBI might play a role in regulating the activity of the niche upon environmental stimulation. DBI is an important player in regulating SVZ neurogenesis and might have a special role in the plasticity of the niche and its response to external factors.

2. Materials and Methods

2.1 Materials

2.1.1 Chemical reagents

Chemical Reagent	Company
Agar	Fluka
Bromo-2-deoxyuridine (BrdU)	Sigma-Aldrich
Citric acid	Grüssing
DAPI (Hoechst)	Sigma-Aldrich
EDTA	PanReac Applichem
Ethanol	Sigma-Aldrich
Hydrochloric acid (HCl)	VWR
Isoflurane	Zoetis
Ketavet (100mg/ml)	Pfizer
Mowiol	Calbiochem
Roti-Histofix, 4% Paraformaldehyde (PFA) solution	Roth
Rompun (2%)	Bayer
Sodium azide (NaN_3)	Roth
Sodium chloride (NaCl)	Sigma-Aldrich
Sodium chloride 0.9% sterile (NaCl)	Braun
Sodium citrate	Riedel-de Haën
Sodium dihydrogen phosphate monohydrate (NaH_2PO_4)	Sigma-Aldrich
Sodium hydroxide (NaOH)	VWR
Sodium phosphate dibasic heptahydrate ($Na_2HPO_4 \cdot 7H_2O$)	VWR
Tamoxifen	Sigma-Aldrich
Tris base	Applichem
Triton X-100	Merck

Tween-20	Sigma-Aldrich

Table 2.1. Chemical reagents

2.1.2 Buffers

PBS (1x)

NaCl	8 g/L (137 mM)
Na_2HPO_4	1.44 g/L (10 mM)
KH_2PO_4	0.24 g/L (1.8 mM)
KCl	0.2 g/L (2.7 mM)

- Adjust the pH to 7.4 with 0.1M HCl.
- Bring the finale volume of the solution to 1L with dH2O.

1M Tris pH=8 buffer

Tris	141.14 g/L

- Adjust the pH to 8 with 1M HCl.

Citric acid antigen retrieval Buffer A

Citric acid	19.21 g/L (0.1M)

Citric acid antigen retrieval Buffer B

Sodium citrate	24.9 g/L (0.1M)

Citric acid antigen retrieval Buffer

9 mL Citric acid antigen retrieval Buffer A +

41 mL Citric acid antigen retrieval Buffer B +

450 mL distilled watter

2.2 Methods

2.2.1 Animal experiments

Animals

During this study I used WT C57BL/6 mice (Charles River) and four transgenic mouse lines: Nestin-Cre described by Tronche et al. (1999), Nestin-CreERT2 described by Lagace et al. (2007), DBI-flox described by Neess et al. (2011) and gamma2F77I described by Cope et al. (2004). All mice were housed in standard housing conditions following the regulations of the German Cancer Research Center and of the University of Heidelberg at a twelve-hour dark/light cycle with free access to food and water. For some experiments the mice were housed in an enriched environment: an open plastic box 400x600x320 (length x width x height) with beading, colorful toys and free access to running wheels. The mice housed in the enriched environment cage had as well free access to food and water. All experiments were approved by the Regierungspräsidium Karlsruhe (G 215/14). Animal handling was performed by trained staff certified by the Federation of European Laboratory Animal Science Associations (FELASA).

Monkey brain sample

For the monkey DG staining I used a 1 year old Rhesus monkey brain obtained from EUPRIM-Net biobank (www.euprim-net.eu). The brain was fixed in 4% PFA for 24 h and further cut into 0.5 cm slabs which were postfixed for 1 week in 4% PFA. The slabs were than cryoprotected in 30% sucrose for 72h and subsequently frozen on dry ice. For analysis the brain pieces were sectioned with a Leica VT1000S vibratome in 50 μm coronal sections which were analyzed according to the staining protocol described kept in PBS and 0.05% natrium azide at 4°C.

Human brain sample

Pieces of the hippocampus from two human male donors (17 and a 22 year old) were obtained from the NIH Neurobiobank. The experiments were approved by the ethics committee of the NIH and the sample donation was accepted by the Tissue

Access Committee of the NHI Neurobiobank (https://neurobiobank.nih.gov/; Request 275).

The brain pieces were dissected postmortem at the NIH and directly frozen at -80°C. Further, they were defrosted, postfixed in 4% PFA for 5 days, cryoprotected in 30% sucrose for 72h and then frozen on dry ice. The brain pieces were kept frozen until sectioning with a cryostat (Leica Biosystems, Germany) in 50 μm coronal sections which were kept in PBS and 0,05% natrium azide at 4°C. The brain slices were used for immunohistochemistry using the following protocol: permeabilization and blocking overnight in 5%BSA, 1% Triton in PBS solution, 2 days incubation in primary antibody (in 5% BSA, 1% Triton in PBS), washing 3 times with PBS for 10 minutes, secondary antibody incubation overnight (in 5% BSA, 1% Triton), washing 3 times with PBS for 10 minutes followed by mounting with Mowiol.

Histology and Immunofluorescence

Mice were anesthetized with an intraperitoneal injection of ketamine-xylazine or Rompun (2% 1:6 diluted; Bayer) and Ketavet (100mg/ml; 1:15 diluted; Pfizer) in 0.9% NaCl (Braun) and were transcardially perfused with ice-cold PBS for 5 minutes followed by perfusion with 4% PFA solution for 5-8 minutes. The brains were dissected out and postfixed overnight in 4% PFA solution buffered (pH 7). The tissue was further washed twice with PBS and stored at 5°C in PBS with 0.05% sodium azide. For analysis the brains were cut with a Leica VT1000S vibratome in 50μm thick slices. Immunohistochemistry was performed following a free-floating staining protocol. The brain slices were first incubated for one hour at room temperature (RT) in a 3% BSA, 0.2%-0.3% Triton PBS solution in order to achieve proper permeabilization and blocking. The tissue slices were further incubated overnight at 5°C in a 3% BSA, 0.2% Triton in PBS solution containing the primary antibodies. On the next day the sections were washed 3 times for 10 minutes with PBS and incubated for 1.5-2h at RT in a 3% BSA, 0.2% Triton PBS solution containing the secondary antibody. After the second incubation, the brain slices were washed 3 times for 10 minutes with PBS and mounted onto glass slides. The preparates were left for 20 minutes in a dark space for the tissue

slices to dry after which were mounted with Mowiol. In the case of the monkey brain, the slices were incubated in a 5% BSA, 1% Triton PBS solution overnight at 5°C for permeabilization and blocking and were further incubated in a 5% BSA, 1% Triton PBS solution containing the primary antibody at RT between 2 and 5 days. The brain slices were than washed 3 times for 10 minutes with PBS and were incubated overnight in a 5% BSA, 1% Triton PBS solution containing the secondary antibody. For BrdU stainings, before starting the regular staining protocol, the brain slices were incubated in a 1M HCl solution for 30 minutes at 37°C in order to denature the DNA and were thereafter incubated for 15 minutes at RT in Tris buffer pH 8 to bring the tissue to a neutral pH. For stainings which included the detection of Tbr2 using the rabbit anti Tbr2 antibody from Abcam, I performed before the regular staining protocol a citric acid - citrate buffer antigen retrieval according to the protocol published by Houssaini et al., 2013. The sections were analyzed using a Zeiss LSM 700 confocal microscope.

Primary antibodies

Antibody	Company	Application	Concentration
Rabbit anti-DBI	Santa Cruz	IHC	1:100
Rabbit anti-DBI	Frontier Institute Japan	IHC	1:1000
Mouse anti-GFAP	Sigma	IHC	1:500
Chicken anti-Nestin	Novus	IHC	1:200
Goat anti-SOX2	Santa Cruz	IHC	1:500
Rabbit anti-Tbr2	Abcam	IHC	1:200
Mouse anti-Mash1	BD PharMingen	IHC	1:500
Goat anti-DCX	Santa Cruz	IHC	1:500
Mouse anti-NeuN	Chemicon	IHC	1:1000
Chicken anti-EGFP	Abcam	IHC	1:1000
Rabbit anti-DsRed	Clontech Living Colors	IHC	1:1000
Rabbit anti-Ki67	Abcam	IHC	1:200

Table 2.2. Primary antibodies

Secondary antibodies

Antibody	Company	Application	Concentration
Donkey anti-rabbit Cy3	Jackson Immuno Research Laboratories	IHC	1:1000
Donkey anti-goat Alexa 647	Invitrogen	IHC	1:1000
Donkey anti-chicken Alexa 488	Invitrogen	IHC	1:1000
Donkey anti-chicken Alexa 488	Jackson Immuno Research Laboratories	IHC	1:1000
Donkey anti-mouse Alexa 488	Invitrogen	IHC	1:1000
Donkey anti-mouse Alexa 647	Invitrogen	IHC	1:1000
Donkey anti-mouse DyLight 405	Jackson Immuno Research Laboratories	IHC	1:500
Donkey anti-rabbit DyLight 405	Jackson Immuno Research Laboratories	IHC	1:500
Donkey anti-chicken DyLight 405	Jackson Immuno Research Laboratories	IHC	1:500
Donkey anti-rabbit Alexa 488	Invitrogen	IHC	1:1000

Table 2.3. Secondary antibodies

Viral vector construction

For the present study I used several lentiviruses. To create the lentiviruses needed I modified by cloning the pCDH lentiviral backbone and generated the following plasmids:

1) DBI KD: pCDH-EF1-H1-shRNADBIa-EGFP;
2) DBI KD: pCDH-EF1-H1-shRNADBIb-EGFP;

3) Ctrl KD: pCDH-EF1-H1-shRNAscrambled-tdTomato;
4) DBI OE: pCDH-EF1- DBI-T2A-tdTomato;
5) Ctrl OE: pCDH-EF1-EGFP;
6) GFAP-tdTomato virus: pCDH-GFAPpromoter-tdTomato;
7) DBI KD: pCDH-EF1-LoxP-H1-shRNADBIa-EGFP-(inverted)-LoxP;
8) Ctrl KD: pCDH-EF1-LoxP-H1-shRNAscrambled-mCherry (inverted)-LoxP;
9) DBI OE: pCDH-EF1-LoxP-DBI-T2A-tdTomato (inverted)-LoxP;
10) Ctrl OE: pCDH-EF1-LoxP- EGFP (inverted)-LoxP;
11) ODN OE: pCDH-EF1-LoxP-ODN-T2A-tdTomato-LoxP.

For DBI KD I used two shRNA sequences described by Alfonso et al., 2012: DBIa: GCTGTTCATCTACAGTCACTT targeting the coding sequence of mouse DBI, and DBIb: CCTGTGAGGACATAATGC targeting the 3'UTR of mouse DBI.
Viruses 1) and 2) were created by cloning the sequences for H1-shRNA DBIa (virus 1) and for H1-shRNA DBIb (virus 2) into a pCDH plasmid expressing EGFP after the EF1 promoter. Virus 3) was produced by cloning the sequence for H1-shRNAscrambled into a pCDH plasmid expressing tdTomato after the EF1 promoter. Virus 4) was created by cloning the sequence for DBI in a pCDH vector in front of the sequence for T2A-tdTomato, in frame with the tdTomato sequence.

The backbone of the Cre-dependent viruses was constructed by subcloning the LoxP sites and the protein mCherry situated between the two LoxP sites from a retroviral vector kindly provided by Prof. Oscar Marin (MRC Centre for Developmental Neurobiology, King's College, London, UK) into the pCDH lentiviral backbone. For obtaining virus 7) I cloned the DBI KD sequence (a) together with the H1 promoter (H1-shRNAa into the new generated pCDH backbone and replaced the mCherry sequence with the inverted sequence of EGFP. For obtaining virus 8) I cloned a shRNAscrambled sequence together with the H1 promoter (H1- shRNAscrambled) into the new generated pCDH backbone. For creating DBI OE virus 9) and ODN OE virus 11) I replaced the mCherry sequence from the previously described pCDH backbone with the inverted sequence of DBI-T2A-tdTomato (for virus 5) and with the inverted sequence of ODN-T2A-tdTomato (for virus 11). Virus 10) was generated by

replacing the mCherry sequence with the inverted sequence of EGFP (Dumitru et al., 2017).

Virus production

Viral production was achieved by transfecting the packaging cell line HEK293, using a calcium transfection protocol, with the viral backbone vector together with the VSVG and Δ-helper plasmids. Two days after the calcium transfection, the viral particles were purified and concentrated by ultracentrifugation, obtaining a final viral solution which was further titrated using a serial dilution method. The viral preparates used presented a viral titer in the range of 10^6-10^8 cfu/ml.

Intracranial virus injection

All procedures were approved by the Regierungspräsidium Karlsruhe (G 215/14) and were in agreement with the regulation of the German Cancer Research Center and of the University of Heidelberg. For intracranial injection the animal was first anesthetized via isoflurane inhalation. Following, the head of the mouse was fixed in a stereotactic device and the animal was kept under a constant flow of air mixed with isoflurane during the entire procedure. For injecting the viral mixes (Ctrl and KD or OE) in the hippocampus without great loss of nervous tissue, I made use of pulled glass capillary with sharp tips. After mounting the capillary tube to the arm of the stereotactic device the virus was loaded. To target the DG I used the following age dependent coordinates: P7 old mice (from Bregma) -1.5mm anteroposterior, +/-1.5mm mediolateral, -1.7mm dorsoventral; mice older that P15 (from Bregma) -2mm anteroposterior, +/-1.7mm mediolateral, -2mm dorsoventral. An electrical dentist drill was used for making a small hole through the skull at the right coordinates. After bringing the tip of the glass capillary to the right position, the viral mix was slowly injected in the brain and 3 to 10 minutes were given for the mix to diffuse within the tissue. Finally the tip of the pipette was carefully removed from the brain and the skin was stitched using sterile resorbing fibers.

Electrophysiology

Whole-cell patch-clamp recordings were performed using 3-4 weeks old, males and females, wild-type C57Bl/6 (n = 4) and gamma2 mutant mice (n = 6). The mice were deeply anaesthetized by isoflurane inhalation and were perfused transcardially with 30 ml sucrose solution containing (in mM) 212 sucrose, 26 NaHCO3, 1.25 NaH2PO4, 3 KCl, 7 $MgCl_2$, 10 glucose and 0.2 CaCl2, cooled to 4 °C and oxygenated with carbogen gas (95% O2/ 5% CO2, pH 7.4). 250 µm thick acute horizontal sections were performed using a vibratome (Slicer HR2, Sigmann Elektronik, Germany). The tissue was further incubated at room temperature for 1 hour in oxygenated extracellular solution containing (in mM) 125 NaCl, 25 $NaHCO_3$, 1.25 NaH_2PO_4, 2.5 KCl, 2 $CaCl_2$, 1 $MgCl_2$ and 25 glucose. The individual slices were transferred into a submerged, superfused chamber (perfusion rate 3.0 ml/min with oxygenated extracellular solution heated up to 30-32°C). Epifluorescence and DIC optics were used to visualize the fluorescently labeled cells in the DG. The recording pipettes were pulled from borosilicate capillaries with the tip resistance of 6-8 MΩ, filled with a high Cl^- solution containing (in mM) 127.5 KCl, 11 EGTA, 10 Hepes, 1 $CaCl_2$, 2 $MgCl_2$ and 2 Mg-ATP (pH 7.3). During measurements was not correct for liquid junction potentials. Florescent cells with a RG-like morphology were identified in the SGZ. Into the cell soma individual current steps ranging from -100 to 100 pA (delta 20 pA) were injected in current-clamp mode and as tested for the presence of action potentials. Sequential local puffs of GABA (50 µM) or GABA/ODN (50 µM /20 µM) (each with a duration of 1 sec at 0.01 bar) were further applied onto the patched stem cells in voltage-clamp mode at a holding potential of -60 mV. The stimulus was delivered and the data acquisition was performed with the PatchMaster software (HEKA). The signal was filtered at 3 kHz and digitized at 20 kHz. The data was analyzed with the HEKA software FitMaster and the results were presented as mean ± SEM. Further statistical analysis was performed with SigmaPlot (Systat). The electrophysiological measurements were performed by Angela Neitz.

Quantification and statistical analysis

For all quantifications presented pictures from at least 3 brain slices/mouse were analyzed. In the case of the conditional DBI KO using the NestinCre^{ERT2}/DBI$^{lx/lx}$ mice, the density of the NSCs (RG-like Nestin^{+}/SOX2^{+} cells) or dividing cells (Ki67^{+} cells) present in the SGZ was determined by dividing the number of cells to the volume of the granular layer in which they were identified.

For experiments involving Cre-dependent lentiviruses was chosen to express the data as cell percentage instead of absolute cell numbers to rule out effects resulting from *in vivo* titer differences between Ctrl and OE or KD viruses, between differences generated by the location of the infection site in the DG and by the density of the cell infected population. To reduce all the technical errors and biases the same animal was injected with both control and experiment virus. The percentage of NSCs (RG-like GFAP^{+}/SOX2^{+}/virus^{+} cells), TACs (GFAP^{-}/SOX2^{+}/virus^{+} cells), Astrocytes (GFAP^{+}/virus^{+}/astrocyte morphology), neuroblasts (DCX^{+}/virus^{+} cells) and adult-born neurons (DCX^{-}/virus^{+} neuron morphology) were quantified within the population of infected cells, separately for the KD or OE and control population. The percentages of the different progenitors were evaluated using two different stainings: GFAP, dsRed, EGFP, SOX2 was used to quantify the NSCs, ANPs and stem cells, while NeuN, dsRed, EGFP, DCX was used to identify the neuroblasts and the adult-born neurons. The overlap between the cell markers used as well as the technical differences between the two stainings and the averaging between animals can explain why the percentage summation for the different progenitors does not result to 100. Double infected cells with Ctrl and OE or KD viruses were considered to be OE or respectively KD. Although it cannot be excluded that some Nestin-negative infected cells express the shRNA but not the fluorescent marker, these cells do not constitute a confound because they were not included in our analysis which comprise labeled cells only. Most importantly, control-labeled cells (red) were Nestin+ at the time of the infection and, hence, cannot be shRNA DBI+ and not green.

For experiments involving non-Cre dependent lentiviruses the percentage of SOX2^{+} progenitors was quantified within the virus infected population in DG, separately for Ctrl and KD or OE infected cells two weeks after the infection. The

quantification of neuroblasts or neurons in this type of experiment is not feasible as one cannot make a difference between the cells infected directly by the virus and the cells that were produced by virus infected stem cells. Because of the turnover of ANPs, the SOX2 progenitors quantified two weeks after infection include only infected stem cells and ANPs originating from the infected stem cells.

To test the role of DBI in enriched environment and exercise, NestinCre mice were injected with Cre-dependent DBI KD virus (viruses 7 from viral vector construction part). The mice were kept for 3 weeks either in standard housing conditions or in an enriched environment with free access to running wheels. For this experiment, presented in figure 6, the non-infected part of the DG was considered control while the part of the DG infected with the KD virus was analyzed as DBI KD. To exclude the possibility that the procedure itself leads to the effects found the experiment was repeated by injecting the mice with control virus (viruses 8 from viral vector construction part), experiment presented in supplemental figure 3. For this experiment the areas of the DG infected with the control virus versus non-infected areas of the DG were compared. For both experiments the average density of neuroblasts (DCX^+ cells) and of dividing cells ($Ki67^+$ cells) was determined in the DG by dividing the number of cells counted to the volume of the granular layer in which they were counted. Within these experiments the percentage of proliferating NSCs was determined as percentage RG-like $Nestin^+/SOX2^+/Ki67^+$ cells of all NSCs in the analyzed volume.

The statistical analyses presented were performed using the SigmaPlot software (Systat). All data sets were first checked if they are normally distributed using the Shapiro-Wilk normality test. Parametric tests were used for normally distributed datasets and non-parametric tests for datasets that were not normally distributed. For all analyses where control and experiment values were obtained in the same mouse (for examples viral mix injections) paired comparison tests were used.

The Materials and Methods chapter was adapted after Dumitru and colleagues (2017).

3. RESULTS

3.1 DBI is expressed in the adult neurogenic niches in rodents and primates

DBI is strongly expressed in the SVZ and RMS, specifically in NSCs and TACs (Alfonso et al., 2012). The important regulatory function DBI has in postnatal SVZ neurogenesis raised the pertinent question whether the protein plays a similar role in the other well-studied adult neurogenic niche, the SGZ.

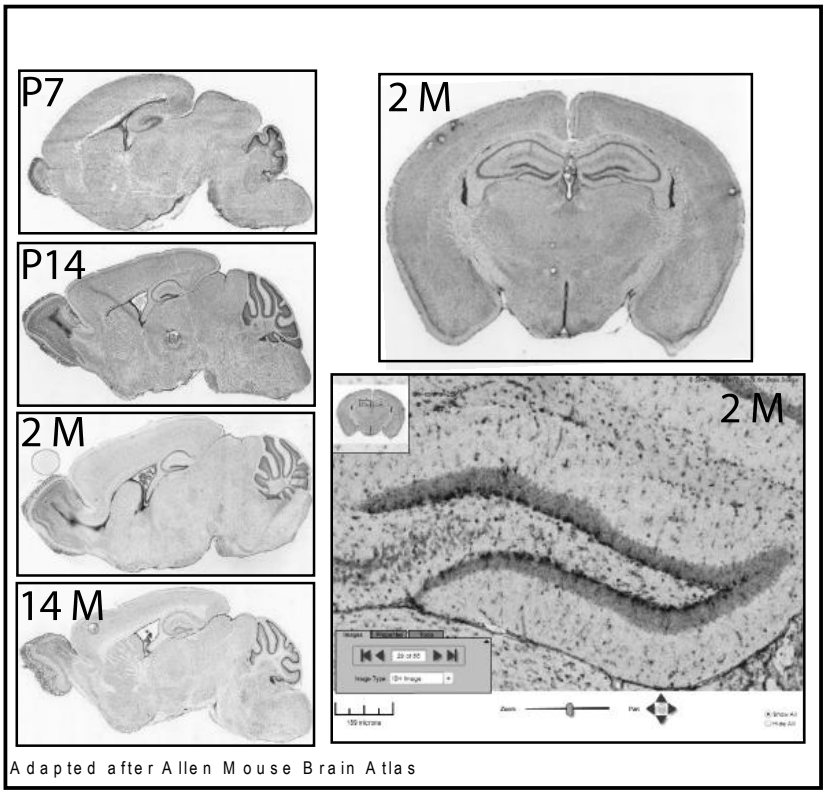

Figure 6.1. DBI mRNA is present in the SVZ, RMS and DG in postnatal and adult mice. The pictures presented depict *in situ* hybridizations for DBI in sagittal and coronal slices of the mouse brain at different ages. DBI (black signal) is clearly present in the DG and is especially localized to the SGZ. P7/P14: postnatal day 7/14. 2M/14M: 2/14 months old Pictures adapted after Allen Mouse Brain Atlas.

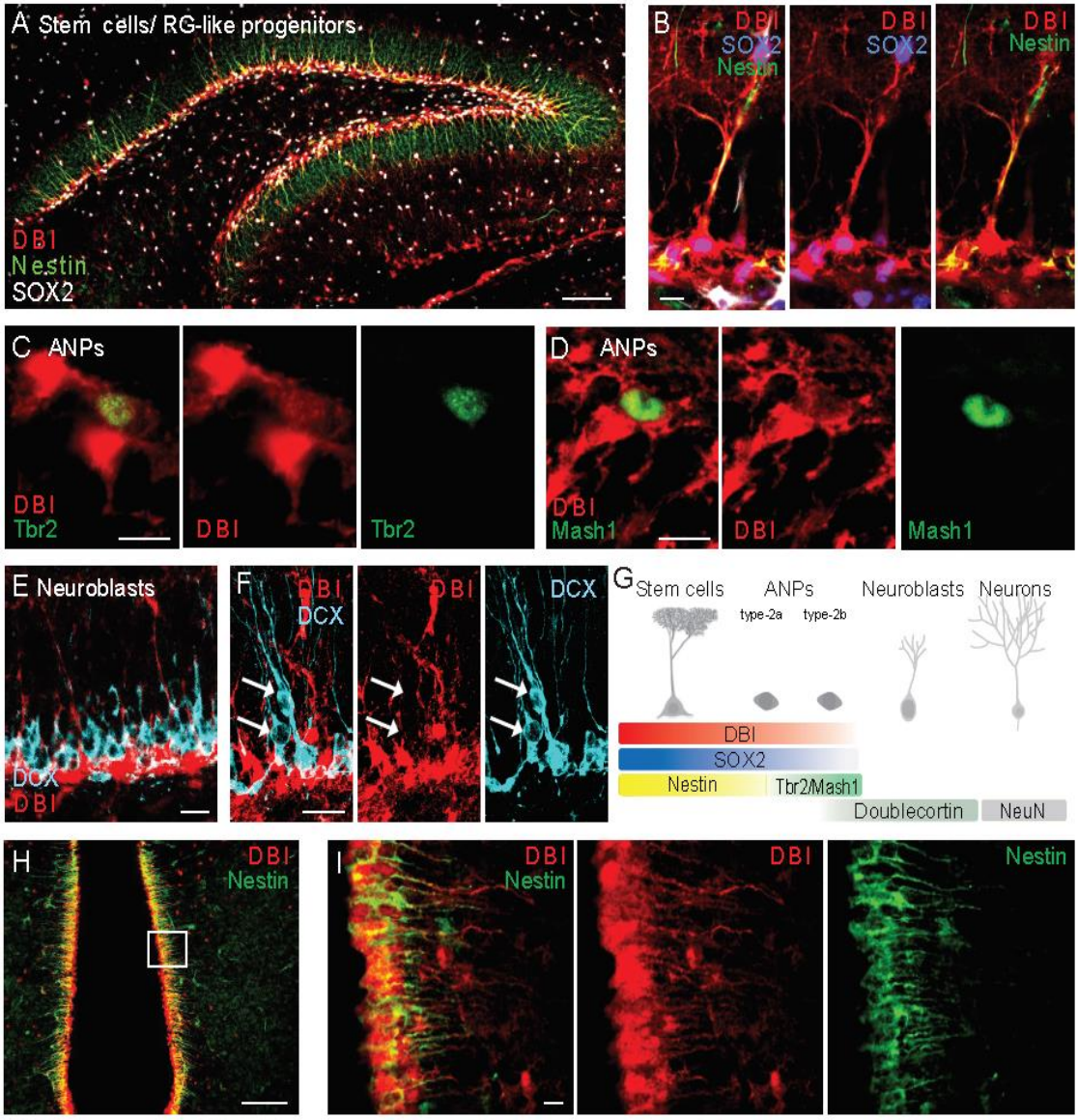

Figure 6.2. DBI is expressed in NSCs and ANPs in the SGZ and Tanycytes in the third ventricle.

(A) Overview of the DG in a coronal brain section of a 3-week-old mouse stained with antibodies against DBI (red), Nestin (green), and SOX2 (white).

(B) RG-like stem cells positive for Nestin^{+} (green) and SOX2^{+} (blue) in the DG of a 2-month old mouse express DBI (red).

(C and D) DBI immunoreactivity (red) is detected in a subpopulation of ANPs labeled with Tbr2 (green in C) and Mash1 (green in D).

(E and F) DG brain section of a 3-week-old (E) and 2-month-old (F) mouse showing that DBI (red) does not co-localize with the neuroblast marker DCX (cyan). Arrows in (F) indicate two DCX-positive cells.
(G) Scheme summarizing the expression pattern of DBI and other cell-type markers in the SGZ.
(H) Overview of the third ventricle in a coronal brain section of a 2-month-old mouse stained with antibodies against DBI (red) and Nestin (green).
(I) Magnification of boxed area in (H) showing tanycytes positive for DBI (red) and Nestin (green).
Scale bars represent 100 mm in (A) and (H); 10 mm in (B), (C), (D), and (I); and 20 mm in (E) and (F). Figure and figure legend were reproduced from Dumitru and colleagues (2017).

A careful analysis of DBI *in situ* hybridization pictures from the Allen Mouse Brain Atlas (**Figure 6.1)** showed that DBI mRNA is specifically localized in the SGZ. I tested DBI expression by immunohistochemistry and found a strong DBI signal in the SGZ. DBI expression was localized to SGZ RG-like cells, positive for Nestin and SOX2, identified as NSCs (**Figure 6.2 A and B**). Almost all stem cells had a strong DBI signal (97.8 ± 0.38%; mean ± s.e.m.; n = 6 mice) present in the cell body as well as in the long radial process and in the bushy tuft-like end-process (**Figure 6.2 B**). DBI was also expressed in all $SOX2^+$ astrocytes but at lower levels compared to the SGZ NSCs (data not shown). DBI was expressed in 87.16 ± 1.01% of the $Nestin^-/Sox2^+$ early TACs (Type 2a cells; mean ± s.e.m.; n = 6 mice) and in 31.07 ± 2.39% of the $Tbr2^+$ or $Mash1^+$ late TACs (Type 2b cells; mean ± s.e.m.; n = 6 mice; **Figure 6.2 A-D**). Among DCX^+ neuroblasts, only 10.73 ± 1.15% (mean ± s.e.m.; n = 6 mice) expressed DBI. However, these cells were most likely TACs that already started expressing DCX, as 96.28 ± 0.64% (mean ± s.e.m.; n = 6 mice) of the DBI positive cells also expressed SOX2 (**Figure 6.2 A, B and E**). I did not detect DBI expression in any of the granule cells (data not shown).

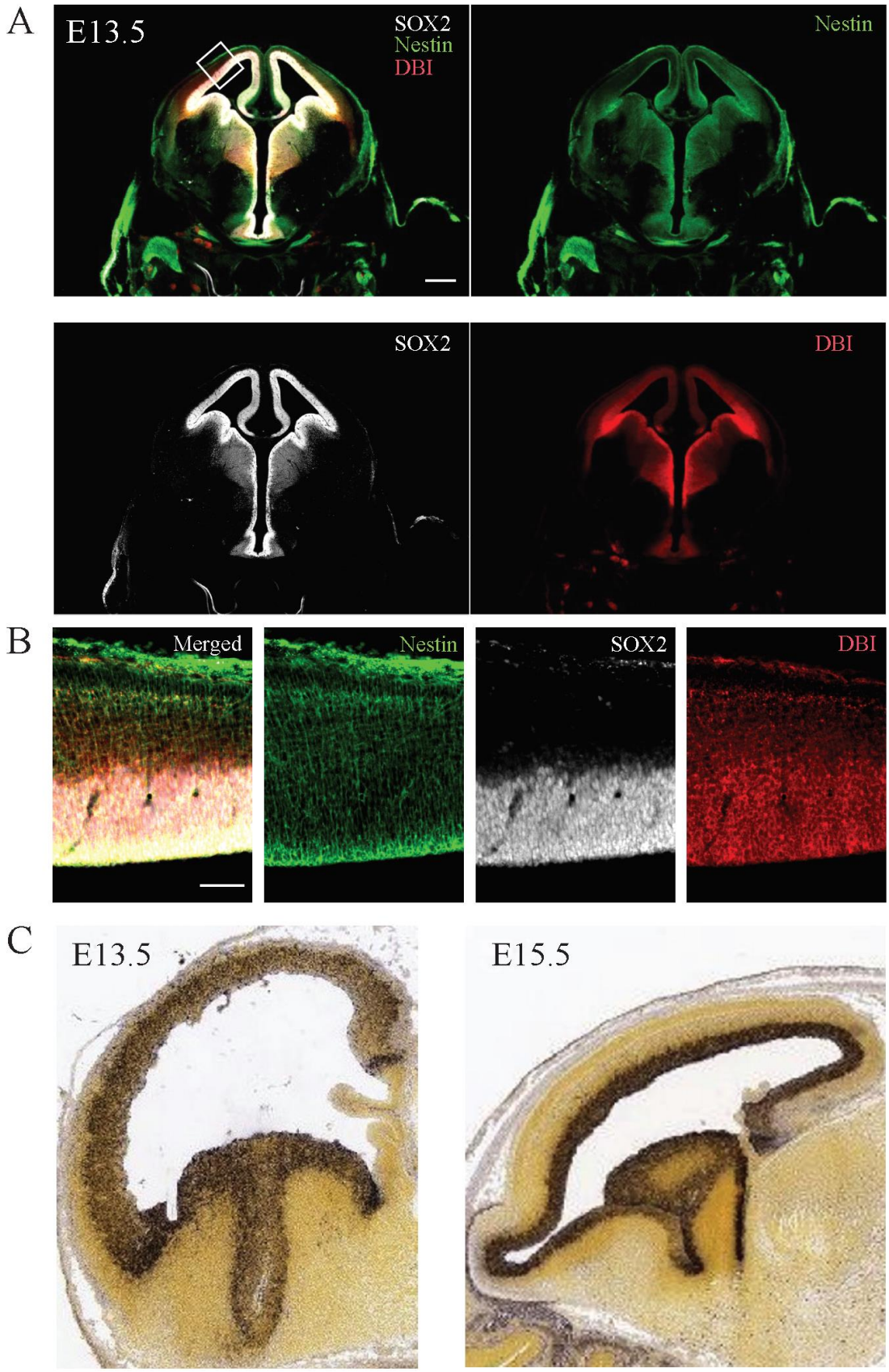
A
E13.5
SOX2
Nestin
DBI
Nestin
SOX2
DBI
B
Merged
Nestin
SOX2
DBI
C
E13.5
E15.5

Figure 6.3. DBI is expressed in the RG cells during mouse brain development.
(A) Overview of E13.5 developing mouse brain in a coronal brain section stained with antibodies against DBI (red), Nestin (green), and SOX2 (white).
(B) Magnification of boxed area in (A) showing a part of the pallial cortex positive for DBI (red), Nestin (green), and SOX2 (white).
(C) DBI *in situ* hybridizations in sagittal slices of the developing mouse brain at E13,5 and E15,5. DBI (black) is present in the ventricular and subventricular zones of the pallium and the ganglionic eminences. Scale bars represent 500 µm in (A) and 50 µm in (B). Pictures adapted after Allen Mouse Brain Atlas.

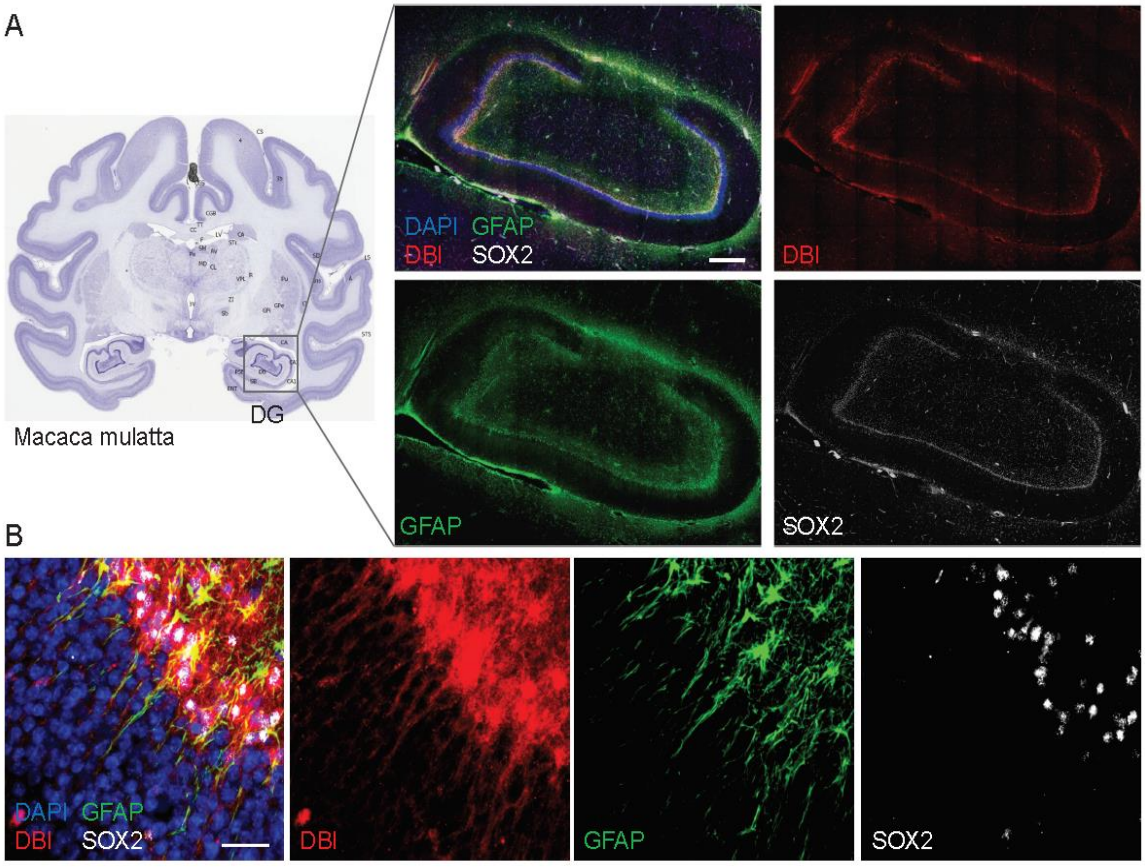

Figure 6.4. DBI is expressed in adult neural progenitors in Rhesus monkey DG.
(A) Overview of the DG in a coronal section from a 1-year-old Rhesus monkey brain. DBI (red) in the SGZ exhibits a similar expression pattern as the NSCmarkers GFAP (green) and SOX2 (white).

(B) Higher magnification showing co-localization of $GFAP^+$ (green), $SOX2^+$ (white), and DBI (red).
Scale bars represent 500 mm in (A) and 30 mm in (B). The picture of the coronal brain slice of Macaca mulatta has been taken from BrainMaps: An Interactive Multiresolution Brain Atlas; http://brainmaps.org. Figure and figure legend were reproduced from Dumitru and colleagues (2017).

The strong DBI presence in both SVZ and SGZ and its specific localization to the stem cells raised the question whether DBI is also expressed in the other adult neurogenic niche in the mouse brain. The walls of the 3rd host cells with RG-like morphology called Tanycytes. α-Tanycytes populating the ventral wall of the ventricle have stem cell properties producing neurons postnatally, which integrate in the adjacent parenchyma. All Tanycytes in the walls of the 3rd ventricle presented a strong DBI expression which co-localized with the stem cell markers Nestin and SOX2 (**Figure 6.2 H and I**). Thus, DBI is expressed in stem cells in all adult neurogenic niches of the mouse brain.

Adult neurogenesis recapitulates embryonic neurogenesis sharing similar developmental stages and regulatory mechanisms. Therefore, I tested whether DBI is also expressed during development in the mouse brain. At E13.5 I found that DBI was present in the ventricular and subventricular zones of both pallium and subpallium (the ganglionic eminences). Careful analysis showed DBI to be strongly expressed in all $Nestin^+$ $SOX2^+$ RG cells both in the cell body and in the long radial process (**Figure 6.3 A and B**). Furthermore, DBI *in situ* hybridization pictures from the Allen developing mouse brain atlas showed the presence of DBI mRNA in the ventricular and subventricular zones of both the pallium and the subpallium (**Figure 6.3 C**).

Next, I tested the presence of DBI in the adult SGZ of the Rhesus monkey and in humans. In the Rhesus monkey, a careful immunohistological analysis revealed that DBI was specifically expressed in SGZ and was localized in RG-like, $GFAP^+$ $SOX2^+$ putative stem cells and non-RG-like $GFAP^-$ $SOX2^+$ putative TACs (**Figure 6.4 A and B**). In the human DG, I found that DBI was specifically expressed in SGZ $GFAP^+$ cells; however, because of technical reasons, it was not possible to precisely identify

whether DBI was expressed in putative stem cells or in astrocytes (**Figure 6.5 A and B**).

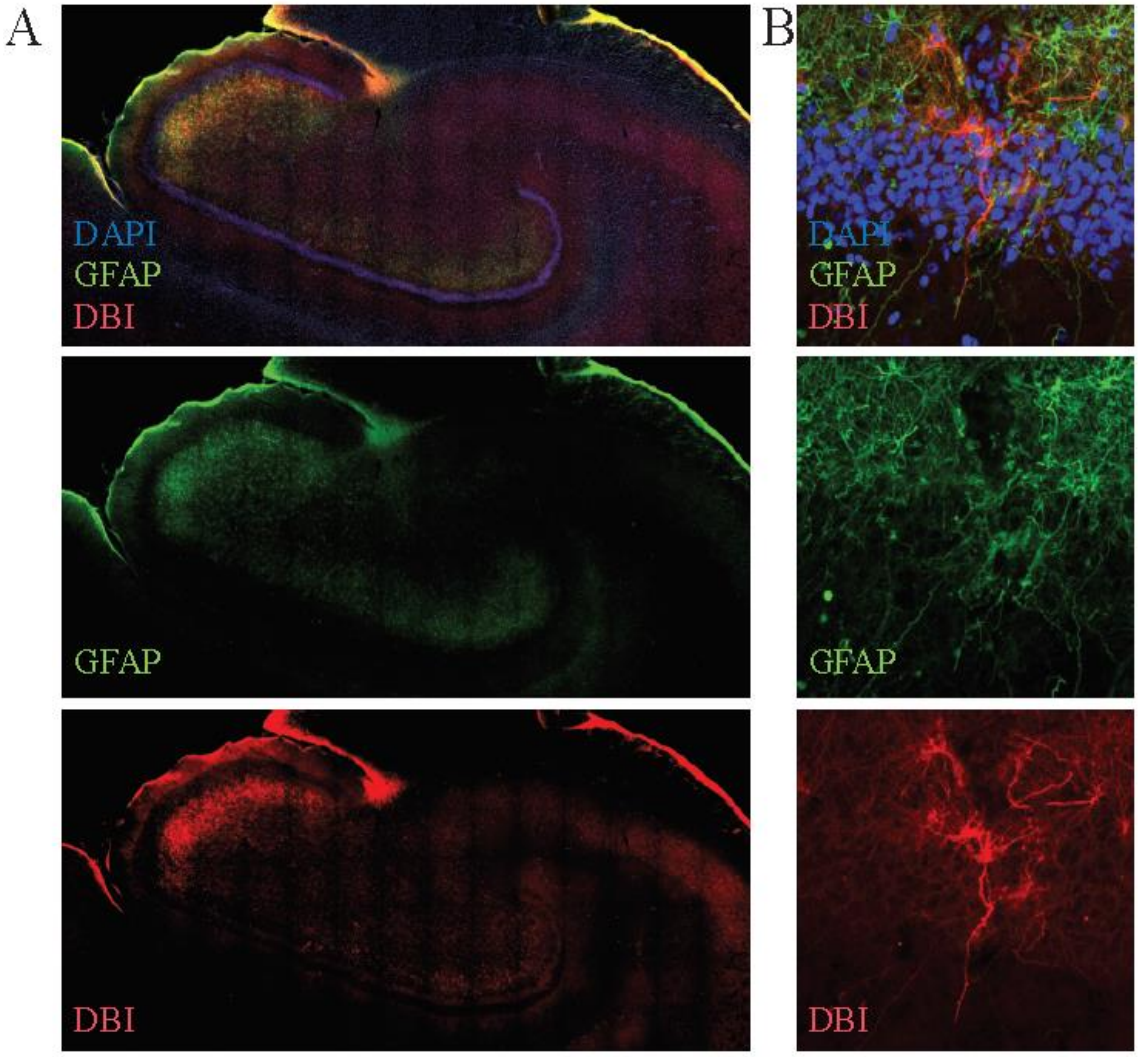

Figure 6.5. DBI is expressed in SGZ of human DG.

(A) Overview of the DG in a coronal section from a 23-year-old human male. The post-mortem human brain hippocampus was coronally sliced and stained with antibodies against DBI (red), GFAP (green), and SOX2 (white).

(B) Higher magnification of the DG and SGZ showing co-localization of $GFAP^{+}$ (green) and DBI (red).

3.2 DBI conditional knockout in the SGZ leads to a reduction in the number of stem cells and in their proliferation

To investigate the functional role of DBI in the SGZ I took recourse to genetically modified mice in which the expression of a tamoxifen-dependent Cre recombinase (Cre^{ERT2}) is driven by a Nestin promoter. In this mouse model the sequence of DBI is flanked by loxP sites: $NestinCre^{ERT2}/DBI^{lx/lx}$ (Neess et al., 2011; Zhu et al., 2014). Tamoxifen administration to the before mentioned mice leads to the knockout (KO) of DBI in the Nestin expressing cells. Therefore, I administered tamoxifen for one week to two months old $NestinCre^{ERT2}/DBI^{lx/lx}$ mice to ensure DBI KO in SVZ and SGZ adult stem cells and in their progeny. I used as controls littermates that did not express the Cre recombinase ($DBI^{lx/lx}$) which also received the tamoxifen treatment, and $NestinCre^{ERT2}/DBI^{lx/lx}$ mice to which I administered a saline solution instead of tamoxifen. Three weeks after the treatment, tamoxifen administration led to a partial deletion of DBI in the $NestinCre^{ERT2}/DBI^{lx/lx}$ mice in comparison to the $DBI^{lx/lx}$ mice and to the mice treated with saline solution. As expected, DBI was only deleted in SGZ NSCs and TACs but not in astrocytes, as they do not express Nestin (**Figure 6.6 A and B**). I evaluated the number of SGZ NSCs and Ki67 positive (proliferating) SGZ NSCs and found no significant difference between the two control groups. However, DBI deletion led to a statistically significant decrease both in the number of SGZ NSCs and in the number of proliferating NSCs, indicating that DBI plays a role in regulating adult SGZ neurogenesis (**Figure 6.6 C and D**).

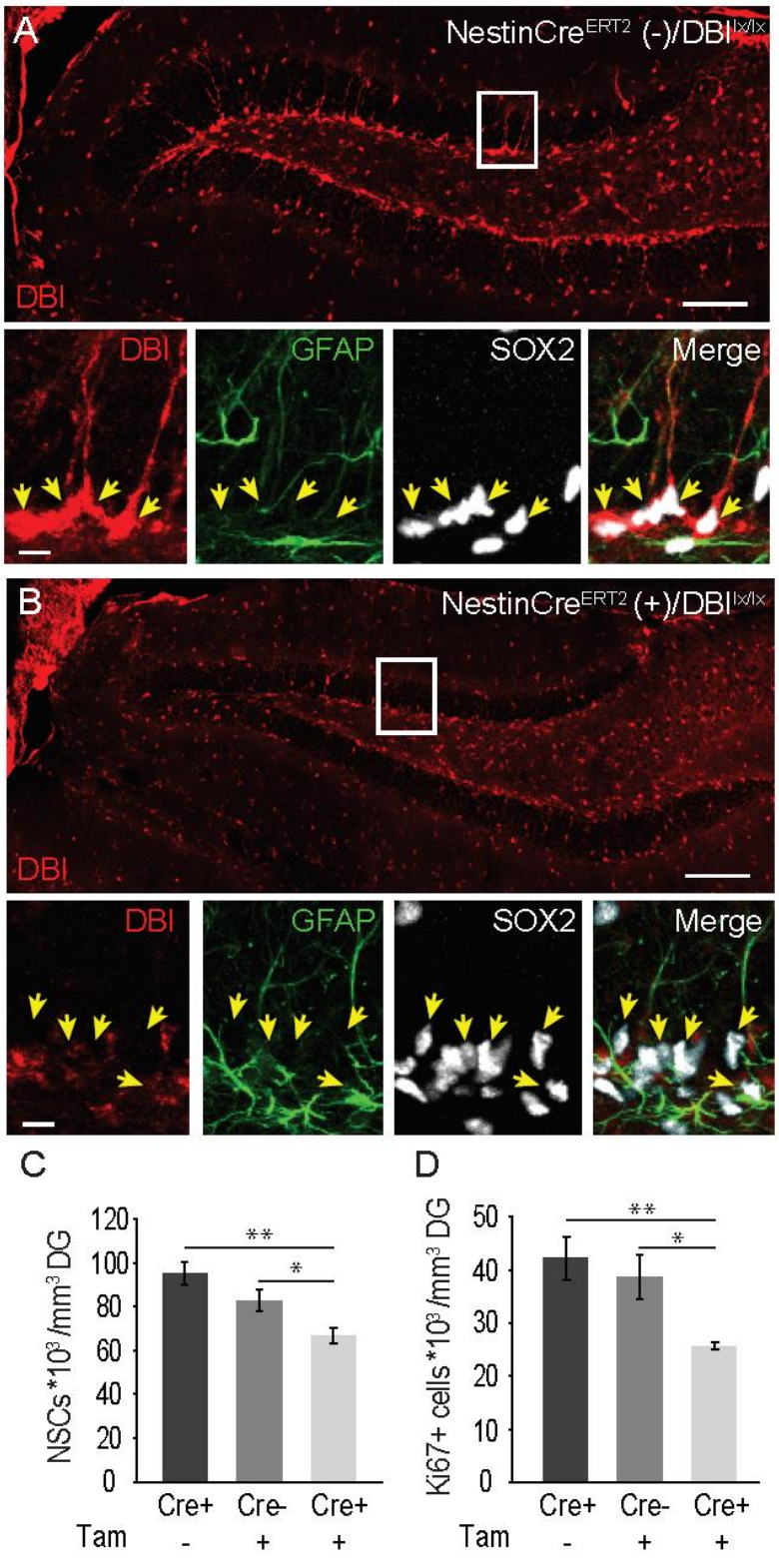

Figure 6.6. Conditional DBI KO reduces the number of DG NSCs and their proliferation. (A and B) Overview of the DG in a coronal brain section of a 2-month-old NestinCreERT2(-)/DBIlx/lx (A) and Nestin CreERT2(+) /DBIlx/lx (B) mouse. Small panels in (A) and (B) show higher magnifications of the boxed areas and depict stainings for DBI (red), GFAP (green), and SOX2 (white) 3 weeks after 1 week of tamoxifen treatment. Arrows indicate $GFAP^+/SOX2^+$ cells in the SGZ, demonstrating successful DBI ablation in (B). (C) Quantitative evaluation (mean ± SEM) of $Nestin^+/SOX2^+$ RG-like NSCs in the DG of control mice (NestinCreERT2 (+)/DBIlx/lx no tamoxifen, black bar, and NestinCreERT2(-)/DBIlx/lx tamoxifen treated, dark gray

bar) and DBI conditional KO mice (NestinCreERT2(+)/DBIlx/lx tamoxifen treated, light gray bar). Cre+ Tam-: 1,730 cells in 7 mice; Cre- Tam+: 1,589 cells in 7 mice, Cre+ Tam+: 1,407 cells in 7 mice; *p < 0.05, **p < 0.01, one-way ANOVA followed by Holm-Sidak method for all pairwise comparison.
(D) Quantitative evaluation (mean ± SEM) of Ki67+ dividing cells in the DG of mice from the three groups as in (C). Cre+ Tam-: 757 cells in 7 mice; Cre- Tam+: 728 cells in 7 mice; Cre+ Tam+: 544 cells in 7 mice; *p < 0.05, **p < 0.01, one-way ANOVA followed by Holm-Sidak method for all pairwise comparison.
Scale bars represent 100 mm in the overview and 10 mm in the magnified images. Figure and figure legend were reproduced from Dumitru and colleagues (2017).

3.3 In vivo manipulation of DBI expression levels influences postnatal and adult SGZ neurogenesis

To specifically determine how DBI regulates the SGZ NSCs and TACs, I made use of viral strategies that allow the concomitant manipulation of DBI expression and labeling of the infected stem cells and of their progeny. For this purpose, I used lentiviruses containing the inverted sequences of a short hairpin RNA (shRNA) targeting DBI (DBI KD) and the reporter protein EGFP flanked by LoxP sites. EGFP expression is controlled by a general promoter (EF1) and can occur only upon inversion of the floxed cassette following recombination by a Cre enzyme. As control, I generated similar lentiviruses expressing a scrambled shRNA sequence and mCherry (**Figure 6.7 A**). To compare between DBI KD and control infected cells and overcome any technical variations generated by the injection site or the mice used, the viruses were injected as a mix of control and DBI KD in the same mouse. I injected a mix of the two viruses in the DG of postnatal 7 (P7) or three months old mice expressing Cre recombinase in the $Nestin^+$ cells. In these mice, the floxed cassette containing the reporter proteins would be inverted only in the Nestin expressing stem cells. Two weeks after injection I found in the SGZ infected stem cells and progeny originating from these cells (**Figure 6.7 B**). I evaluated the efficiency of the DBI KD by

immunohistochemistry and found that cells infected with the KD virus did not present DBI expression. The regions of the SGZ infected with the KD virus showed in average a decrease of 62% in DBI signal indicating that the viral DBI KD was successful (**Figure 6.8 A**).

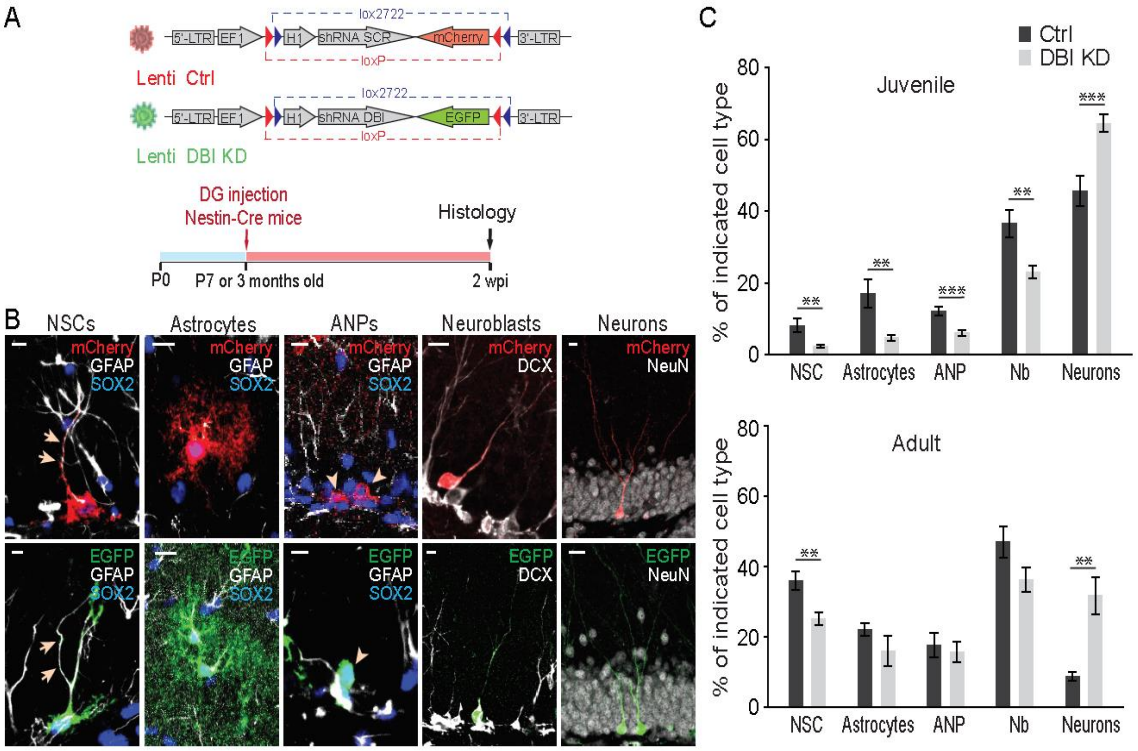

Figure 6.7. DBI KD in stem cells *in vivo* reduces the progenitor pool and favors a neuronal fate.

(A) Top: vector maps of the Cre-dependent DBI KD and the corresponding control lentivirus. Bottom: scheme depicting experimental procedure pertaining to injection of viral mixes of DBI KD and Ctrl lentiviruses into the DG of either P7 (juvenile) or 3-month-old (adult) Nestin-Cre mice.

(B) Examples of SGZ stem cells and their progeny 2 weeks after infection with Ctrl (upper panels, red signal) or DBI KD (lower panels, green signal) lentiviruses, co-immunostained for GFAP (white), SOX2 (blue), DCX (white), or NeuN (white). Arrows point to processes of infected stem cells positive for GFAP, and arrowheads show infected ANPs positive for SOX2, but negative for GFAP.

(C) Graphs show the proportion of the different cell types in the niche quantified as a percentage of all infected cells and expressed as mean ± SEM following DBI KD experiments in juvenile (top) or adult (bottom) NestinCre mice. Juvenile: Ctrl: 776 virus+ cells; DBI KD: 1,973 virus+ cells; n = 10 mice; **p < 0.01; ***p < 0.001; NSCs and astrocytes: Wilcoxon signed-rank test; ANPs, neuroblasts, and neurons: two-tailed paired t test. Adult: Ctrl: 695 virus+ cells; DBI KD: 916 virus+ cells; n = 5 mice; **p < 0.01, two-tailed paired t test. Abbreviations: NSC, neural stem cells; ANP, amplifying neural progenitor; Nb, neuroblast.
Scale bars represent 10 mm. Figure and figure legend were reproduced from Dumitru and colleagues (2017).

I further tested whether the virus led to cytotoxicity or whether DBI KD increased cell death. For this purpose, I measured the number of cells positive for activated Caspase 3 in the DG area infected with KD virus and compared it to the uninfected area. The numbers of cells expressing activated Caspase 3 were not different between the two areas indicating that DBI KD does not increase cell death (**Figure 6.8 B**).

Two weeks after the viral mix injection I evaluated the proportion of labelled NSCs ($GFAP^+/SOX2^+$ RG-like morphology), TACs ($GFAP^-/SOX2^+$), neuroblasts (DCX^+), young neurons ($DCX^-/NeuN^+$), and astrocytes ($GFAP^+$, astrocyte morphology) within the red (control) and green (DBI KD) cell population. In both juvenile (P7) and adult mice, I found a decrease in the proportion of NSCs, TACs, astrocytes and neuroblasts and an increase in the number of adult-born neurons. These results indicate that DBI KD induces a drop in the early progenitor pool and favours a concomitant shift towards a more neurogenic fate (**Figure 6.7 C**). I found higher proportions of stem cells in the adult mice and the speed with which these cells produce neurons was noticeably lower (**Figure 6.7 C**). Therefore, the results obtained in mature mice reproduced the decrease with age in the stem cell pool and the lower speed with which neurogenesis takes place described in previous studies (Encinas et al., 2011; Rao et al., 2005; Riddle and Lichtenwalner, 2007).

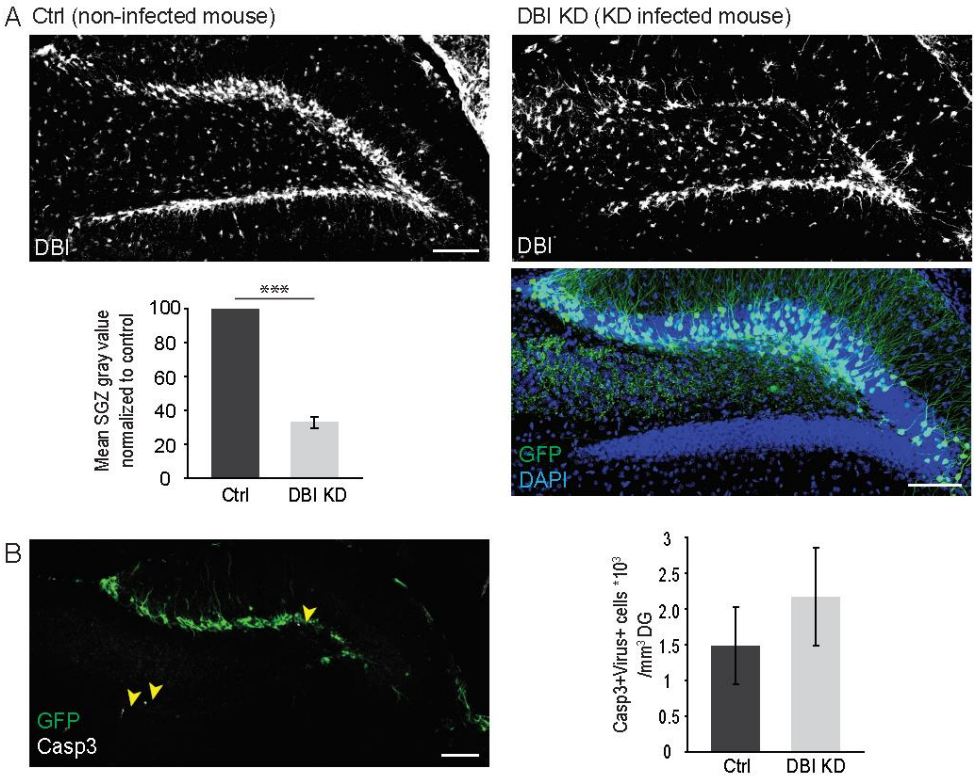

Figure 6.8. Reduced DBI expression does not affect cell survival.

(A) DBI expression visualized as immunostaining (white) in the DG in a control mouse (left panel) and 2 weeks post DBI KD / EGFP lentivirus injection (right panel). The bottom image shows green (DBI KD infected cells) and blue (DAPI) channels from the upper picture providing evidence that the infected upper blade exhibits normal morphology. Quantification of DBI KD effect measured as DBI signal intensity (mean ± SEM, n = 8 images per condition, **p<0.001, two-tailed paired t test).

(B) Representative picture of a DG from a 1-month old NestinCre mouse injected with DBI KD lentivirus, 3 weeks post injection. EGFP expression (green) allows the visualization of lentivirus infected cells. The signal in white indicates ActiveCaspase3 (Casp3) staining. Right: Quantification indicates that there is no difference in the number of apoptotic Casp3+ cells in control and DBI KD mice (mean ± SEM, n = 14 brain sections from 5 mice, p = 0.26, two-tailed paired t test).

Scale bars represent 200 μm in (A) and (B). Figure and figure legend were reproduced from Dumitru and colleagues (2017).

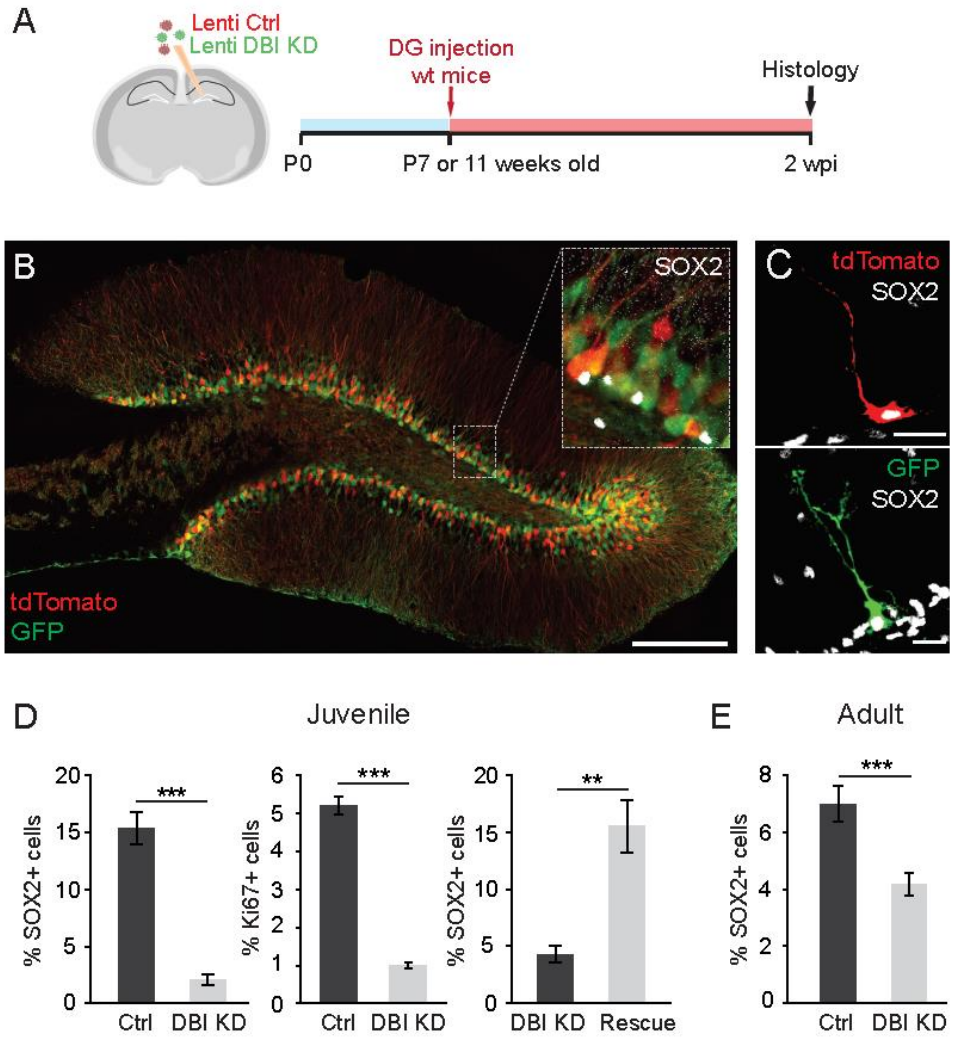

Figure 6.9. DBI KD regulates the production of neuronal progenitors in juvenile and adult mice.

(A) Scheme depicting the experimental protocol.

(B) Overview of the DG in a coronal brain section from a 6 weeks old wild-type mouse infected at 1 month of age with DBI KD (green cells) and Ctrl lentiviruses (red cells).

(C) Example of a Ctrl infected $SOX2^{+}$ (white) RG-like cell in the SGZ expressing tdTomato and a DBI KD infected $SOX2^{+}$ (white) RG-like cell in the SGZ expressing $EGFP^{+}$ (green).

(D) Left: Quantification of $SOX2^+$ progenitors within the DG expressed as percentage (mean ± SEM) of virus infected red (Ctrl) and green (DBI KD) cells, from mice injected at P7 (Ctrl 3824 $virus^+$ cells; DBI KD: 13066 $virus^+$ cells; n = 12 mice, ***p<0.001). Middle: Quantification of $Ki67^+$ progenitors expressed as percentage (mean ± SEM) of virus infected red (Ctrl) and green (DBI KD) cells at 14 days post injection in P7 mice (Ctrl: 532 $virus^+$ cells; DBI KD: 3695 $virus^+$ cells; n = 4 mice; ***p < 0.001; two-tailed paired t test). Right: A viral mix of KD DBIb lentivirus (expressing a shRNA sequence targeting the UTR of the DBI mRNA) and of DBI OE lentivirus (expressing only the coding region) was injected in the DG of P7 mice. The mice were sacrificed 2 weeks after surgery. The graph depicts the quantification of $SOX2^+$ progenitors expressed as percentage (mean ± SEM) of infected cells with either DBI KD lentivirus or with DBI KD plus DBI OE lentivirus (Ctrl 174 $virus^+$ cells; DBI KD 2781 $virus^+$ cells; rescue 179 $virus^+$ cells; n = 7 mice; **p < 0.01; two-tailed paired t test).

(E) Quantification of SOX2+ neural progenitors in 1 month old mice injected with control and DBI KD lentiviruses: Ctrl 737 $virus^+$ cells; DBI KD 6311 $virus^+$ cells; n = 5 mice; ***p < 0.001; two-tailed paired t test).

Scale bars represent 200μm in (B), 20μm in (C). Figure and figure legend were reproduced from Dumitru and colleagues (2017).

To confirm the previous findings and exclude any possible influence of the genetically modified mouse lines, the results were reproduced in a wild type (wt) background. For this purpose I used an alternative approach involving non-Cre-dependent lentiviruses that enable co-expression of the shRNA against DBI and the reporter protein EGFP in all infected cells. As control, I designed a similar lentivirus expressing scrambled shRNA and tdTomato (**Figure 6.9 A**). These viruses have the advantage of infecting and labelling any cell independently of the Cre expression; however, after analysing the infection site, it is not possible to distinguish the cells produced by infected stem cells from the ones which were infected directly by the virus (**Figure 6.9 B**). Therefore, I took recourse to a different analysis strategy by quantifying the percentage of SOX2 progenitors (NSCs and TACs) within the KD and

control infected populations. DBI KD led to a decrease in the percentage of $SOX2^+$ progenitors similar to the results obtained with Cre dependent viruses. Furthermore, the absence of DBI also reduced proliferation within the DBI KD infected population, reproducing the results obtained after conditional DBI KO (**Figure 6.9 D**).

To further test the specificity of the approach, I performed a rescue experiment for DBI KD by co-infecting the cells with a DBI overexpression lentivirus. To this purpose, I designed a lentivirus expressing a shRNA targeting the 5' untranslated region (5'UTR) of the DBI mRNA and EGFP (shRNAb). For the OE I designed a lentivirus expressing DBI linked through the peptide T2A to tdTomato. The shRNAb expressed by the KD virus targeted the endogenous DBI but not the one expressed by the OE virus which does not contain a 5'UTR. By injecting a mix of DBI KD and DBI OE virus in juvenile wt mice I found that overexpressing DBI rescued the KD phenotype to almost control levels indicating the specificity of the performed manipulations (**Figure 6.9 E**).

As a complementary approach to the loss of function experiments, I performed gain of function studies using a viral strategy that allows labelling the stem cells and their progeny and the specific overexpression of DBI in these cells. To this end I designed a lentivirus encoding the floxed and inverted sequence of DBI linked through T2A to tdTomato and controlled by the general promoter EF1. The expression of DBI and tdTomato occurs only after Cre-dependent recombination of the floxed cassette. As control I designed a lentivirus presenting the inverted sequence of EGFP flanked by loxP sites. I injected a mix of the Cre-dependent DBI OE and control lentiviruses in the DG of juvenile (P7) NestinCre mice and analysed the niche two weeks later (**Figure 6.7 A**). I evaluated the proportion of labeled NSCs ($GFAP^+/SOX2^+$ RG-like morphology), ANPs ($GFAP^-/SOX2^+$), neuroblasts (DCX^+), young neurons ($DCX^-/NeuN^+$), and astrocytes ($GFAP^+$, astrocyte morphology) within the red (DBI OE) and green (control) cell populations. In contrast to the results of the KD experiment, DBI OE led to an increase in the proportion of NSCs, TACs and astrocytes and to a decrease in the proportion of adult-born neurons (**Figure 6.10 A**). Upon performing the experiment in adult mice (two months old) I found a similar expansion of the early progenitor population, especially of the stem cell pool and a decrease in the number of

adult-born neurons (**Figure 6.10 B**). To determine whether the expanded stem cell pool leads later on to an increase in neurogenesis I injected a mix of the OE and the control Cre-dependent lentiviruses in the DG of two months old mice and waited for three months to test the long term effects of DBI OE on the niche. After this longer time point I still found a significantly higher number of stem cells in the DBI OE cell population, showing that DBI produces an expansion of the stem cell pool also after long expression times and not only temporarily (**Figure 6.10 B**). There was no difference in the number of mature adult-born neurons between control and OE groups, indicating that the higher number of neuroblasts found two weeks after DBI OE developed into neurons. In addition, this result suggests that DBI OE does not lead to an increase in neurogenesis in the long run but rather expands the progenitor pool (**Figure 6.10 B**). Altogether the results of the gain and loss of function experiments show that DBI is important for regulating the balance between preserving the stem cell pool and neurogenesis in the SGZ.

3.4 DBI and ODN regulate the activity of SGZ NSCs by negatively modulating GABA induced currents via the $GABA_A$ channel

The previous results showed that DBI is important for regulating postnatal and adult SGZ neurogenesis. The next step in understanding the role DBI plays in the SGZ was to determine its action mechanism. DBI has multiple potential action mechanisms; the protein was shown to bind to the benzodiazepine binding site of the $GABA_A$ channel (the central benzodiazepine receptor) and to modulate its activity (Alfonso et al., 2012; Bormann, 1991; Hill et al., 2010). However, DBI also binds to the peripheral benzodiazepine receptor and acts as an acyl-CoA ester transporter (Knudsen et al., 1993; Neess et al., 2015; Rosendal et al., 1993; Selvaraj et al., 2015; Vock et al., 2010). Our lab previously showed that DBI and its cleavage product ODN regulate the proliferation of SVZ TACs by binding to the $GABA_A$ receptor and negatively modulating the GABA currents. Similar to DBI, ODN binds with high affinity to the

$GABA_A$ receptor; however, it binds only with low affinity to the peripheral benzodiazepine receptor and it does not bind acyl-CoA esters. Thus, to determine whether DBI regulates SGZ neurogenesis by modulating the activity of the $GABA_A$ receptor I tested whether overexpressing ODN can reproduce the results obtained by overexpressing DBI. To this end I designed a Cre-dependent lentivirus similar to the one used to overexpress DBI, containing the inverted sequence of ODN in frame with T2A and tdTomato flanked by loxP sites. I used as control a lentivirus containing the inverted sequence of EGFP alone. For both viruses, expression is driven by the general promoter EF1, just as in the case of DBI OE and control virus. I injected a mix of the ODN OE and control lentivirus in the DG of juvenile mice and analyzed the niche two weeks later (**Figure 6.10 C**). After analyzing the different progenitors in the niche I found in the cell population overexpressing ODN considerable more stem cells than in the control infected cells and an increase in the population of TACs and neuroblasts, very similar to the results obtained after overexpressing DBI (**Figure 6.10 C**). Therefore, the results suggest that DBI regulates adult SGZ neurogenesis by modulating the $GABA_A$ receptor.

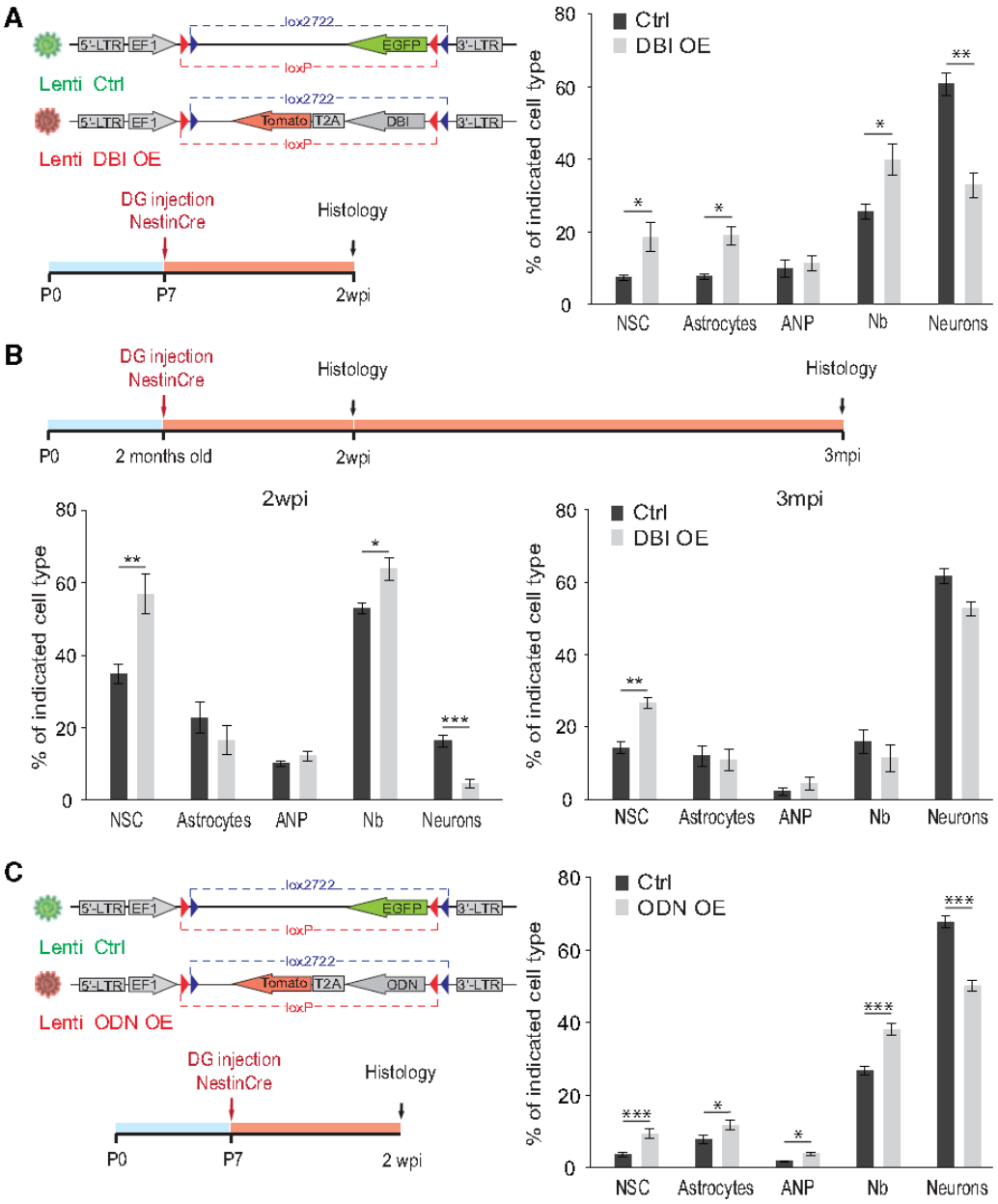

Figure 6.10. DBI/ODN OE in stem cells *in vivo* favors the expansion of the progenitor pool.

(A) Top: vector maps of the Cre-dependent DBI OE and the corresponding control lentivirus. Bottom: scheme depicting experimental procedure pertaining to injection of viral mixes of DBI OE and Ctrl lentiviruses into the DG of P7 NestinCre mice. Right: graph shows the proportion of the indicated cell types in the niche quantified as percentage of all infected cells and expressed as mean ± SEM following DBI OE (Ctrl:

8,114 virus+ cells; DBI OE: 341 virus+ cells; n = 6 mice; *p < 0.05, **p < 0.01; two-tailed paired t test).

(B) Top: scheme depicting experimental procedure. Adult NestinCre mice were injected with viral mixes of DBI OE and Ctrl lentiviruses into the DG and analyzed either 2 weeks or 3 months post injection. Bottom: graphs show the proportion of the indicated cell types in the niche quantified as percentage of all infected cells and expressed as mean ± SEM following DBI OE at either 2 weeks post-injection (left) (Ctrl: 2,862 virus+ cells; DBI OE: 535 virus+ cells; n = 4 mice; *p < 0.05, **p < 0.01, ***p < 0.001; two-tailed paired t test) or 3 months post-injection (right) (Ctrl: 4,096 virus+ cells; DBI OE: 324 virus+ cells; n = 4 mice; *p < 0.05, **p < 0.01, ***p < 0.001; two-tailed paired t test).

(C) Left: vector maps of the Cre-dependent ODN OE with the corresponding control lentivirus and scheme depicting experimental procedure pertaining to injection of viral mixes of ODN OE and Ctrl lentiviruses into the DG of P7 NestinCre mice. Right: graph shows the proportion of the indicated cell types in the niche quantified as percentage of all infected cells and expressed as mean ± SEM following ODN OE (Ctrl: 4,226 virus+ cells; ODN OE: 1,074 virus+ cells; n = 8 mice; *p < 0.05, ***p < 0.001; two-tailed paired t test).

Abbreviations: NSC, neural stem cells; ANP, amplifying neural progenitor; Nb, neuroblast. Figure and figure legend were reproduced from Dumitru and colleagues (2017).

To directly measure whether DBI influences the activity of the receptor in stem cells I generated a lentivirus expressing tdTomato driven by a GFAP promoter that allows the identification of the NSCs in acute brain slices (**Figure 6.11 A**). I injected this lentivirus in the DG of juvenile mice and one to two weeks later Angela Neitz patched cells in the SGZ expressing tdTomato and having a RG-like morphology.

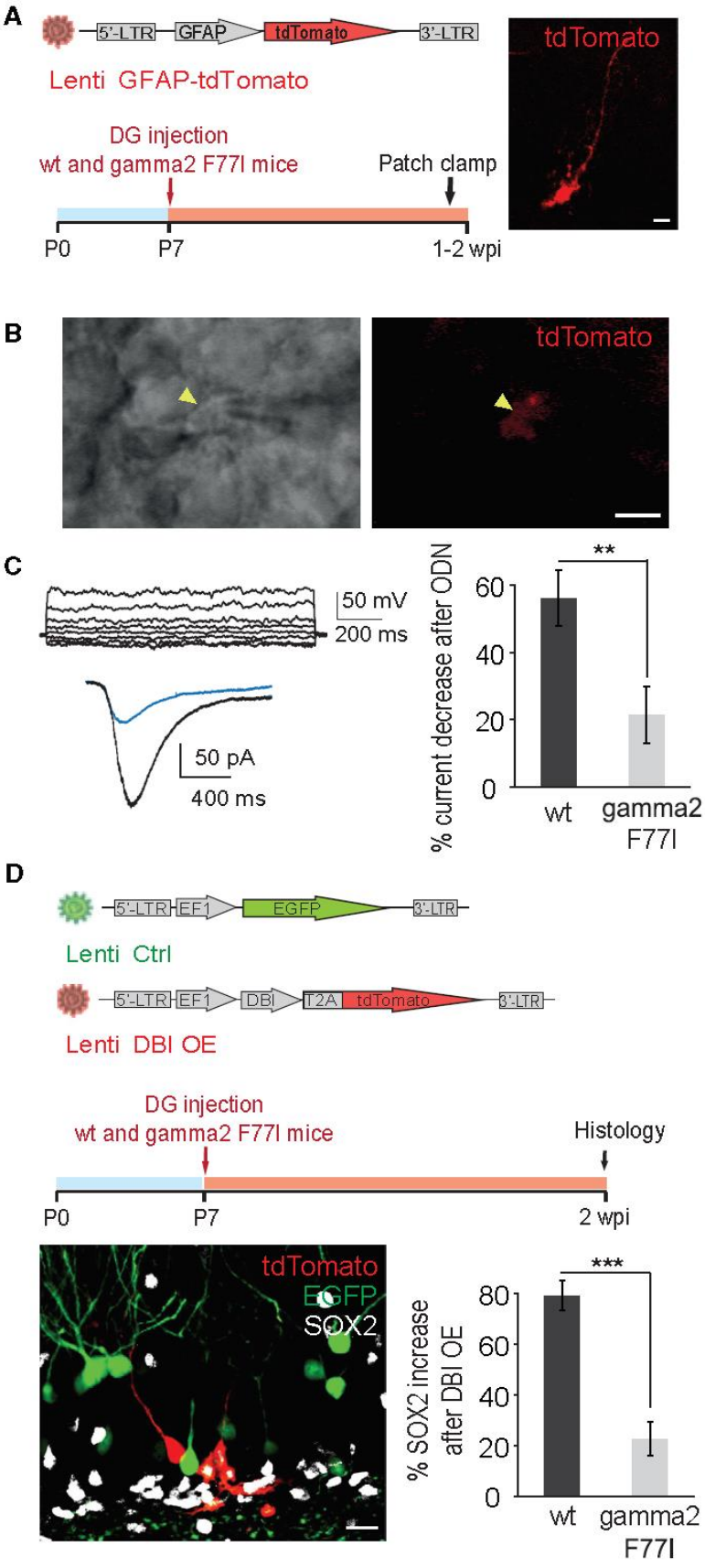

Figure 6.11. DBI reduces $GABA_A$-induced currents in hippocampal NCSs, thereby affecting the progenitor pool.

(A) Left: scheme depicting the lentiviral construct and the experimental procedure: a lentivirus expressing tdTomato from a GFAP promoter was injected in the DG of either wild-type or gamma2 F77I mice at P7. Mice were sacrificed between 1 and 2 weeks after injection, and patch clamp recordings were performed on $tdTomato^+$ cells. Right: representative image of an infected $tdTomato^+$ RG-like cell in the SGZ 1 week after injection.

(B) Left: a light microscope image of a patched stem cell. The cell is indicated by the

arrowhead, and the tip of the patch pipette is visible on the right side of the cell. Right: tdTomato expression in the same patched stem cell, indicated by the arrowhead.
(C) Left top: recordings from a fluorescently labeled stem cell that does not exhibit action potentials following 20 pA current steps ranging from -100 pA to 100 pA injected into the cell soma. Left bottom: representative example showing inward currents obtained in response to local puff application of GABA (black trace) or GABA plus ODN (blue trace) in a wild-type stem cell. Right: quantification of current responses obtained by local puff application of GABA plus ODN in wild-type stem cells (black bar) and gamma2 F77I mutant stem cells (gray bar). Each bar represents the GABA current in the presence of ODN expressed as a percentage of the current in the absence of ODN (mean ± SEM; wild-type: 11 cells in 4 mice; gamma2 F77I: 11 cells in 6 mice; **$p < 0.01$; two-tailed t test).
(D) Top: scheme depicting the lentiviral constructs and the experimental procedure: a mix of DBI OE and control lentiviruses was injected in the DG of either wild-type or gamma2 F77I mice at P7. Mice were sacrificed 2 weeks after injection. Bottom: a representative picture of virally infected cells positive for SOX2 in a wild-type mouse and quantification of $SOX2^+$ cells overexpressing DBI (quantified as the increase in the percentage of $SOX2^+$ cells when comparing control-infected cells and DBI OE cells) in wild-type (black bar) or in gamma2 F77I mice (gray bar) (mean ± SEM; wild-type Ctrl 3,132 $virus^+$ cells; wild-type DBI OE: 372 virus+ cells; n = 9; gamma2 F77I Ctrl: 3,965 $virus^+$ cells; gamma2 F77I DBI OE: 1,582 $virus^+$ cells; n = 8 mice; ***$p < 0.001$; Mann-Whitney rank-sum test).
Scale bars in (A) and (B) represent 10 mm. Figure and figure legend were reproduced from Dumitru and colleagues (2017). All electrophysiological measurements were performed by Angela Neitz.

The SGZ NSCs display particular electrophysiological characteristics, different from neurons: they have a high input resistance and do not fire after current injection. The stem cells also express $GABA_A$ receptors and present tonic GABA responses which are enhanced by the GABA agonist muscimol and by benzodiazepines like diazepam and are abolished by the GABA antagonist bicuculine (Shin et al., 2011;

Song et al., 2012). Therefore, we selected the cells that had electrophysiological characteristics of stem cells and measured GABA induced currents in voltage clamp mode at a holding potential of -60mV after applying puffs of either GABA or GABA and ODN (**Figure 6.11 A-C**). As expected, we found currents after GABA application. Furthermore, these currents were partially inhibited by co-application of ODN, indicating that DBI and respectively ODN can bind to the $GABA_A$ receptors on the stem cells and negatively modulate the activity of the channel (**Figure 6.11 C**).

The next step was to determine whether DBI binding to the benzodiazepine binding site was mediating the phenotypes found after DBI KD and DBI OE. To answer this question we made use of mice carrying a phenylalanine (F) to isoleucine (I) substitution at position 77 in the N-terminal domain of the γ_2 subunit (gamma2 F77I); mutation which reduces binding to the benzodiazepine binding site (Cope et al., 2004; Ogris et al., 2004). Patch clamp measurements in the gamma2 F77I mice showed that the ODN-mediated reduction in GABA currents was almost abolished in mutant NSCs, indicating that ODN negatively modulates the activity of the $GABA_A$ channel by binding to the benzodiazepine binding site (**Figure 6.11 C**).

If DBI regulates the activity of the stem cells via this mechanism, the effects should be diminished in the gamma2 F77I mice. To test this hypothesis I injected in the DG of juvenile gamma2 F77I and wt mice a mix of DBI OE and control lentiviruses and evaluated the proportion of $SOX2^+$ progenitors within the OE and control cell populations. The wt mice showed an increase in the proportion of $SOX2^+$ progenitors as described before; however, I found a drastically mitigated effect in the gamma2 F77I mice (**Figure 6.11 D**). Altogether, the data presented indicate that DBI regulates the activity of the SGZ NSCs by binding to the $GABA_A$ receptor and negatively modulating the GABA induced currents.

3.5 DBI is required for the pro-proliferative effect of voluntary exercise and enriched environment

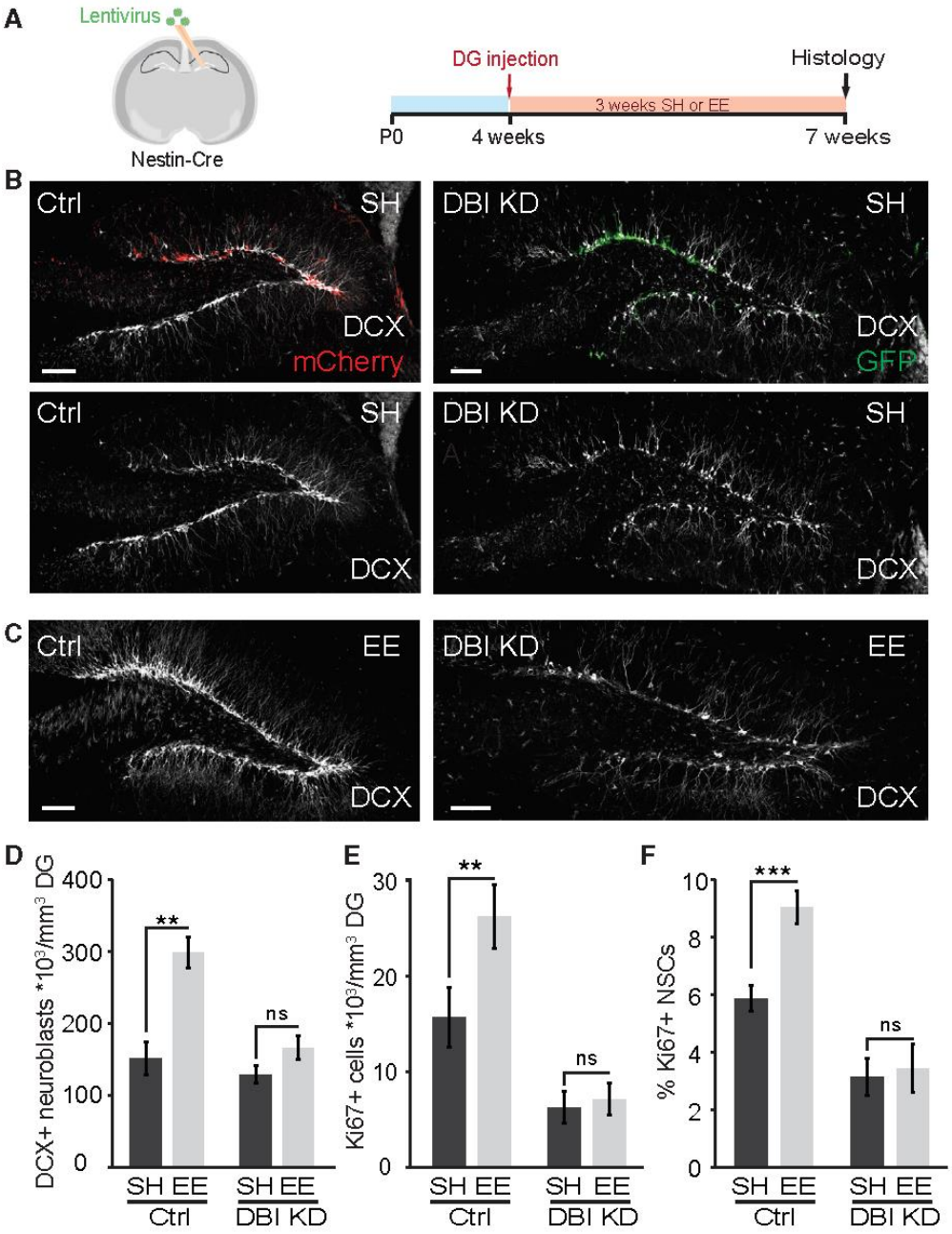

Figure 6.12. DBI KD prevents the pro-neurogenic effect of EE.

(A) Schematic drawing depicting the experimental protocol.

(B) Coronal brain sections showing a representative Ctrl (left) and DBI KD (right)-infected DG from mice kept in standard housing (SH). Upper panels show double labeling for DCX (white) and mCherry (red) or EGFP (green). Lower panels show DCX labeling only for better visualization of the signal.
(C) Coronal brain sections showing DCX labelling (white) in a representative Ctrl (left) and a DBI KD (right) DG from mice kept in an enriched environment (EE).
(D) Quantification of DCX+ neuroblasts per mm3 (mean ± SEM) in non-infected DGs (Ctrl) and in DBI KD-infected DGs from mice housed in SH or EE (Ctrl non-infected SH: 2,997 cells in 9 mice; Ctrl non-infected EE: 7,576 cells in 12 mice; infected with DBI KD virus SH: 3,269 cells in 7 mice; infected with DBI KD virus EE: 4,404 cells in 9 mice; $^{**}p < 0.01$; Mann-Whitney rank-sum test).
(E) Quantification of Ki67+ cells per mm3 (mean ± SEM) in non-infected DGs (Ctrl) and in DBI KD DGs from mice housed in SH or EE (Ctrl non-infected SH: 307 cells in 9 mice; Ctrl non-infected EE: 1,043 cells in 13 mice; infected with DBI KD virus SH: 80 cells in 6 mice; infected with DBI KD virus EE: 175 cells in 9 mice; $^{**}p < 0.01$; two-tailed t test).
(F) Percentage of proliferating NSCs (mean ± SEM) in non-infected DGs (Ctrl) and in DBI KD-infected DGs from mice housed in SH or EE (Ctrl non-infected SH: 1,971 RG-like $Nestin^+/SOX2^+$ cells in 10 mice; Ctrl non-infected EE: 2,111 RG-like $Nestin^+/SOX2^+$ cells in 12 mice; injected with DBI KD virus SH: 3,233 RG-like $Nestin^+/SOX2^+$ cells in 7 mice; injected with DBI KD virus EE: 1,625 RG-like $Nestin^+/SOX2^+$ cells in 8 mice; $^{***}p < 0.001$; two-tailed t test).
Scale bars represent 100 mm. Figure and figure legend were reproduced from Dumitru and colleagues (2017).

A natural question that follows in this study relates to the physiological function of DBI in the SGZ. I found that DBI is important for regulating the activity of the SGZ NSCs by modulating GABA signaling. GABA influences SGZ neurogenesis at multiple levels and was proposed to couple the electrical activity in the hippocampus to the dynamics of SGZ neurogenesis. Furthermore, optogenetic silencing of the DG PV-positive interneurons abolished the survival increase found after EE. This finding

suggests that GABA signaling is responsible for mediating the pro-neurogenic effect of EE to the SGZ niche (Song et al., 2013). Therefore, I investigated whether DBI plays a role in regulating SGZ neurogenesis in special situations like EE and physical exercise. To test this hypothesis I injected in four weeks old Nestin-Cre mice Cre-dependent DBI KD lentivirus and used the non-infected DG as control. The mice were housed in EE with free access to running wheels for three weeks after which they were sacrificed (**Figure 6.12 A**). I analyzed the number of DCX^+ neuroblasts present in the DG infected with KD virus and compared it to non-infected DGs. As expected, EE and voluntary running lead to a strong increase in the number of neuroblasts; however, DBI KD prevented this increase (**Figure 6.12 B-D**). Voluntary exercise was shown to enhance the activation of the NSCs and especially to increase the proliferation of NSCs and of TACs (Dranovsky et al., 2011; Gebara et al., 2016; Kempermann et al., 1997). Data presented in this study shows that DBI is important for progenitor proliferation. After analyzing the number of $Ki67^+$ cells in the SGZ I found a strong increase in SGZ proliferation after EE and voluntary exercise, as described in previous studies (Kempermann et al., 1997). However, this effect was abolished by DBI KD (**Figure 6.12 B, C and E**). DBI is strongly expressed in SGZ NSCs and I showed before that DBI is important for regulating their activity; therefore, I tested the proliferation rate of the SGZ NSCs in the KD and control DGs. As expected, EE and physical exercise lead to an increase in SGZ NSCs proliferation, increase which was abolished by the absence of DBI (**Figure 6.12 B, C and F**). Thus, the present data show that DBI is essential for the pro-neurogenic and especially for the pro-proliferative effect of enriched environment and physical exercise.

To avoid any possibility that the effects found were caused by the viral manipulation I repeated the experiment by injecting 4 weeks old mice with control Cre-dependent lentivirus and used as control the non-infected DGs. After housing the mice for 3 weeks in EE with free access to running wheels I found in both the control infected DGs and in the non-infected DGs a strong increase in the number of neuroblasts. Therefore, the abolished pro-neurogenic effect of EE found after DBI KD was caused by the absence of DBI and not by the viral manipulation (**Figure 6.13 A**).

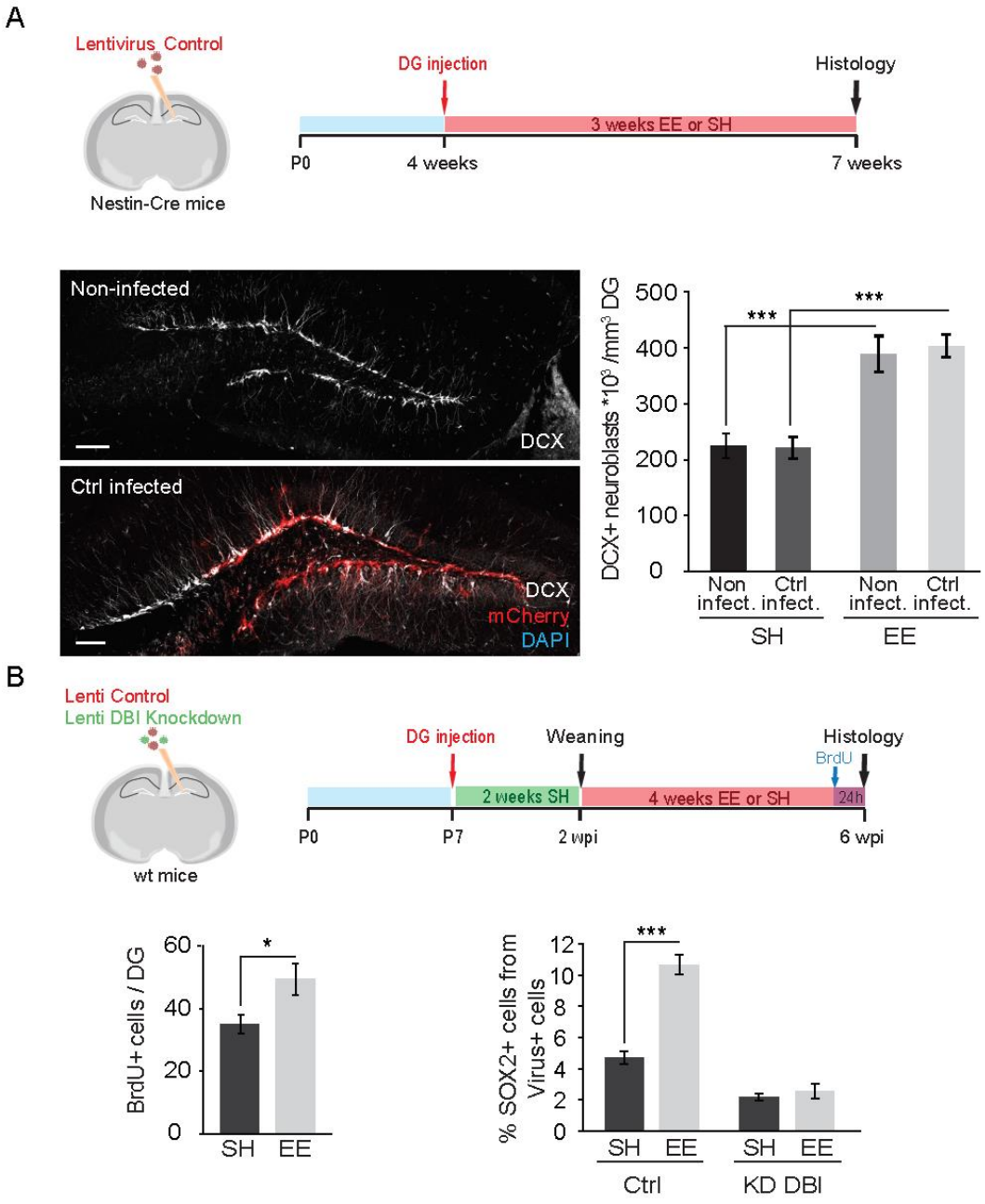

Figure 6.13. DBI regulates the SGZ stem cell niche under EE.

(A) Top: Scheme depicting the experimental setup. Bottom left: Coronal brain sections showing an overview of a non-infected (upper panel) and an infected DG with Ctrl virus (red for mCherry) (lower panel). The brain slices were stained for DCX (white). Bottom right: Quantification of the number of DCX+ neuroblasts per mm3 (mean ±

SEM) in non-infected DGs and Ctrl lentivirus infected DGs from mice kept either under SH (non-infected DGs: 1459 cells; DGs infected with Ctrl lentivirus expressing scrambled shRNA and mCherry: 2303 cells; n = 6 mice) or EE conditions (non-infected DGs: 4039 cells; DGs infected with Ctrl lentivirus expressing scrambled shRNA and mCherry: 4412 cells; n = 5 mice, ***p<0.001, one-way ANOVA followed by Holm-Sidak method for all pairwise comparison). There is no significant differences between non-infected and Ctrl-infected DGs from mice kept under similar conditions.
(B) Top: Schematic depicting the experimental setup. Bottom left: Quantification of BrdU+ cells (mean ± SEM) per DG slice in SH and EE housed mice (SH: n = 16 mice; EE: n = 15 mice; *p < 0.05; two-tailed t test). Bottom right: Quantification of $SOX2^+$ progenitors expressed as percentage (mean ± SEM) of infected cells in Ctrl $virus^-$ and KD DBI virus-injected mice kept under SH or EE conditions (SH Ctrl: 1031 $virus^+$ cells in 16 mice; EE Ctrl 518 $virus^+$ cells in 15 mice; SH KD DBI: 8756 $virus^+$ cells in 16 mice; EE KD DBI 5443 $virus^+$ cells in 15 mice; ***p < 0.001; two-tailed paired t test).
Abbreviations: SH – standard housing, EE – enriched environment. Scale bars represent 100μm. Figure and figure legend were reproduced from Dumitru and colleagues (2017).

Similar results were obtained when DBI ablation was achieved by non-Cre-dependent lentiviruses in wt mice (**Figure 6.13 A**). EE and Physical exercise increase the number of $SOX2^+$ progenitors in SGZ because of the enhanced proliferation and survival of the neural progenitors (Fabel et al., 2009; Gebara et al., 2016; Kronenberg et al., 2003; Vivar et al., 2013). DBI KD inhibited almost completely the pronounced increase in $SOX2^+$ progenitors in the DG of mice subjected to EE (**Figure 6.13 B**). These results are further proving that DBI is required to promote the pro-neurogenic and pro-proliferative effect of EE and exercise.

4. Discussion

4.1 DBI is expressed in embryonic and adult neural stem cells

DBI is highly expressed in certain areas of the adult brain such as the walls of the lateral and 3rd ventricle, the RMS and the hippocampus (Alfonso et al., 2012; Alho et al., 1989; Alho et al., 1985; Alho et al., 1991; Alho et al., 1995). In the SVZ, DBI is strongly and specifically expressed in all NSCs and in a population of TACs (Alfonso et al., 2012). I investigated in this study the presence of DBI in the other postnatal and adult neurogenic niches. After a detailed immunohistological analysis I found that DBI is strongly expressed in the SGZ, both in juvenile and in adult mice and is specifically localized in stem cells and early progenitors. DBI expression levels decline along with the developmental stage of the SGZ neural progenitors, resembling its expression pattern in the SVZ. The early proliferative TACs still express high levels of the protein; however, the late and more committed Type 2b cells, show low DBI expression as reflected both by the number of DBI-positive cells and their expression levels. Finally, only few neuroblasts express DBI, albeit at very low levels, while in mature neurons DBI signal is not detectable.

Multiple factors are expressed both in SVZ and SGZ neural progenitors. Well characterized stem cell markers like Nestin, SOX2 and GFAP, as well as factors important for the differentiation of neuronal progenitors including Mash1, Tbr2 and NeuroD are present in both niches (Kempermann et al., 2015). These proteins are often essential during basic processes in the biology of stem cells and early progenitors. Meanwhile, other proteins are found exclusively in one niche. These are often factors responsible for cell commitment to a certain fate (Kempermann et al., 2015; Lim and Alvarez-Buylla, 2016). Indeed, these factors drive SVZ-derived progenitors to produce GABAergic neurons or SGZ-derived progenitors to produces glutamatergic neurons. Such an example is Prox1 which is expressed only in SGZ progenitors and is essential for determining granule cell fate (Lavado et al., 2010). Olig2 is preferentially expressed in the SVZ and is responsible for generating oligodendrocytes, which are only produced in very small numbers in the SGZ (Kempermann et al., 2003; Steiner et al.,

2004). The presence of DBI in stem cells and uncommitted TACs from both the SVZ and SGZ suggests that the function of this protein might be related to early cellular processes in neurogenesis, general to different neurogenic niches. Thus, it is likely that DBI is expressed in other neural stem cells regardless of the niche they are populating. I also explored the presence of DBI in the less described neurogenic niche localized close to the hypothalamus, namely the wall of the 3rd ventricle. Using immunohistochemistry I found that DBI is strongly expressed in all Nestin^{+} SOX2^{+} Tanycytes lining the walls of the 3rd ventricle. The α-Tanycytes populating the ventral wall of the 3rd ventricle were shown to act as stem cells and to postnatally produce neurons that integrate into the surrounding parenchyma and are important for regulating feeding behavior and fat metabolism (Dietrich and Horvath, 2012; Lee et al., 2012). Interestingly, a previous study suggested that DBI is involved in regulating energy homeostasis (Compere et al., 2010).

Adult neurogenesis recapitulates the stages of embryonic neurogenesis and shares many regulatory factors and mechanisms. Therefore, I investigated the presence of DBI during embryonic development and found that all Nestin^{+} SOX2^{+} RG cells strongly express DBI at E 13,5. DBI is present in the ventricular and subventricular zones of both the neocortex and the ganglionic eminences. Thus, DBI is not only expressed in all adult neural stem cells but also in RG cells during embryonic development. Embryonic RG cells and adult NSCs display both similarities and differences. During embryonic development RG cells must divide quickly to produce a high number of neurons and glial cells that compose the brain; therefore, they are highly proliferative (Arai et al., 2011; Gotz and Huttner, 2005). At early embryonic stages (E11.5 –E14.5) all RG cells produce neurons and already express high levels of neurogenic fate determinants. Thus, RG cells resemble more the TAPs found in adult neurogenesis (Gotz et al., 2016). Adult NSCs present several similarities to glial cells. However, they must present extra mechanisms to ensure the preservation of the stem cell pool and of multipotency over longer periods of time (Gotz et al., 2016). Adult NSCs divide less than RG cells, have a much longer cell cycle and present very low levels of neurogenic fate determinants (Arai et al., 2011; Beckervordersandforth et al., 2010; Bonaguidi et al., 2011; Gotz and Huttner, 2005; Gotz et al., 2016; Morshead et al., 1994). The

presence of DBI in both embryonic and adult neural stem cells suggests that DBI plays a role in regulating fundamental processes in the biology of the early neural progenitors. There are numerous examples of factors that regulate the activity of the stem cells and are present both during embryonic and adult neurogenesis such as wnt, notch, sonic hedgehog and bone morphogenetic protein (BMP) (Gotz et al., 2016; Urban and Guillemot, 2014). Some factors play similar roles while others produce completely different outcomes in RG cells and adult NSCs. A good example is BMP which keeps the stem cells proliferating in the embryo while it promotes quiescence of the stem cells in the adult brain (Caronia et al., 2010; Mira et al., 2010; Urban and Guillemot, 2014). Therefore, it will be interesting to determine in the future whether DBI plays similar roles in embryonic and adult neurogenesis and whether it acts via similar mechanisms.

DBI is present in all eukaryotes and is highly conserved; therefore, I tested whether DBI is present also in adult neurogenic niches from other species. In the Rhesus monkey, an immunohistological analysis showed that DBI is strongly expressed in the SGZ and is present in all $GFAP^+$ $SOX2^+$ RG-like putative NSCs. DBI is also expressed in $SOX2^+$ cells which do not display a RG-like morphology suggesting its presence also in TACs. In human tissue, I found that DBI is present in the SGZ, localized in GFAP+ cells. Unfortunately, there are few studies targeting the human SGZ and therefore also few tools available to study the niche. Many antibodies used to detect well-established markers for the identifications of adult neural progenitors do not provide good results in the human tissues. Furthermore, the suboptimal postmortem tissue preparation and fixation further decrease the quality of the immunostainings. Therefore, technical issues prevented a precise identification of the cell types expressing DBI. The protein co-localizes in the adult human SGZ with $GFAP^+$; however, it was not possible to determine whether these $GFAP^+$ cells were astrocytes or SGZ NSCs.

DBI is thus expressed in all adult neurogenic niches in mice and across species in the adult SGZ in the rhesus monkey and in humans. Furthermore, DBI is strongly expressed during development in RG stem cells. The presence of the protein in all neurogenic niches indicates a strong connection between DBI and neurogenesis.

Moreover, the expression of DBI completely overlaps with the expression pattern of SOX2, which is a well-known stem cells marker and an essential factor for the induction and maintenance of self-renewal and pluripotency (Zhang and Cui, 2014). Furthermore, high DBI expression also overlaps with Nestin expression in the nervous system. Therefore, high DBI expression represents a potential marker for neural stem cells and a potential indicator for stemness in the nervous system.

4.2 DBI is important for regulating the balance between preserving the progenitor pool and generating neurons

DBI plays an important regulatory role in the SVZ. SGZ and SVZ present many similarities and share common regulatory mechanisms. Thus, I investigated the potential of DBI as a regulator of postnatal and adult SGZ neurogenesis. To this end I took recourse to three in vivo strategies to manipulate DBI expression levels in the SGZ NSCs: an inducible genetic system (NestinCre^{ERT2}/DBI$^{lx/lx}$ mouse line in which DBI can be deleted specifically in the Nestin expressing stem cells and in their progeny after tamoxifen administration); a combination of a genetic system (Nestin-Cre mouse line) and lentiviral injections in the DG which allows specific labeling and DBI KD or OE in stem cells and their progeny; and injections of lentiviruses that knockdown or overexpress DBI in the DG of wt mice. The NestinCre^{ERT2}/DBI$^{lx/lx}$ mice allowed me to determine the role DBI plays in the SGZ without the usage of any viral manipulation. However, DBI KO is only partial and one cannot determine with certainty which cells lack DBI. The combination of Nestin-Cre mice and Cre-dependent lentiviruses allowed the specific labeling of SGZ stem cells and their progeny and the manipulation of DBI expression levels in these cells. Using this strategy we could achieve almost complete DBI KD and strong DBI OE in the infected cells and determine the role DBI has in the SGZ NSCs. Furthermore, in this technique, one targets the SGZ without affecting the other postnatal neurogenic niches which also present Nestin expressing progenitors. Last but not least the lentiviral injection in wt mice allowed me to test the effects I found with the other methods in a wt background without any genetic modifications

that could influence the results. Thus, each strategy has advantages and disadvantages but together they constructed a clear image of the role DBI has in the SGZ and confirmed that the phenotypes found were caused by changes in DBI expression levels and not by technical artifacts.

All three techniques showed that reducing or ablating DBI expression in stem cells leads to a reduction of the population of SGZ NSCs while DBI OE leads to an expansion of the stem cell pool, indicating the importance of DBI for regulating the activity of SGZ NSCs. Viral DBI KD infections analyzed after a short period of time (2 weeks post injection) resulted also in a decrease in the number of TACs, astrocytes and neuroblasts and to an increase in the number of adult-born neurons. At the same time, DBI OE infections analyzed at similar time post injection had opposite effects leading not only to an expansion of the pool of SGZ NSCs but also of TACs, neuroblasts and astrocytes and to a decrease in the number of adult-born neurons. Long-term (3 months post injection) DBI OE treatment resulted in an expanded stem cell pool; however, the number of neuroblasts and adult-born neurons produced by the cells overexpressing DBI were comparable to controls. Thus, DBI ablation increases neuronal differentiation while DBI OE expands the pool of early progenitors.

The most remarkable finding associated with manipulating DBI OE is the expansion of the SGZ stem cell pool. The most plausible scenario is that DBI keeps the stem cells into symmetric proliferation enhancing self-renewal. Three months after DBI OE, the expansion of the NSCs pool persisted in the SGZ, indicating that DBI is a potent regulator of self-renewal even after long periods of high expression levels. After longer DBI OE the number of neuroblasts and adult-born neurons was not different from the control population. In the SVZ DBI was shown to increase the number of cell-divisions without affecting the cell cycle length (Alfonso et al., 2012). Therefore, DBI OE in the SGZ most likely enhances symmetrical division of the stem cells and increases the number of times the TACs reenter the cell cycle. In this case, the early progenitors would undergo more rounds of division which would delay their differentiation. Thus, one finds after short term DBI OE a higher number of early progenitors but a lower number of adult-born neurons. After a long period of DBI OE the progenitors overexpressing DBI would have enough time to exit cell cycle and

become adult-born neurons. This would explain why the difference between the number of neuroblasts produced in the OE and the control population disappears. However, three months of DBI OE did not lead to an increase in the number of adult-born neurons. Therefore, DBI enhances the pool of stem cells but does not finally lead to an increase in neurogenesis under homeostatic conditions, even after longer time points. This indicates that DBI might be responsible for maintaining the SGZ stem cell pool rather than for neuron production. However, even though in homeostatic conditions the increased stem cell population does not lead to an increase in neurogenesis, the additional stem cells could be used to produce more neurons in specific situations.

4.3 DBI regulates the activity of neural stems cell by negatively modulating GABA-mediated currents

DBI plays an important role in regulating postnatal and adult SGZ neurogenesis. An important step in understanding the role of DBI as a neurogenic regulator is to determine its mechanism of action. DBI was shown before to act as a negative modulator of the $GABA_A$ receptor (the central benzodiazepine receptor) in cultured spinal cord neurons (Bormann et al., 1985; Costa and Guidotti, 1991). In addition, DBI binds to the TSPO receptor (the peripheral benzodiazepine receptor) and regulates the cholesterol flow into the mitochondria (Selvaraj et al., 2015; Vock et al., 2010). Moreover, DBI also binds acyl-CoA esters and acts as an acyl-CoA ester transporter and pool former playing an important role in lipid metabolism (Knudsen et al., 1993; Neess et al., 2015; Rosendal et al., 1993). Therefore, there are several potential molecular mechanisms via which DBI could influence SGZ neurogenesis. Our lab showed that in the SVZ, DBI negatively modulates the activity of the $GABA_A$ receptor in TACs and enhances their proliferation via this mechanism and not through its binding to the TSPO. Similar to its action in the SVZ, DBI increased the proliferation of SGZ NSCs and TACs via binding to the $GABA_A$ receptor. Electrophysiological recordings from SGZ stem cells during application of GABA or GABA plus ODN

showed that ODN significantly reduces GABA induced currents. The reduction in GABA currents induced by ODN was strongly diminished in gamma2 F77I mice, which present a mutation in the gamma2 subunit of the GABAA receptor that decreases binding to the benzodiazepine binding site. This confirms that ODN negatively modulates the activity of the $GABA_A$ receptor by binding to the benzodiazepine binding site. This mouse line constitutes an optimal system to test whether DBI modulates neurogenesis via the $GABA_A$ receptor. If DBI is regulating SGZ neurogenesis by modulating $GABA_A$ currents, DBI and ODN should have an ameliorated phenotype in the mice presenting the gamma2 F77I mutation. Indeed overexpressing DBI in the gamma2 F77I mutant mice prevented the phenotype found in wt mice; namely an expansion of the pool of $SOX2^+$ early progenitors. This experiment constitutes a definitive proof to conclude that DBI regulates the activity of the SGZ stem cells and thereby SGZ neurogenesis by binding to the benzodiazepine binding site of the $GABA_A$ receptor. One cannot exclude the possibility of DBI acting also via TSPO or via its function as acyl-CoA esters reservoir; however, this is unlikely as ODN OE reproduced the effects found after DBI OE and ODN binds only with low affinity to TSPO and lacks the aminoacid residues necessary for binding acyl-CoA esters. Furthermore, inhibiting *in vitro* the activity of TSPO did not interfere with DBI's pro-proliferative phenotype in SVZ progenitors while reducing its binding to the $GABA_A$ receptor by competitive inhibition almost abolished the phenotype. These results are further proof that DBI does not regulate neurogenesis via TSPO but via the $GABA_A$ receptor.

The studies undertaken by Song et al. found a 'diametric regulation' of stem cell proliferation and of TAC and neuroblast survival in the SGZ niche. Tonic GABA, spilled-over from the synapses of PV-positive interneurons was shown to keep the stem cells quiescent and to reduce the proliferation of the activated stem cells (Song et al., 2012). PV-positive interneurons make immature synapses with the newborn progeny, providing their first phasic input and supporting their survival and development (Song et al., 2013). Thus, GABA seems to keep the SGZ stem cells quiescent and at the same time to have a pro-survival effect in TACs and neuroblasts. I showed that DBI regulates SGZ neurogenesis by negatively modulating GABA signaling in NSCs and

TACs. Therefore, the results presented in this study fit very well with the data presented by the Song lab. DBI KD, which results in enhanced GABA signaling, leads to a reduction in the number of stem cells and TACs, similarly to the findings obtained by increasing GABA currents with either benzodiazepines or optogenetically. DBI OE has opposite effects to DBI KD and similar results to reduced GABA signaling, namely enhanced stem cell activation and enhanced proliferation. Furthermore, the effects found by the Song lab were dependent on the presence of the γ_2 subunit of the $GABA_A$ receptor (Song et al., 2013). DBI binds to the benzodiazepine binding site of the receptor present on the extracellular side between the α and the γ_2 subunits. Along the same lines, diazepam treatment increases GABA signaling and reduces stem cell proliferation in the SGZ (Song et al., 2013). Meanwhile, deletion of the γ_2 subunit, which would correspond to reduced GABA currents, leads to similar results as DBI OE, namely increased stem cells activation, increased stem cell symmetrical division, and self-renewal (Lorez et al., 2000). Furthermore, deleting of the γ_2 subunit leads to an increase in the astrocyte generation, phenotype which was also found after DBI OE (Song et al., 2013). The very similar effects obtained either by directly manipulating GABA signaling or by manipulating DBI expression levels provide further proof that DBI regulates adult SGZ neurogenesis by negatively modulating GABA signaling via the γ_2 containing $GABA_A$ channel.

Numerous reports show that DBI acts as a negative allosteric modulator of the GABA receptor both in cultured spinal cord neurons as well as in neural progenitors (Alfonso et al., 2012; Bormann et al., 1985; Costa and Guidotti, 1991). However, in neurons of the thalamic reticular nucleus, DBI was found to act as a positive modulator of the $GABA_A$ receptor (Christian et al., 2013; Farzampour et al., 2015). A possible explanation for the activity of DBI as a dual modulator can be found in the subunit composition of the $GABA_A$ channels present in the membrane of the stem cells and of the thalamic neurons. The $GABA_A$ receptor is a heteropentameric channel composed of 2α, 2β and a γ or a δ subunit. There are six types of α subunits, three types of β subunits and 3 types of γ subunits (Sieghart, 2015; Sigel and Buhr, 1997). Different combination of the possible α,β and γ subunits of the $GABA_A$ channel could be responsible for the different actions of DBI. Thus, DBI could differently regulate the cells present in the

niche according to the types of $GABA_A$ receptors they express. The measurements undertaken in this study demonstrate that DBI negatively modulates the activity of the $GABA_A$ receptor present on SGZ NSCs. Whether DBI plays a different role in other cells in niche is to be tested in the future. However, this perspective is unlikely as DBI is only expressed in the SGZ NSCs and TACs and in a very small number of neuroblasts. Moreover, DBI was shown to negatively modulate GABA currents in SVZ TACs and neuroblasts and it is likely that it exerts a similar action in the SGZ. However, the mechanistic details which allow DBI to acts as both a positive and a negative modulator of the $GABA_A$ receptor and whether DBI could also act as a positive modulator in the SGZ remain to be elucidated in the future.

It is still an open question whether the DBI produced by the stem cells acts in a solely autocrine fashion or it could also diffuse to surrounding neuroblasts and neurons. The results presented here render the possibility of a paracrine action unlikely as in the experiments using lentiviral strategies, cells overexpressing DBI were closely located to control cells. In spite of this proximity, large differences were found between the OE and control cells. This indicates that DBI acts in an autocrine fashion. However, the results presented here cannot exclude an influence of DBI on the neighboring cells. Furthermore, the results obtained for the control populations in the KD and in the OE experiments were not identical. This could be caused by technical differences between the viruses or by DBI diffusing from the OE infected cells to the control infected cells. Therefore, the possibility of DBI acting in a paracrine fashion cannot be completely excluded.

DBI adds another regulatory component to the current models of adult neurogenesis. According to the model proposed by Encinas and colleagues, a quiescent RG-like stem cell divides about three times asymmetrically, giving rise to another stem cell and to an intermediate progenitor, and subsequently transforms into an astrocyte (Encinas et al., 2011). In this model, a depletion of stem cells would ensue over time, which would explain the age dependent decrease in neurogenesis. In the model proposed by Song and colleagues, RG-like quiescent stem cells are thought either to be activated and undergo asymmetric division producing ANPs and astrocytes, or to divide symmetrically, giving rise to two RG-like stem cells (Bonaguidi et al., 2011). In

this model, symmetric division of the NSCs supports the expansion of the stem cell pool. Further experiments will hopefully shed light on the validity of these models (Bonaguidi et al., 2012). However, in both scenarios, by modulating the proliferation of the SGZ stem cells, DBI regulates the balance between preserving the stem cell pool and neuron production.

4.4 DBI is involved in mediating the pro-neurogenic effect of EE and physical exercise

Adult neurogenesis is influenced by external factors: EE is known to lead to an increase in the survival of the adult-born neurons while physical exercise leads to an increase in proliferation of the stem cells and TACs (Kempermann et al., 1997; Vivar et al., 2013). Running was also shown to enhance the activity of local inhibitory neurons in the hippocampus, including the PV-positive cells (Schoenfeld et al., 2013). Moreover, PV-positive interneurons in the hippocampus receive excitatory input from the granule cells; thus, they qualify as an indicator for the activity of the local network (Hu et al., 2014; Song et al., 2016). Therefore, tonic and phasic GABA released from the PV-positive neurons were proposed to link the dynamics of neurogenesis to the activity of the DG network. Moreover, Song et al. showed that silencing the activity of the PV-positive interneurons practically abolishes the increase in survival induced by EE (Song et al., 2013). This indicates that GABA signalling is necessary for the pro-neurogenic effect of EE. A similar manipulation of the SOM-positive interneurons had no effect on neurogenesis with or without EE indicating that GABA release from the PV-positive interneurons provides a specific link between environmental enrichment and the survival of the adult-born neurons.

The diametric regulation of stem cell proliferation and TAC and neuroblast survival provided by GABA in the SGZ was proposed to provide flexibility to the niche and to serve the ‘time-stamping’ of the adult-born neurons, essential for remembering situations in the right temporal context and order (Aimone et al., 2009; Song et al., 2016). However, this type of regulation cannot explain the dynamics of the

niche in situations of EE and physical activity. GABA regulation can provide a mechanism for the pro-neurogenic effect of EE by enhancing the survival and development of TACs and neuroblasts; however, cannot account for the pro-proliferative effect of voluntary physical exercise. Often in EE experiments, the animals are housed with free access to running wheels which leads to an increase in both the activation of stem cells and their proliferation as well as in survival and development of the TACs and neuroblasts. An increase in physical activity could lead to an increase in the activity of the PV-positive interneurons which could explain the enhanced survival found for the TACs and the neuroblasts. However, the increase in GABA released by the PV-positive interneurons should reduce the activation of the stem cells and their proliferation. I showed that DBI is expressed only in NSCs and TACs but not in neuroblasts. Moreover, DBI expression levels decrease along with the commitment and differentiation stages from one cell type to the other. This study also showed that DBI reduces GABA signalling on NSCs and early TACs, which express DBI at high levels. Via this mechanism DBI enhances the proliferation of the early progenitors and allows an activation of the stem cells and an expansion of the stem cell pool. Therefore, during EE and physical exercise, DBI could decrease GABA currents in NSCs and early TACs without interfering with the GABA signal in neuroblasts and adult-born neurons, as it is not expressed in these cells. Based on our data I cannot exclude a paracrine action of DBI on neuroblasts and neurons. However, this possibility is unlikely as large functional differences were found when comparing control cells and cells overexpressing DBI found in close apposition. Therefore, DBI is most likely acting in an autocrine fashion.

Knocking down DBI in SGZ NSCs and their progeny blocked the increase in proliferation that normally occurs after EE and physical exercise. The lack of DBI not only affected proliferation but also impaired the increase in the number of DCX neuroblasts expected after EE. Most likely the lack of DBI combined with high GABA release induced by physical exercise led to a dramatic reduction in stem cells activation and TAC proliferation that in turn resulted in a low production of neuroblasts. The present study shows that DBI allows both the pro-proliferative and, most likely as a consequence of this, also the pro-neurogenic effect of EE and physical exercise.

Therefore, I hypothesize that the function of DBI in the SGZ is to maintain the progenitor pool, in particular, the stem cell pool, to be used when the conditions demand it. Furthermore, DBI could allow a specific regulation of the GABA signal in early and late progenitors as it is expressed in the NSCs and TACs but not in neuroblasts and adult-born neurons. This differential GABA regulation could lead to an increase in the proliferation of the stem cells and Type 2a TACs and a simultaneous increase in survival of Type 2b TACs and neuroblasts after EE and physical exercise. This regulation of the GABA signal by DBI would explain the simultaneous pro-proliferative and pro-neurogenic effects of these environmental changes. Therefore, DBI and GABA regulate SGZ neurogenesis in a close partnership enabling multiple levels of control which makes the niche dynamic and ready to respond to the needs of the local network.

5. Conclusions

This study shows the presence of DBI not only in the SGZ but in all postnatal and adult mouse neurogenic niches and across species in the rhesus monkey and in humans as well as during development. Moreover, given that the highest expression of DBI is found in neural stem cells, I propose DBI expression as an indicator of stemness potential in the brain. I clearly demonstrated that DBI binds to the benzodiazepine binding site of the $GABA_A$ receptor on SGZ NSCs and reduces GABA mediated currents. This, in turn, increases the proliferation of SGZ progenitors, SGZ stem cells self-renewal rate and astrocyte production. Via this mechanism DBI regulates the balance between preserving the stem cell pool and neuron generation.

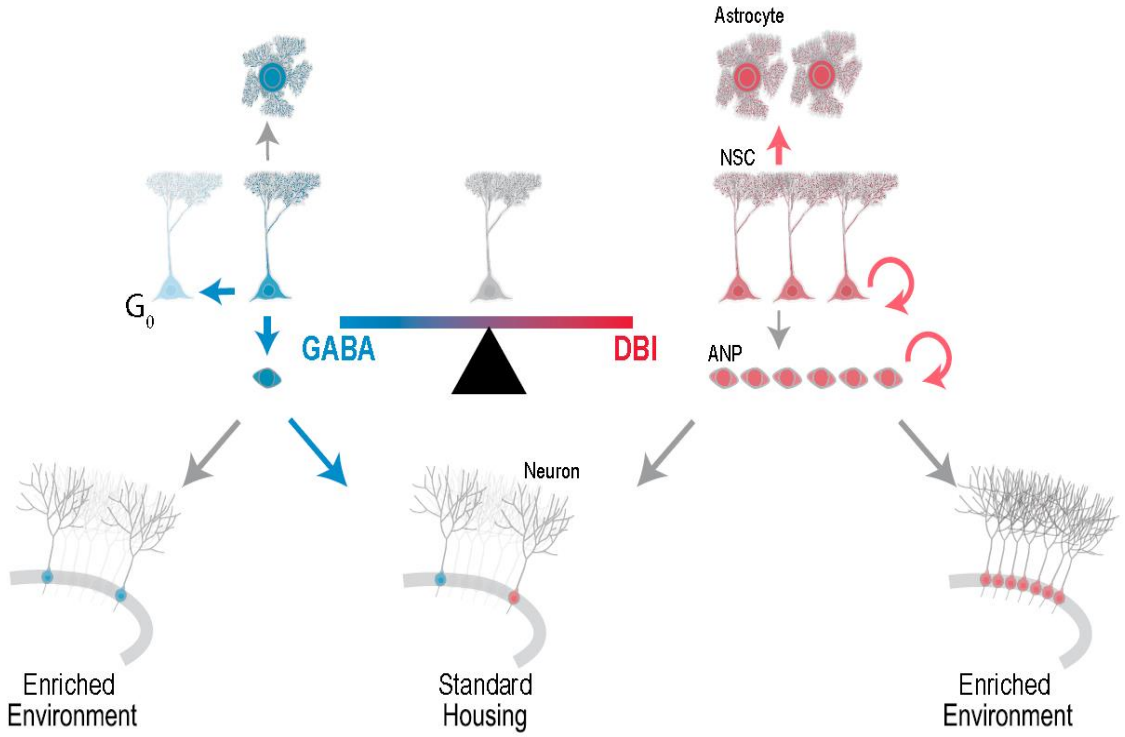

Figure 8.1. Scheme Summarizing DBI Function in SGZ Neuronal Progenitors. DBI reduces GABA signaling in neural stem cells. GABA activity promotes stem cell quiescence (Song et al., 2012) and differentiation to a neuronal fate, while DBI favors progenitor self-renewal and differentiation to astrocytes. A thus enlarged neuronal

progenitor pool would, under conditions of enriched environment, give rise to an increase in neuronal production. Figure and figure legend were reproduced from Dumitru and colleagues (2017).

DBI controls both SVZ and SGZ neurogenesis in spite of the different output of the two niches: while the SVZ produces mostly GABAergic, inhibitory neurons, the SGZ produces glutamatergic, excitatory cells. Thus, DBI is a general regulator of postnatal and adult neurogenesis. Furthermore, this study shows that DBI is essential for the pro-proliferative and for the pro-neurogenic effect of EE and physical exercise. In summary, by negatively modulating the GABA signal, DBI provides a new regulatory mechanism in the SGZ niche which promotes the expansion and preservation of the stem cell pool and together with GABA controls and adapts the output of the niche to the needs of the local network.

6. Outlook

The present study shows that DBI is strongly expressed in all adult neurogenic niches including the α-Tanycytes of the 3rd ventricle and during development. However, the role DBI plays in the 3rd ventricle and during development was not investigated. A future goal is to check whether DBI is also regulating the activity of the Tanycytes and, most importantly, to determine the function of DBI in regulating developmental neurogenesis. Considering the high expression of the protein in RG-cells, it is likely that DBI has an important function in developmental neurogenesis.

A question that remains open in this study is whether DBI acts in an autocrine or in a paracrine fashion. The viral OE experiments presented here show differences between DBI OE and control infected cell populations in spite of the close proximity between the cells. This indicates that DBI acts in an autocrine fashion. However, the results presented here cannot exclude an influence of DBI on the neighboring cells. Using high titers of DBI OE virus and comparing the results from different control/OE viral mix ratios could allow clearer interpretations.

Another important open question relates to whether changes in the environment affect DBI expression or its action mechanism. This study demonstrates that DBI is necessary for the pro-neurogenic and pro-proliferative effect of EE and physical exercise. Therefore, it would be interesting to investigate whether DBI is in turn controlled by EE or physical exercise, for example by analyzing DBI expression levels under these conditions. Both in the SVZ and the SGZ, DBI is expressed in all the stem cells but only in a certain population of the TACs. It would be interesting to investigate whether the percentage of TACs expressing DBI is affected by changes in the environment.

The interplay between GABA and DBI in regulating adult neurogenesis is complex and it is still not known in which conditions DBI could also act as a positive modulator of the channel. This most likely depends on the local concentration of DBI and on the subunit composition of the $GABA_A$ receptor. Further studies are needed to

elucidate these aspects especially as the potential of DBI to completely revert its action would have complex influences on regulating neurogenesis.

Last but not least, it would be important to determine the signaling downstream of DBI. In this study, I bring convincing data showing that DBI acts by modulating GABA signaling. However, there is still very little known about the connection between GABA signaling and cell proliferation. *In vitro* and *in vivo* studies in which neural progenitors could be treated with GABA and/or DBI followed by microarrays or RNA sequencing could help to elucidate the downstream mechanisms followed by DBI/GABA activation.

7. Bibliography

Aguilar-Arredondo, A., Arias, C., and Zepeda, A. (2015). Evaluating the functional state of adult-born neurons in the adult dentate gyrus of the hippocampus: from birth to functional integration. Rev Neurosci *26*, 269-279.

Aimone, J.B., Wiles, J., and Gage, F.H. (2009). Computational influence of adult neurogenesis on memory encoding. Neuron *61*, 187-202.

Alfonso, J., Le Magueresse, C., Zuccotti, A., Khodosevich, K., and Monyer, H. (2012). Diazepam binding inhibitor promotes progenitor proliferation in the postnatal SVZ by reducing GABA signaling. Cell Stem Cell *10*, 76-87.

Alho, H., Bovolin, P., Jenkins, D., Guidotti, A., and Costa, E. (1989). Cellular and subcellular localization of an octadecaneuropeptide derived from diazepam binding inhibitor: immunohistochemical studies in the rat brain. J Chem Neuroanat *2*, 301-318.

Alho, H., Costa, E., Ferrero, P., Fujimoto, M., Cosenza-Murphy, D., and Guidotti, A. (1985). Diazepam-binding inhibitor: a neuropeptide located in selected neuronal populations of rat brain. Science *229*, 179-182.

Alho, H., Harjuntausta, T., Schultz, R., Pelto-Huikko, M., and Bovolin, P. (1991). Immunohistochemistry of diazepam binding inhibitor (DBI) in the central nervous system and peripheral organs: its possible role as an endogenous regulator of different types of benzodiazepine receptors. Neuropharmacology *30*, 1381-1386.

Alho, H., Kolmer, M., Harjuntausta, T., and Helen, P. (1995). Increased expression of diazepam binding inhibitor in human brain tumors. Cell Growth Differ *6*, 309-314.

Altman, J. (1969). Autoradiographic and histological studies of postnatal neurogenesis. IV. Cell proliferation and migration in the anterior forebrain, with special reference to persisting neurogenesis in the olfactory bulb. J Comp Neurol *137*, 433-457.

Altman, J., and Das, G.D. (1965). Autoradiographic and histological evidence of postnatal hippocampal neurogenesis in rats. J Comp Neurol *124*, 319-335.

Arai, Y., Pulvers, J.N., Haffner, C., Schilling, B., Nusslein, I., Calegari, F., and Huttner, W.B. (2011). Neural stem and progenitor cells shorten S-phase on commitment to neuron production. Nat Commun *2*, 154.

Awapara, J., Landua, A.J., Fuerst, R., and Seale, B. (1950). Free gamma-aminobutyric acid in brain. J Biol Chem *187*, 35-39.

Baumann, S.W., Baur, R., and Sigel, E. (2003). Individual properties of the two functional agonist sites in GABA(A) receptors. J Neurosci *23*, 11158-11166.

Baur, R., and Sigel, E. (2005). Benzodiazepines affect channel opening of GABA A receptors induced by either agonist binding site. Mol Pharmacol *67*, 1005-1008.

Baur, R., Tan, K.R., Luscher, B.P., Gonthier, A., Goeldner, M., and Sigel, E. (2008). Covalent modification of GABAA receptor isoforms by a diazepam analogue provides evidence for a novel benzodiazepine binding site that prevents modulation by these drugs. J Neurochem *106*, 2353-2363.

Beckervordersandforth, R., Tripathi, P., Ninkovic, J., Bayam, E., Lepier, A., Stempfhuber, B., Kirchhoff, F., Hirrlinger, J., Haslinger, A., Lie, D.C., *et al.* (2010). In vivo fate mapping and expression analysis reveals molecular hallmarks of prospectively isolated adult neural stem cells. Cell Stem Cell *7*, 744-758.

Berchtold, N.C., Chinn, G., Chou, M., Kesslak, J.P., and Cotman, C.W. (2005). Exercise primes a molecular memory for brain-derived neurotrophic factor protein induction in the rat hippocampus. Neuroscience *133*, 853-861.

Berchtold, N.C., Kesslak, J.P., and Cotman, C.W. (2002). Hippocampal brain-derived neurotrophic factor gene regulation by exercise and the medial septum. J Neurosci Res *68*, 511-521.

Bergmann, O., Spalding, K.L., and Frisen, J. (2015). Adult Neurogenesis in Humans. Cold Spring Harb Perspect Biol *7*, a018994.

Bettler, B., Kaupmann, K., Mosbacher, J., and Gassmann, M. (2004). Molecular structure and physiological functions of GABA(B) receptors. Physiol Rev *84*, 835-867.

Bianchi, M.T. (2010). Context dependent benzodiazepine modulation of GABA(A) receptor opening frequency. Curr Neuropharmacol *8*, 10-17.

Bianchi, M.T., Botzolakis, E.J., Lagrange, A.H., and Macdonald, R.L. (2009). Benzodiazepine modulation of GABA(A) receptor opening frequency depends on activation context: a patch clamp and simulation study. Epilepsy Res *85*, 212-220.

Bloksgaard, M., Bek, S., Marcher, A.B., Neess, D., Brewer, J., Hannibal-Bach, H.K., Helledie, T., Fenger, C., Due, M., Berzina, Z., *et al.* (2012). The acyl-CoA binding

protein is required for normal epidermal barrier function in mice. J Lipid Res *53*, 2162-2174.

Bonaguidi, M.A., Song, J., Ming, G.L., and Song, H. (2012). A unifying hypothesis on mammalian neural stem cell properties in the adult hippocampus. Curr Opin Neurobiol *22*, 754-761.

Bonaguidi, M.A., Wheeler, M.A., Shapiro, J.S., Stadel, R.P., Sun, G.J., Ming, G.L., and Song, H. (2011). In vivo clonal analysis reveals self-renewing and multipotent adult neural stem cell characteristics. Cell *145*, 1142-1155.

Bond, A.M., Ming, G.L., and Song, H. (2015). Adult Mammalian Neural Stem Cells and Neurogenesis: Five Decades Later. Cell Stem Cell *17*, 385-395.

Bormann, J. (1991). Electrophysiological characterization of diazepam binding inhibitor (DBI) on GABAA receptors. Neuropharmacology *30*, 1387-1389.

Bormann, J., Ferrero, P., Guidotti, A., and Costa, E. (1985). Neuropeptide modulation of GABA receptor C1- channels. Regul Pept Suppl *4*, 33-38.

Bovolin, P., Schlichting, J., Miyata, M., Ferrarese, C., Guidotti, A., and Alho, H. (1990). Distribution and characterization of diazepam binding inhibitor (DBI) in peripheral tissues of rat. Regul Pept *29*, 267-281.

Braestrup, C., and Squires, R.F. (1977). Specific benzodiazepine receptors in rat brain characterized by high-affinity (3H)diazepam binding. Proc Natl Acad Sci U S A *74*, 3805-3809.

Brickley, S.G., Cull-Candy, S.G., and Farrant, M. (1999). Single-channel properties of synaptic and extrasynaptic GABAA receptors suggest differential targeting of receptor subtypes. J Neurosci *19*, 2960-2973.

Buhr, A., Baur, R., and Sigel, E. (1997). Subtle changes in residue 77 of the gamma subunit of alpha1beta2gamma2 GABAA receptors drastically alter the affinity for ligands of the benzodiazepine binding site. J Biol Chem *272*, 11799-11804.

Buhr, A., and Sigel, E. (1997). A point mutation in the gamma2 subunit of gamma-aminobutyric acid type A receptors results in altered benzodiazepine binding site specificity. Proc Natl Acad Sci U S A *94*, 8824-8829.

Calzolari, F., Michel, J., Baumgart, E.V., Theis, F., Gotz, M., and Ninkovic, J. (2015). Fast clonal expansion and limited neural stem cell self-renewal in the adult subependymal zone. Nat Neurosci *18*, 490-492.

Carlen, M., Cassidy, R.M., Brismar, H., Smith, G.A., Enquist, L.W., and Frisen, J. (2002). Functional integration of adult-born neurons. Curr Biol *12*, 606-608.

Caronia, G., Wilcoxon, J., Feldman, P., and Grove, E.A. (2010). Bone morphogenetic protein signaling in the developing telencephalon controls formation of the hippocampal dentate gyrus and modifies fear-related behavior. J Neurosci *30*, 6291-6301.

Chaker, Z., Codega, P., and Doetsch, F. (2016). A mosaic world: puzzles revealed by adult neural stem cell heterogeneity. Wiley Interdiscip Rev Dev Biol *5*, 640-658.

Charara, A., Pare, J.F., Levey, A.I., and Smith, Y. (2005). Synaptic and extrasynaptic GABA-A and GABA-B receptors in the globus pallidus: an electron microscopic immunogold analysis in monkeys. Neuroscience *131*, 917-933.

Christian, C.A., Herbert, A.G., Holt, R.L., Peng, K., Sherwood, K.D., Pangratz-Fuehrer, S., Rudolph, U., and Huguenard, J.R. (2013). Endogenous positive allosteric modulation of GABA(A) receptors by diazepam binding inhibitor. Neuron *78*, 1063-1074.

Clark, P.J., Brzezinska, W.J., Puchalski, E.K., Krone, D.A., and Rhodes, J.S. (2009). Functional analysis of neurovascular adaptations to exercise in the dentate gyrus of young adult mice associated with cognitive gain. Hippocampus *19*, 937-950.

Compere, V., Lanfray, D., Castel, H., Morin, F., Leprince, J., Dureuil, B., Vaudry, H., Pelletier, G., and Tonon, M.C. (2010). Acute food deprivation reduces expression of diazepam-binding inhibitor, the precursor of the anorexigenic octadecaneuropeptide ODN, in mouse glial cells. J Mol Endocrinol *44*, 295-299.

Cope, D.W., Wulff, P., Oberto, A., Aller, M.I., Capogna, M., Ferraguti, F., Halbsguth, C., Hoeger, H., Jolin, H.E., Jones, A., *et al.* (2004). Abolition of zolpidem sensitivity in mice with a point mutation in the GABAA receptor gamma2 subunit. Neuropharmacology *47*, 17-34.

Corda, M.G., Ferrari, M., Guidotti, A., Konkel, D., and Costa, E. (1984). Isolation, purification and partial sequence of a neuropeptide (diazepam-binding inhibitor) precursor of an anxiogenic putative ligand for benzodiazepine recognition site. Neurosci Lett *47*, 319-324.

Costa, E., and Guidotti, A. (1991). Diazepam binding inhibitor (DBI): a peptide with multiple biological actions. Life Sci *49*, 325-344.

Crowther, A.J., and Song, J. (2014). Activity-dependent signaling mechanisms regulating adult hippocampal neural stem cells and their progeny. Neurosci Bull *30*, 542-556.

Cutting, G.R., Lu, L., O'Hara, B.F., Kasch, L.M., Montrose-Rafizadeh, C., Donovan, D.M., Shimada, S., Antonarakis, S.E., Guggino, W.B., Uhl, G.R., *et al.* (1991). Cloning of the gamma-aminobutyric acid (GABA) rho 1 cDNA: a GABA receptor subunit highly expressed in the retina. Proc Natl Acad Sci U S A *88*, 2673-2677.

Davies, P.A., Hanna, M.C., Hales, T.G., and Kirkness, E.F. (1997). Insensitivity to anaesthetic agents conferred by a class of GABA(A) receptor subunit. Nature *385*, 820-823.

Dayer, A.G., Ford, A.A., Cleaver, K.M., Yassaee, M., and Cameron, H.A. (2003). Short-term and long-term survival of new neurons in the rat dentate gyrus. J Comp Neurol *460*, 563-572.

De Mateos-Verchere, J.G., Leprince, J., Tonon, M.C., Vaudry, H., and Costentin, J. (1998). The octadecaneuropeptide ODN induces anxiety in rodents: possible involvement of a shorter biologically active fragment. Peptides *19*, 841-848.

DeFelipe, J., Lopez-Cruz, P.L., Benavides-Piccione, R., Bielza, C., Larranaga, P., Anderson, S., Burkhalter, A., Cauli, B., Fairen, A., Feldmeyer, D., *et al.* (2013). New insights into the classification and nomenclature of cortical GABAergic interneurons. Nat Rev Neurosci *14*, 202-216.

Dietrich, M.O., and Horvath, T.L. (2012). Fat incites tanycytes to neurogenesis. Nat Neurosci *15*, 651-653.

Doetsch, F., Garcia-Verdugo, J.M., and Alvarez-Buylla, A. (1997). Cellular composition and three-dimensional organization of the subventricular germinal zone in the adult mammalian brain. J Neurosci *17*, 5046-5061.

Dranovsky, A., Picchini, A.M., Moadel, T., Sisti, A.C., Yamada, A., Kimura, S., Leonardo, E.D., and Hen, R. (2011). Experience dictates stem cell fate in the adult hippocampus. Neuron *70*, 908-923.

Dumitru, I., Neitz, A., Alfonso, J., and Monyer, H. (2017). Diazepam Binding Inhibitor Promotes Stem Cell Expansion Controlling Environment-Dependent Neurogenesis. Neuron *94*, 125-137 e125.

Duran, J.M., Anjard, C., Stefan, C., Loomis, W.F., and Malhotra, V. (2010). Unconventional secretion of Acb1 is mediated by autophagosomes. J Cell Biol *188*, 527-536.

Elholm, M., Bjerking, G., Knudsen, J., Kristiansen, K., and Mandrup, S. (1996). Regulatory elements in the promoter region of the rat gene encoding the acyl-CoA-binding protein. Gene *173*, 233-238.

Encinas, J.M., Michurina, T.V., Peunova, N., Park, J.H., Tordo, J., Peterson, D.A., Fishell, G., Koulakov, A., and Enikolopov, G. (2011). Division-coupled astrocytic differentiation and age-related depletion of neural stem cells in the adult hippocampus. Cell Stem Cell *8*, 566-579.

Eriksson, P.S., Perfilieva, E., Bjork-Eriksson, T., Alborn, A.M., Nordborg, C., Peterson, D.A., and Gage, F.H. (1998). Neurogenesis in the adult human hippocampus. Nat Med *4*, 1313-1317.

Ernst, A., Alkass, K., Bernard, S., Salehpour, M., Perl, S., Tisdale, J., Possnert, G., Druid, H., and Frisen, J. (2014). Neurogenesis in the striatum of the adult human brain. Cell *156*, 1072-1083.

Ernst, A., and Frisen, J. (2015). Adult neurogenesis in humans- common and unique traits in mammals. PLoS Biol *13*, e1002045.

Esposito, M.S., Piatti, V.C., Laplagne, D.A., Morgenstern, N.A., Ferrari, C.C., Pitossi, F.J., and Schinder, A.F. (2005). Neuronal differentiation in the adult hippocampus recapitulates embryonic development. J Neurosci *25*, 10074-10086.

Fabel, K., Fabel, K., Tam, B., Kaufer, D., Baiker, A., Simmons, N., Kuo, C.J., and Palmer, T.D. (2003). VEGF is necessary for exercise-induced adult hippocampal neurogenesis. Eur J Neurosci *18*, 2803-2812.

Fabel, K., Wolf, S.A., Ehninger, D., Babu, H., Leal-Galicia, P., and Kempermann, G. (2009). Additive effects of physical exercise and environmental enrichment on adult hippocampal neurogenesis in mice. Front Neurosci *3*, 50.

Farmer, J., Zhao, X., van Praag, H., Wodtke, K., Gage, F.H., and Christie, B.R. (2004). Effects of voluntary exercise on synaptic plasticity and gene expression in the dentate gyrus of adult male Sprague-Dawley rats in vivo. Neuroscience *124*, 71-79.

Farrant, M., and Nusser, Z. (2005). Variations on an inhibitory theme: phasic and tonic activation of GABA(A) receptors. Nat Rev Neurosci *6*, 215-229.

Farrukh, I.S., Peng, W., Orlinska, U., and Hoidal, J.R. (1998). Effect of dehydroepiandrosterone on hypoxic pulmonary vasoconstriction: a Ca(2+)-activated K(+)-channel opener. Am J Physiol *274*, L186-195.

Farzampour, Z., Reimer, R.J., and Huguenard, J. (2015). Endozepines. Adv Pharmacol *72*, 147-164.

Feldblum, S., Erlander, M.G., and Tobin, A.J. (1993). Different distributions of GAD65 and GAD67 mRNAs suggest that the two glutamate decarboxylases play distinctive functional roles. J Neurosci Res *34*, 689-706.

Ferrarese, C., Vaccarino, F., Alho, H., Mellstrom, B., Costa, E., and Guidotti, A. (1987). Subcellular location and neuronal release of diazepam binding inhibitor. J Neurochem *48*, 1093-1102.

Ferrero, P., Santi, M.R., Conti-Tronconi, B., Costa, E., and Guidotti, A. (1986). Study of an octadecaneuropeptide derived from diazepam binding inhibitor (DBI): biological activity and presence in rat brain. Proc Natl Acad Sci U S A *83*, 827-831.

Filippov, V., Kronenberg, G., Pivneva, T., Reuter, K., Steiner, B., Wang, L.P., Yamaguchi, M., Kettenmann, H., and Kempermann, G. (2003). Subpopulation of nestin-expressing progenitor cells in the adult murine hippocampus shows electrophysiological and morphological characteristics of astrocytes. Mol Cell Neurosci *23*, 373-382.

Fox, C.J., Russell, K.I., Wang, Y.T., and Christie, B.R. (2006). Contribution of NR2A and NR2B NMDA subunits to bidirectional synaptic plasticity in the hippocampus in vivo. Hippocampus *16*, 907-915.

Franek, M., Pagano, A., Kaupmann, K., Bettler, B., Pin, J.P., and Blahos, J. (1999). The heteromeric GABA-B receptor recognizes G-protein alpha subunit C-termini. Neuropharmacology *38*, 1657-1666.

Fritschy, J.M., Meskenaite, V., Weinmann, O., Honer, M., Benke, D., and Mohler, H. (1999). GABAB-receptor splice variants GB1a and GB1b in rat brain: developmental regulation, cellular distribution and extrasynaptic localization. Eur J Neurosci *11*, 761-768.

Frolov, A., and Schroeder, F. (1998). Acyl coenzyme A binding protein. Conformational sensitivity to long chain fatty acyl-CoA. J Biol Chem *273*, 11049-11055.

Fuentealba, L.C., Rompani, S.B., Parraguez, J.I., Obernier, K., Romero, R., Cepko, C.L., and Alvarez-Buylla, A. (2015). Embryonic Origin of Postnatal Neural Stem Cells. Cell *161*, 1644-1655.

Furutachi, S., Miya, H., Watanabe, T., Kawai, H., Yamasaki, N., Harada, Y., Imayoshi, I., Nelson, M., Nakayama, K.I., Hirabayashi, Y., *et al.* (2015). Slowly dividing neural progenitors are an embryonic origin of adult neural stem cells. Nat Neurosci *18*, 657-665.

Ge, S., Goh, E.L., Sailor, K.A., Kitabatake, Y., Ming, G.L., and Song, H. (2006). GABA regulates synaptic integration of newly generated neurons in the adult brain. Nature *439*, 589-593.

Ge, S., Yang, C.H., Hsu, K.S., Ming, G.L., and Song, H. (2007). A critical period for enhanced synaptic plasticity in newly generated neurons of the adult brain. Neuron *54*, 559-566.

Gebara, E., Bonaguidi, M.A., Beckervordersandforth, R., Sultan, S., Udry, F., Gijs, P.J., Lie, D.C., Ming, G.L., Song, H., and Toni, N. (2016). Heterogeneity of Radial Glia-Like Cells in the Adult Hippocampus. Stem Cells *34*, 997-1010.

Goncalves, J.T., Bloyd, C.W., Shtrahman, M., Johnston, S.T., Schafer, S.T., Parylak, S.L., Tran, T., Chang, T., and Gage, F.H. (2016a). In vivo imaging of dendritic pruning in dentate granule cells. Nat Neurosci *19*, 788-791.

Goncalves, J.T., Schafer, S.T., and Gage, F.H. (2016b). Adult Neurogenesis in the Hippocampus: From Stem Cells to Behavior. Cell *167*, 897-914.

Goodman, T., and Hajihosseini, M.K. (2015). Hypothalamic tanycytes-masters and servants of metabolic, neuroendocrine, and neurogenic functions. Front Neurosci *9*, 387.

Gotz, M., and Huttner, W.B. (2005). The cell biology of neurogenesis. Nat Rev Mol Cell Biol *6*, 777-788.

Gotz, M., Nakafuku, M., and Petrik, D. (2016). Neurogenesis in the Developing and Adult Brain-Similarities and Key Differences. Cold Spring Harb Perspect Biol *8*.

Gray, P.W., Glaister, D., Seeburg, P.H., Guidotti, A., and Costa, E. (1986). Cloning and expression of cDNA for human diazepam binding inhibitor, a natural ligand of an allosteric regulatory site of the gamma-aminobutyric acid type A receptor. Proc Natl Acad Sci U S A *83*, 7547-7551.

Green, C.S., and Bavelier, D. (2008). Exercising your brain: a review of human brain plasticity and training-induced learning. Psychol Aging *23*, 692-701.

Guidotti, A., Forchetti, C.M., Corda, M.G., Konkel, D., Bennett, C.D., and Costa, E. (1983). Isolation, characterization, and purification to homogeneity of an endogenous polypeptide with agonistic action on benzodiazepine receptors. Proc Natl Acad Sci U S A *80*, 3531-3535.

Hadingham, K.L., Wingrove, P., Le Bourdelles, B., Palmer, K.J., Ragan, C.I., and Whiting, P.J. (1993). Cloning of cDNA sequences encoding human alpha 2 and alpha 3 gamma-aminobutyric acidA receptor subunits and characterization of the benzodiazepine pharmacology of recombinant alpha 1-, alpha 2-, alpha 3-, and alpha 5-containing human gamma-aminobutyric acidA receptors. Mol Pharmacol *43*, 970-975.

Hastings, N.B., and Gould, E. (1999). Rapid extension of axons into the CA3 region by adult-generated granule cells. J Comp Neurol *413*, 146-154.

Hedblom, E., and Kirkness, E.F. (1997). A novel class of GABAA receptor subunit in tissues of the reproductive system. J Biol Chem *272*, 15346-15350.

Hill, L.E., Droste, S.K., Nutt, D.J., Linthorst, A.C., and Reul, J.M. (2010). Voluntary exercise alters GABA(A) receptor subunit and glutamic acid decarboxylase-67 gene expression in the rat forebrain. J Psychopharmacol *24*, 745-756.

Hu, H., Gan, J., and Jonas, P. (2014). Interneurons. Fast-spiking, parvalbumin(+) GABAergic interneurons: from cellular design to microcircuit function. Science *345*, 1255263.

Inta, D., Alfonso, J., von Engelhardt, J., Kreuzberg, M.M., Meyer, A.H., van Hooft, J.A., and Monyer, H. (2008). Neurogenesis and widespread forebrain migration of distinct GABAergic neurons from the postnatal subventricular zone. Proc Natl Acad Sci U S A *105*, 20994-20999.

Jarry, M., Diallo, M., Lecointre, C., Desrues, L., Tokay, T., Chatenet, D., Leprince, J., Rossi, O., Vaudry, H., Tonon, M.C., *et al.* (2010). The vasoactive peptides urotensin II and urotensin II-related peptide regulate astrocyte activity through common and distinct mechanisms: involvement in cell proliferation. Biochem J *428*, 113-124.

Jin, P., Zhang, J., Rowe-Teeter, C., Yang, J., Stuve, L.L., and Fu, G.K. (2004). Cloning and characterization of a GABAA receptor gamma2 subunit variant. J Biol Chem *279*, 1408-1414.

Jones, K.A., Borowsky, B., Tamm, J.A., Craig, D.A., Durkin, M.M., Dai, M., Yao, W.J., Johnson, M., Gunwaldsen, C., Huang, L.Y., *et al.* (1998). GABA(B) receptors function as a heteromeric assembly of the subunits GABA(B)R1 and GABA(B)R2. Nature *396*, 674-679.

Kaila, K., Price, T.J., Payne, J.A., Puskarjov, M., and Voipio, J. (2014). Cation-chloride cotransporters in neuronal development, plasticity and disease. Nat Rev Neurosci *15*, 637-654.

Kempermann, G., Gast, D., Kronenberg, G., Yamaguchi, M., and Gage, F.H. (2003). Early determination and long-term persistence of adult-generated new neurons in the hippocampus of mice. Development *130*, 391-399.

Kempermann, G., Jessberger, S., Steiner, B., and Kronenberg, G. (2004). Milestones of neuronal development in the adult hippocampus. Trends Neurosci *27*, 447-452.

Kempermann, G., Kuhn, H.G., and Gage, F.H. (1997). More hippocampal neurons in adult mice living in an enriched environment. Nature *386*, 493-495.

Kempermann, G., Song, H., and Gage, F.H. (2015). Neurogenesis in the Adult Hippocampus. Cold Spring Harb Perspect Biol *7*, a018812.

Knudsen, J., Mandrup, S., Rasmussen, J.T., Andreasen, P.H., Poulsen, F., and Kristiansen, K. (1993). The function of acyl-CoA-binding protein (ACBP)/diazepam binding inhibitor (DBI). Mol Cell Biochem *123*, 129-138.

Kokoeva, M.V., Yin, H., and Flier, J.S. (2005). Neurogenesis in the hypothalamus of adult mice: potential role in energy balance. Science *310*, 679-683.

Krall, J., Balle, T., Krogsgaard-Larsen, N., Sorensen, T.E., Krogsgaard-Larsen, P., Kristiansen, U., and Frolund, B. (2015). GABAA receptor partial agonists and antagonists: structure, binding mode, and pharmacology. Adv Pharmacol *72*, 201-227.

Kronenberg, G., Reuter, K., Steiner, B., Brandt, M.D., Jessberger, S., Yamaguchi, M., and Kempermann, G. (2003). Subpopulations of proliferating cells of the adult hippocampus respond differently to physiologic neurogenic stimuli. J Comp Neurol *467*, 455-463.

Kucken, A.M., Wagner, D.A., Ward, P.R., Teissere, J.A., Boileau, A.J., and Czajkowski, C. (2000). Identification of benzodiazepine binding site residues in the gamma2 subunit of the gamma-aminobutyric acid(A) receptor. Mol Pharmacol *57*, 932-939.

Kuhn, H.G., Dickinson-Anson, H., and Gage, F.H. (1996). Neurogenesis in the dentate gyrus of the adult rat: age-related decrease of neuronal progenitor proliferation. J Neurosci *16*, 2027-2033.

Kullmann, D.M., Ruiz, A., Rusakov, D.M., Scott, R., Semyanov, A., and Walker, M.C. (2005). Presynaptic, extrasynaptic and axonal GABAA receptors in the CNS: where and why? Prog Biophys Mol Biol *87*, 33-46.

Lagace, D.C., Whitman, M.C., Noonan, M.A., Ables, J.L., DeCarolis, N.A., Arguello, A.A., Donovan, M.H., Fischer, S.J., Farnbauch, L.A., Beech, R.D., *et al.* (2007). Dynamic contribution of nestin-expressing stem cells to adult neurogenesis. J Neurosci *27*, 12623-12629.

Lavado, A., Lagutin, O.V., Chow, L.M., Baker, S.J., and Oliver, G. (2010). Prox1 is required for granule cell maturation and intermediate progenitor maintenance during brain neurogenesis. PLoS Biol *8*.

Lee, D.A., Bedont, J.L., Pak, T., Wang, H., Song, J., Miranda-Angulo, A., Takiar, V., Charubhumi, V., Balordi, F., Takebayashi, H., *et al.* (2012). Tanycytes of the hypothalamic median eminence form a diet-responsive neurogenic niche. Nat Neurosci *15*, 700-702.

Levy, W.B., Redburn, D.A., and Cotman, C.W. (1973). Stimulus-coupled secretion of gamma-aminobutyric acid from rat brain synaptosomes. Science *181*, 676-678.

Li, G., Fang, L., Fernandez, G., and Pleasure, S.J. (2013). The ventral hippocampus is the embryonic origin for adult neural stem cells in the dentate gyrus. Neuron *78*, 658-672.

Li, Y., Luikart, B.W., Birnbaum, S., Chen, J., Kwon, C.H., Kernie, S.G., Bassel-Duby, R., and Parada, L.F. (2008). TrkB regulates hippocampal neurogenesis and governs sensitivity to antidepressive treatment. Neuron *59*, 399-412.

Lihrmann, I., Plaquevent, J.C., Tostivint, H., Raijmakers, R., Tonon, M.C., Conlon, J.M., and Vaudry, H. (1994). Frog diazepam-binding inhibitor: peptide sequence, cDNA cloning, and expression in the brain. Proc Natl Acad Sci U S A *91*, 6899-6903.

Lim, D.A., and Alvarez-Buylla, A. (2016). The Adult Ventricular-Subventricular Zone (V-SVZ) and Olfactory Bulb (OB) Neurogenesis. Cold Spring Harb Perspect Biol *8*.

Liu, X., Wang, Q., Haydar, T.F., and Bordey, A. (2005). Nonsynaptic GABA signaling in postnatal subventricular zone controls proliferation of GFAP-expressing progenitors. Nat Neurosci *8*, 1179-1187.

Lledo, P.M., Alonso, M., and Grubb, M.S. (2006). Adult neurogenesis and functional plasticity in neuronal circuits. Nat Rev Neurosci *7*, 179-193.

Lois, C., Garcia-Verdugo, J.M., and Alvarez-Buylla, A. (1996). Chain migration of neuronal precursors. Science *271*, 978-981.

Loomis, W.F., Behrens, M.M., Williams, M.E., and Anjard, C. (2010). Pregnenolone sulfate and cortisol induce secretion of acyl-CoA-binding protein and its conversion into endozepines from astrocytes. J Biol Chem *285*, 21359-21365.

Lorez, M., Benke, D., Luscher, B., Mohler, H., and Benson, J.A. (2000). Single-channel properties of neuronal GABAA receptors from mice lacking the 2 subunit. J Physiol *527 Pt 1*, 11-31.

Ludewig, A.H., Klapper, M., Wabitsch, M., Doring, F., and Nitz, I. (2011a). Differential expression of alternative Acyl-CoA binding protein (ACBP) transcripts in an inducible human preadipocyte cell line. Horm Metab Res *43*, 440-442.

Ludewig, A.H., Nitz, I., Klapper, M., and Doring, F. (2011b). Identification of a novel human Acyl-CoA binding protein isoform with a unique C-terminal domain. IUBMB Life *63*, 547-552.

Lugert, S., Basak, O., Knuckles, P., Haussler, U., Fabel, K., Gotz, M., Haas, C.A., Kempermann, G., Taylor, V., and Giachino, C. (2010). Quiescent and active hippocampal neural stem cells with distinct morphologies respond selectively to physiological and pathological stimuli and aging. Cell Stem Cell *6*, 445-456.

Macdonald, R., and Barker, J.L. (1978). Benzodiazepines specifically modulate GABA-mediated postsynaptic inhibition in cultured mammalian neurones. Nature *271*, 563-564.

Magnusson, J.P., and Frisen, J. (2016). Stars from the darkest night: unlocking the neurogenic potential of astrocytes in different brain regions. Development *143*, 1075-1086.

Magnusson, J.P., Goritz, C., Tatarishvili, J., Dias, D.O., Smith, E.M., Lindvall, O., Kokaia, Z., and Frisen, J. (2014). A latent neurogenic program in astrocytes regulated by Notch signaling in the mouse. Science *346*, 237-241.

Mann, E.O., and Paulsen, O. (2007). Role of GABAergic inhibition in hippocampal network oscillations. Trends Neurosci *30*, 343-349.

Masmoudi, O., Gandolfo, P., Leprince, J., Vaudry, D., Fournier, A., Patte-Mensah, C., Vaudry, H., and Tonon, M.C. (2003). Pituitary adenylate cyclase-activating polypeptide (PACAP) stimulates endozepine release from cultured rat astrocytes via a PKA-dependent mechanism. FASEB J *17*, 17-27.

Masmoudi, O., Gandolfo, P., Tokay, T., Leprince, J., Ravni, A., Vaudry, H., and Tonon, M.C. (2005). Somatostatin down-regulates the expression and release of endozepines from cultured rat astrocytes via distinct receptor subtypes. J Neurochem *94*, 561-571.

Matta, J.A., Ashby, M.C., Sanz-Clemente, A., Roche, K.W., and Isaac, J.T. (2011). mGluR5 and NMDA receptors drive the experience- and activity-dependent NMDA receptor NR2B to NR2A subunit switch. Neuron *70*, 339-351.

McIntire, S.L., Reimer, R.J., Schuske, K., Edwards, R.H., and Jorgensen, E.M. (1997). Identification and characterization of the vesicular GABA transporter. Nature *389*, 870-876.

Menn, B., Garcia-Verdugo, J.M., Yaschine, C., Gonzalez-Perez, O., Rowitch, D., and Alvarez-Buylla, A. (2006). Origin of oligodendrocytes in the subventricular zone of the adult brain. J Neurosci *26*, 7907-7918.

Minelli, A., Brecha, N.C., Karschin, C., DeBiasi, S., and Conti, F. (1995). GAT-1, a high-affinity GABA plasma membrane transporter, is localized to neurons and astroglia in the cerebral cortex. J Neurosci *15*, 7734-7746.

Minelli, A., DeBiasi, S., Brecha, N.C., Zuccarello, L.V., and Conti, F. (1996). GAT-3, a high-affinity GABA plasma membrane transporter, is localized to astrocytic processes, and it is not confined to the vicinity of GABAergic synapses in the cerebral cortex. J Neurosci *16*, 6255-6264.

Ming, G.L., and Song, H. (2011). Adult neurogenesis in the mammalian brain: significant answers and significant questions. Neuron *70*, 687-702.

Mira, H., Andreu, Z., Suh, H., Lie, D.C., Jessberger, S., Consiglio, A., San Emeterio, J., Hortiguela, R., Marques-Torrejon, M.A., Nakashima, K., *et al.* (2010). Signaling through BMPR-IA regulates quiescence and long-term activity of neural stem cells in the adult hippocampus. Cell Stem Cell *7*, 78-89.

Mirzadeh, Z., Merkle, F.T., Soriano-Navarro, M., Garcia-Verdugo, J.M., and Alvarez-Buylla, A. (2008). Neural stem cells confer unique pinwheel architecture to the ventricular surface in neurogenic regions of the adult brain. Cell Stem Cell *3*, 265-278.

Mocchetti, I., Einstein, R., and Brosius, J. (1986). Putative diazepam binding inhibitor peptide: cDNA clones from rat. Proc Natl Acad Sci U S A *83*, 7221-7225.

Mohler, H. (2014). Endogenous benzodiazepine site peptide ligands operating bidirectionally in vivo in neurogenesis and thalamic oscillations. Neurochem Res *39*, 1032-1036.

Mongiat, L.A., Esposito, M.S., Lombardi, G., and Schinder, A.F. (2009). Reliable activation of immature neurons in the adult hippocampus. PLoS One *4*, e5320.

Monyer, H., Burnashev, N., Laurie, D.J., Sakmann, B., and Seeburg, P.H. (1994). Developmental and regional expression in the rat brain and functional properties of four NMDA receptors. Neuron *12*, 529-540.

Moragues, N., Ciofi, P., Lafon, P., Odessa, M.F., Tramu, G., and Garret, M. (2000). cDNA cloning and expression of a gamma-aminobutyric acid A receptor epsilon-subunit in rat brain. Eur J Neurosci *12*, 4318-4330.

Morshead, C.M., Reynolds, B.A., Craig, C.G., McBurney, M.W., Staines, W.A., Morassutti, D., Weiss, S., and van der Kooy, D. (1994). Neural stem cells in the adult mammalian forebrain: a relatively quiescent subpopulation of subependymal cells. Neuron *13*, 1071-1082.

Mukhin, A.G., Papadopoulos, V., Costa, E., and Krueger, K.E. (1989). Mitochondrial benzodiazepine receptors regulate steroid biosynthesis. Proc Natl Acad Sci U S A *86*, 9813-9816.

Neess, D., Bek, S., Engelsby, H., Gallego, S.F., and Faergeman, N.J. (2015). Long-chain acyl-CoA esters in metabolism and signaling: Role of acyl-CoA binding proteins. Prog Lipid Res *59*, 1-25.

Neess, D., Bloksgaard, M., Bek, S., Marcher, A.B., Elle, I.C., Helledie, T., Due, M., Pagmantidis, V., Finsen, B., Wilbertz, J., *et al.* (2011). Disruption of the acyl-CoA-binding protein gene delays hepatic adaptation to metabolic changes at weaning. J Biol Chem *286*, 3460-3472.

Nicoll, R.A., and Alger, B.E. (1979). Presynaptic inhibition: transmitter and ionic mechanisms. Int Rev Neurobiol *21*, 217-258.

Nitz, I., Kruse, M.L., Klapper, M., and Doring, F. (2011). Specific regulation of low-abundance transcript variants encoding human Acyl-CoA binding protein (ACBP) isoforms. J Cell Mol Med *15*, 909-927.

Ogris, W., Poltl, A., Hauer, B., Ernst, M., Oberto, A., Wulff, P., Hoger, H., Wisden, W., and Sieghart, W. (2004). Affinity of various benzodiazepine site ligands in mice with a point mutation in the GABA(A) receptor gamma2 subunit. Biochem Pharmacol *68*, 1621-1629.

Olsen, R.W., and Sieghart, W. (2009). GABA A receptors: subtypes provide diversity of function and pharmacology. Neuropharmacology *56*, 141-148.

Olson, A.K., Eadie, B.D., Ernst, C., and Christie, B.R. (2006). Environmental enrichment and voluntary exercise massively increase neurogenesis in the adult hippocampus via dissociable pathways. Hippocampus *16*, 250-260.

Ortega, F., Gascon, S., Masserdotti, G., Deshpande, A., Simon, C., Fischer, J., Dimou, L., Chichung Lie, D., Schroeder, T., and Berninger, B. (2013). Oligodendrogliogenic and neurogenic adult subependymal zone neural stem cells constitute distinct lineages and exhibit differential responsiveness to Wnt signalling. Nat Cell Biol *15*, 602-613.

Overall, R.W., Walker, T.L., Fischer, T.J., Brandt, M.D., and Kempermann, G. (2016). Different Mechanisms Must Be Considered to Explain the Increase in Hippocampal Neural Precursor Cell Proliferation by Physical Activity. Front Neurosci *10*, 362.

Owens, G.P., Chaudhari, N., and Hahn, W.E. (1985). Brain "identifier sequence" is not restricted to brain: similar abundance in nuclear RNA of other organs. Science *229*, 1263-1265.

Owens, G.P., Chaudhari, N., and Hahn, W.E. (1986). Response: brain "identifier sequence". Science *234*, 1006.

Palmer, T.D., Willhoite, A.R., and Gage, F.H. (2000). Vascular niche for adult hippocampal neurogenesis. J Comp Neurol *425*, 479-494.

Paredes, M.F., James, D., Gil-Perotin, S., Kim, H., Cotter, J.A., Ng, C., Sandoval, K., Rowitch, D.H., Xu, D., McQuillen, P.S., *et al.* (2016). Extensive migration of young neurons into the infant human frontal lobe. Science *354*.

Passlick, S., Grauer, M., Schafer, C., Jabs, R., Seifert, G., and Steinhauser, C. (2013). Expression of the gamma2-subunit distinguishes synaptic and extrasynaptic GABA(A) receptors in NG2 cells of the hippocampus. J Neurosci *33*, 12030-12040.

Ponti, G., Obernier, K., and Alvarez-Buylla, A. (2013a). Lineage progression from stem cells to new neurons in the adult brain ventricular-subventricular zone. Cell Cycle *12*, 1649-1650.

Ponti, G., Obernier, K., Guinto, C., Jose, L., Bonfanti, L., and Alvarez-Buylla, A. (2013b). Cell cycle and lineage progression of neural progenitors in the ventricular-subventricular zones of adult mice. Proc Natl Acad Sci U S A *110*, E1045-1054.

Qian, Z., Bilderback, T.R., and Barmack, N.H. (2008). Acyl coenzyme A-binding protein (ACBP) is phosphorylated and secreted by retinal Muller astrocytes following protein kinase C activation. J Neurochem *105*, 1287-1299.

Ramerstorfer, J., Furtmuller, R., Vogel, E., Huck, S., and Sieghart, W. (2010). The point mutation gamma 2F77I changes the potency and efficacy of benzodiazepine site ligands in different GABAA receptor subtypes. Eur J Pharmacol *636*, 18-27.

Rao, M.S., Hattiangady, B., Abdel-Rahman, A., Stanley, D.P., and Shetty, A.K. (2005). Newly born cells in the ageing dentate gyrus display normal migration, survival and neuronal fate choice but endure retarded early maturation. Eur J Neurosci *21*, 464-476.

Reynolds, B.A., and Weiss, S. (1992). Generation of neurons and astrocytes from isolated cells of the adult mammalian central nervous system. Science *255*, 1707-1710.

Riddle, D.R., and Lichtenwalner, R.J. (2007). Neurogenesis in the Adult and Aging Brain. In Brain Aging: Models, Methods, and Mechanisms, D.R. Riddle, ed. (Boca Raton (FL)).

Rochefort, C., Gheusi, G., Vincent, J.D., and Lledo, P.M. (2002). Enriched odor exposure increases the number of newborn neurons in the adult olfactory bulb and improves odor memory. J Neurosci *22*, 2679-2689.

Rosenbaum, D.M., Rasmussen, S.G., and Kobilka, B.K. (2009). The structure and function of G-protein-coupled receptors. Nature *459*, 356-363.

Rosendal, J., Ertbjerg, P., and Knudsen, J. (1993). Characterization of ligand binding to acyl-CoA-binding protein. Biochem J *290 (Pt 2)*, 321-326.

Roth, F.C., and Draguhn, A. (2012). GABA metabolism and transport: effects on synaptic efficacy. Neural Plast *2012*, 805830.

Rudolph, U., Crestani, F., Benke, D., Brunig, I., Benson, J.A., Fritschy, J.M., Martin, J.R., Bluethmann, H., and Mohler, H. (1999). Benzodiazepine actions mediated by specific gamma-aminobutyric acid(A) receptor subtypes. Nature *401*, 796-800.

Rudolph, U., and Mohler, H. (1999). Transgenic and targeted mutant mice in drug discovery. Curr Opin Drug Discov Devel *2*, 134-141.

Ryu, J.R., Hong, C.J., Kim, J.Y., Kim, E.K., Sun, W., and Yu, S.W. (2016). Control of adult neurogenesis by programmed cell death in the mammalian brain. Mol Brain *9*, 43.

Sanai, N., Nguyen, T., Ihrie, R.A., Mirzadeh, Z., Tsai, H.H., Wong, M., Gupta, N., Berger, M.S., Huang, E., Garcia-Verdugo, J.M., *et al.* (2011). Corridors of migrating neurons in the human brain and their decline during infancy. Nature *478*, 382-386.

Sandberg, M.B., Bloksgaard, M., Duran-Sandoval, D., Duval, C., Staels, B., and Mandrup, S. (2005). The gene encoding acyl-CoA-binding protein is subject to metabolic regulation by both sterol regulatory element-binding protein and peroxisome proliferator-activated receptor alpha in hepatocytes. J Biol Chem *280*, 5258-5266.

Scharfman, H., Goodman, J., Macleod, A., Phani, S., Antonelli, C., and Croll, S. (2005). Increased neurogenesis and the ectopic granule cells after intrahippocampal BDNF infusion in adult rats. Exp Neurol *192*, 348-356.

Schoenfeld, T.J., Rada, P., Pieruzzini, P.R., Hsueh, B., and Gould, E. (2013). Physical exercise prevents stress-induced activation of granule neurons and enhances local inhibitory mechanisms in the dentate gyrus. J Neurosci *33*, 7770-7777.

Schofield, P.R., Darlison, M.G., Fujita, N., Burt, D.R., Stephenson, F.A., Rodriguez, H., Rhee, L.M., Ramachandran, J., Reale, V., Glencorse, T.A., *et al.* (1987). Sequence and functional expression of the GABA A receptor shows a ligand-gated receptor super-family. Nature *328*, 221-227.

Schofield, P.R., Pritchett, D.B., Sontheimer, H., Kettenmann, H., and Seeburg, P.H. (1989). Sequence and expression of human GABAA receptor alpha 1 and beta 1 subunits. FEBS Lett *244*, 361-364.

Selvaraj, V., Stocco, D.M., and Tu, L.N. (2015). Minireview: translocator protein (TSPO) and steroidogenesis: a reappraisal. Mol Endocrinol *29*, 490-501.

Shin, M.C., Wakita, M., Xie, D.J., Iwata, S., and Akaike, N. (2011). Synergic effect of diazepam and muscimol via presynaptic GABA(A) receptors on glutamatergic evoked EPSCs. Brain Res *1416*, 1-9.

Sibbe, M., and Kulik, A. (2016). GABAergic Regulation of Adult Hippocampal Neurogenesis. Mol Neurobiol.

Sieghart, W. (2015). Allosteric modulation of GABAA receptors via multiple drug-binding sites. Adv Pharmacol *72*, 53-96.

Sierra, A., Encinas, J.M., Deudero, J.J., Chancey, J.H., Enikolopov, G., Overstreet-Wadiche, L.S., Tsirka, S.E., and Maletic-Savatic, M. (2010). Microglia shape adult hippocampal neurogenesis through apoptosis-coupled phagocytosis. Cell Stem Cell *7*, 483-495.

Sigel, E., and Buhr, A. (1997). The benzodiazepine binding site of GABAA receptors. Trends Pharmacol Sci *18*, 425-429.

Song, H.J., Stevens, C.F., and Gage, F.H. (2002). Neural stem cells from adult hippocampus develop essential properties of functional CNS neurons. Nat Neurosci *5*, 438-445.

Song, J., Andrew, J.C., Olsen, R.H., Song, H., and Ming, G.L. (2014). A diametric mode of neuronal circuitry-neurogenesis coupling in the adult hippocampus via parvalbumin interneurons. Neurogenesis *1:1*.

Song, J., Olsen, R.H., Sun, J., Ming, G.L., and Song, H. (2016). Neuronal Circuitry Mechanisms Regulating Adult Mammalian Neurogenesis. Cold Spring Harb Perspect Biol *8*.

Song, J., Sun, J., Moss, J., Wen, Z., Sun, G.J., Hsu, D., Zhong, C., Davoudi, H., Christian, K.M., Toni, N., *et al.* (2013). Parvalbumin interneurons mediate neuronal circuitry-neurogenesis coupling in the adult hippocampus. Nat Neurosci *16*, 1728-1730.

Song, J., Zhong, C., Bonaguidi, M.A., Sun, G.J., Hsu, D., Gu, Y., Meletis, K., Huang, Z.J., Ge, S., Enikolopov, G., *et al.* (2012). Neuronal circuitry mechanism regulating adult quiescent neural stem-cell fate decision. Nature *489*, 150-154.

Spalding, K.L., Bergmann, O., Alkass, K., Bernard, S., Salehpour, M., Huttner, H.B., Bostrom, E., Westerlund, I., Vial, C., Buchholz, B.A., *et al.* (2013). Dynamics of hippocampal neurogenesis in adult humans. Cell *153*, 1219-1227.

Spurny, R., Ramerstorfer, J., Price, K., Brams, M., Ernst, M., Nury, H., Verheij, M., Legrand, P., Bertrand, D., Bertrand, S., *et al.* (2012). Pentameric ligand-gated ion channel ELIC is activated by GABA and modulated by benzodiazepines. Proc Natl Acad Sci U S A *109*, E3028-3034.

Steiner, B., Kronenberg, G., Jessberger, S., Brandt, M.D., Reuter, K., and Kempermann, G. (2004). Differential regulation of gliogenesis in the context of adult hippocampal neurogenesis in mice. Glia *46*, 41-52.

Stell, B.M., and Mody, I. (2002). Receptors with different affinities mediate phasic and tonic GABA(A) conductances in hippocampal neurons. J Neurosci *22*, RC223.

Suudhof, T.C. (2008). Neurotransmitter release. Handb Exp Pharmacol, 1-21.

Swinnen, J.V., Alen, P., Heyns, W., and Verhoeven, G. (1998). Identification of diazepam-binding Inhibitor/Acyl-CoA-binding protein as a sterol regulatory element-binding protein-responsive gene. J Biol Chem *273*, 19938-19944.

Taliaz, D., Stall, N., Dar, D.E., and Zangen, A. (2010). Knockdown of brain-derived neurotrophic factor in specific brain sites precipitates behaviors associated with depression and reduces neurogenesis. Mol Psychiatry *15*, 80-92.

Tokay, T., Hachem, R., Masmoudi-Kouki, O., Gandolfo, P., Desrues, L., Leprince, J., Castel, H., Diallo, M., Amri, M., Vaudry, H., *et al.* (2008). Beta-amyloid peptide stimulates endozepine release in cultured rat astrocytes through activation of N-formyl peptide receptors. Glia *56*, 1380-1389.

Tronche, F., Kellendonk, C., Kretz, O., Gass, P., Anlag, K., Orban, P.C., Bock, R., Klein, R., and Schutz, G. (1999). Disruption of the glucocorticoid receptor gene in the nervous system results in reduced anxiety. Nat Genet *23*, 99-103.

Ulrich, D., and Bettler, B. (2007). GABA(B) receptors: synaptic functions and mechanisms of diversity. Curr Opin Neurobiol *17*, 298-303.

Urban, N., and Guillemot, F. (2014). Neurogenesis in the embryonic and adult brain: same regulators, different roles. Front Cell Neurosci *8*, 396.

van Praag, H., Kempermann, G., and Gage, F.H. (1999). Running increases cell proliferation and neurogenesis in the adult mouse dentate gyrus. Nat Neurosci *2*, 266-270.

van Praag, H., Kempermann, G., and Gage, F.H. (2000). Neural consequences of environmental enrichment. Nat Rev Neurosci *1*, 191-198.

van Praag, H., Lucero, M.J., Yeo, G.W., Stecker, K., Heivand, N., Zhao, C., Yip, E., Afanador, M., Schroeter, H., Hammerstone, J., *et al.* (2007). Plant-derived flavanol (-)epicatechin enhances angiogenesis and retention of spatial memory in mice. J Neurosci *27*, 5869-5878.

van Praag, H., Schinder, A.F., Christie, B.R., Toni, N., Palmer, T.D., and Gage, F.H. (2002). Functional neurogenesis in the adult hippocampus. Nature *415*, 1030-1034.

Vivar, C., Potter, M.C., and van Praag, H. (2013). All about running: synaptic plasticity, growth factors and adult hippocampal neurogenesis. Curr Top Behav Neurosci *15*, 189-210.

Vock, C., Biedasek, K., Boomgaarden, I., Heins, A., Nitz, I., and Doring, F. (2010). ACBP knockdown leads to down-regulation of genes encoding rate-limiting enzymes in cholesterol and fatty acid metabolism. Cell Physiol Biochem *25*, 675-686.

Walters, R.J., Hadley, S.H., Morris, K.D., and Amin, J. (2000). Benzodiazepines act on GABAA receptors via two distinct and separable mechanisms. Nat Neurosci *3*, 1274-1281.

Whiting, P.J., McAllister, G., Vassilatis, D., Bonnert, T.P., Heavens, R.P., Smith, D.W., Hewson, L., O'Donnell, R., Rigby, M.R., Sirinathsinghji, D.J., *et al.* (1997). Neuronally restricted RNA splicing regulates the expression of a novel GABAA receptor subunit conferring atypical functional properties [corrected; erratum to be published]. J Neurosci *17*, 5027-5037.

Wieland, H.A., Luddens, H., and Seeburg, P.H. (1992). A single histidine in GABAA receptors is essential for benzodiazepine agonist binding. J Biol Chem *267*, 1426-1429.

Xu, Y., Tamamaki, N., Noda, T., Kimura, K., Itokazu, Y., Matsumoto, N., Dezawa, M., and Ide, C. (2005). Neurogenesis in the ependymal layer of the adult rat 3rd ventricle. Exp Neurol *192*, 251-264.

Yang, W., Drewe, J.A., and Lan, N.C. (1995). Cloning and characterization of the human GABAA receptor alpha 4 subunit: identification of a unique diazepam-insensitive binding site. Eur J Pharmacol *291*, 319-325.

Ymer, S., Draguhn, A., Kohler, M., Schofield, P.R., and Seeburg, P.H. (1989a). Sequence and expression of a novel GABAA receptor alpha subunit. FEBS Lett *258*, 119-122.

Ymer, S., Schofield, P.R., Draguhn, A., Werner, P., Kohler, M., and Seeburg, P.H. (1989b). GABAA receptor beta subunit heterogeneity: functional expression of cloned cDNAs. EMBO J *8*, 1665-1670.

Ymer, S., Schofield, P.R., Shivers, B.D., Pritchett, D.B., Luddens, H., Kohler, M., Werner, P., Sontheimer, H., Kettenmann, H., and Seeburg, P.H. (1989c). Molecular studies of the GABAA receptor. J Protein Chem *8*, 352-355.

Young, S.Z., Lafourcade, C.A., Platel, J.C., Lin, T.V., and Bordey, A. (2014). GABAergic striatal neurons project dendrites and axons into the postnatal subventricular zone leading to calcium activity. Front Cell Neurosci *8*, 10.

Zhang, S., and Cui, W. (2014). Sox2, a key factor in the regulation of pluripotency and neural differentiation. World J Stem Cells *6*, 305-311.

Zhao, C., Teng, E.M., Summers, R.G., Jr., Ming, G.L., and Gage, F.H. (2006). Distinct morphological stages of dentate granule neuron maturation in the adult mouse hippocampus. J Neurosci *26*, 3-11.

Zhu, Z., Khan, M.A., Weiler, M., Blaes, J., Jestaedt, L., Geibert, M., Zou, P., Gronych, J., Bernhardt, O., Korshunov, A., *et al.* (2014). Targeting self-renewal in high-grade brain tumors leads to loss of brain tumor stem cells and prolonged survival. Cell Stem Cell *15*, 185-198.

Zhuo, M. (2009). Plasticity of NMDA receptor NR2B subunit in memory and chronic pain. Mol Brain *2*, 4.

8. List of tables

9. List of figures

10. List of abbreviations

Abbreviation	Explanation
ACBP	Acyl-CoA-binding protein
BDNF	Brain-derived neurotrophic factor
BrdU	5-bromo-2-deoxyuridine
CA	*Cornu Ammonis*
DAPI	4',6-diamidino-2-phenylindole
DBI	Diazepam Binding Inhibitor
DCX	Doublecortin
DG	Dentate gryrus
EE	Enriched Environment
F	Phenylalanine
g	Grams
GABA	γ-aminobutyric acid
GFAP	Glial fibrilary acidic protein
I	Isoleucine
i.p.	Intraperitoneal
IPSP	Inhibitory postsynaptic potential
KD	Knockdown
L	Litre
LTP	Long Term Potentiation
M	Molar
MEC	Medial entorhinal cortex
mg	Milligram
ml	Milliliter
NaCl	Sodium chloride
$Na_2HPO_4 \cdot 7H_2O$	Sodium phosphate dibasic heptahydrate
NaH_2PO_4	Sodium dihydrogen phosphate monohydrate

NaN_3	Sodium azide
NMDA	N-methyl-D-aspartate receptor
nRT	Reticular thalamic nucleus
NSCs	Neural stem cells
OB	Olfactory Bulb
ODN	Octadecaneuropeptide
OE	Overexpression
PBS	Phosphate-buffered saline
PBR	Peripheral benzodiazepine receptor
PFA	Paraformaldehyde
PV	Parvalbumin
RMS	Rostral migratory stream
SEM	Standard error of the mean
SGZ	Subgranular zone
SH	Standard housing
SOM	Somatostatin
SVZ	Subventricular zone
TAC	Transit amplifying cells
TTN	Triakontatetraneuropeptide

11. List of publications

Dumitru, I., Neitz, A., Alfonso, J., and Monyer, H. (2017). Diazepam Binding Inhibitor Promotes Stem Cell Expansion Controlling Environment-Dependent Neurogenesis. Neuron *94*, 125-137 e125.

Dumitru, I., Monyer, H. and Alfonso, J. (2016). Mouse Subependymal Zone Explants Cultured on Primary Astrocytes. Bio-protocol 6(14): e1876. DOI: 10.21769/BioProtoc. 1876.

12. Acknowledgements

I must first thank Professor Hannah Monyer and Dr. Julieta Alfonso for offering me the chance to work with them and learn what means to be a neuroscientist. Professor Monyer and Dr. Alfonso were supervisors, my scientific writing professors and the first persons to help when I had a problem. Most important Professor Monyer and Dr. Alfonso were my mentors and gave me good examples of what means to be a scientist. I especially thank Professor Monyer and Dr. Alfonso for really taking the time to help me learn both from my mistakes and from my successes and for guiding me towards becoming an independent scientist.

I also want to thank Professor Thomas Kuner and Dr. Hai-kun Liu for all the good advices, the trust and the guidance during my PhD. They, together with Professor Monyer and with Dr. Alfonso, created a good, supportive and encouraging environment during my TAC meetings.

I would like to thank Dr. Angela Neitz for taking care of the electrophysiological measurements done during this work. Angela was always very helpful in planning the experiments, in taking care of the measurements as well as in helping me analyse and understanding the data.

I thank Jeanette Friemann, Fabian Uch, Regina Hinz-herkommer and Ulrike Amtmann for all the help in the lab. Without Jeanette, Fabian, Regina and Ulla my work would have been much more difficult and my days much longer. I really appreciate that they always helped me in spite of a big amount of work and tight schedule.

I would also like to thank all the members of the Clinical Neurobiology department for creating a challenging and motivating but at the same time supportive and friendly work environment. I especially thank Ceren, Isabelle and Barbara! They were always there when I need help or an opinion. Furthermore, they were not only my colleagues

but also my friends and made working in the lab and science in general to be lots of fun.

I thank Laura Winkel and Anne Herb for the big help with all the administrative issues. Without Laura and Anne I would have been lost in the German bureaucracy.

Last but not least, I must thank my family and my friends, especially my friend Johannes for always being there for me, for always encouraging me and for the trust that I will manage a successful PhD! Without your help, your understanding for the long working hours, the complicated schedule, for the short and seldom vacations I would have never managed it.